

DEPARTMENT OF CHEMISTRY, UNIVERSITY OF JYVÄSKYLÄ
RESEARCH REPORT No. 193

**ION PAIR RECOGNITION BY DITOPIC CROWN ETHER BASED BIS-
UREA AND URANYL SALOPHEN RECEPTORS**

BY

TONI MÄKELÄ

Academic Dissertation for the Degree of
Doctor of Philosophy

*To be presented, by permission of the Faculty of Mathematics and Science of the
University of Jyväskylä, for public examination in Auditorium Kem4,
on June 16th, 2016 at 12 noon.*



UNIVERSITY OF JYVÄSKYLÄ

Copyright ©, 2016
University of Jyväskylä
Jyväskylä, Finland
ISBN 978-951-39-6661-4
ISSN 0357-346X

ABSTRACT

Mäkelä, Toni

Ion Pair Recognition by Ditopic Crown Ether Based bis-Urea and Uranyl Salophen Receptors

Jyväskylä: University of Jyväskylä, 2016, 75 p.

(Department of Chemistry, University of Jyväskylä Research Report Series

ISSN: 0357-346X)

ISBN: 978-951-39-6660-7 (print), 978-951-39-6661-4 (electronic)

This work describes the synthesis of ditopic crown ether based ion pair receptors and their recognition behaviour towards various ion pairs in solid-state, solution, and gas-phase. The receptors consist of crown ether scaffolds for cation recognition and bis-urea or uranyl salophen as anion recognition functionality. As the introduction to the topic, a short description of supramolecular chemistry is given. Then examples of ditopic receptors based on crown ethers and uranyl salophens are presented to give an overview of their ion pair binding behaviour. This is followed by a description of the use of ditopic receptors in further examples of different receptor types, and finally a few examples of more complicated multitopic receptor systems are discussed.

The Results and Discussion section summarizes the results obtained and reported in three published journal articles and one manuscript. In the course of this work, four new crown ether bis-urea receptors and two new crown ether uranyl salophen receptors were prepared. The solid-state ion pair binding behaviour of the crown ether bis-urea receptors was studied in extensive single-crystal X-ray crystallography studies of 33 crystal structures revealing the general characteristics of their ion pair complexation. In addition, the solution behaviour of the receptors revealed strong positive cooperativity toward anion binding when the receptors were complexed with alkali metals. The solution-state behaviour of the receptors was supported by solid-state studies. Lastly, the gas-phase studies by mass spectrometry strongly supported the ion pair complexation behaviour seen in solution.

The two crown ether uranyl salophen receptors were studied in comprehensive solid-state studies with single crystal X-ray crystallography (19 structures) revealing three general interaction motifs in ion pair complexation that depend on the crown ether size and the nature of the ion pair. Interestingly one obtained crystal structure constituted of coordination polymer with repeating $\cdots\text{O}=\text{U}=\text{O}\cdots\text{Na}^+\cdots\text{O}$ units, presenting the intriguing possibility of utilizing these types of receptors in building magnetic materials.

Keywords: supramolecular chemistry, ditopic receptors, ion pair binding, anion binding, crown ethers, urea, uranyl salophens, X-ray crystallography, ^1H NMR titrations

Author's address

Toni Mäkelä
Department of Chemistry
Nanoscience Center
P.O. Box 35
40014 University of Jyväskylä
Finland
toni.p.l.makela@jyu.fi

Supervisors

Acad. Prof. Kari Rissanen
Department of Chemistry
Nanoscience Center
P.O. Box 35
40014 University of Jyväskylä
Finland

Docent Manu Lahtinen
Department of Chemistry
P.O. Box 35
40014 University of Jyväskylä
Finland

Reviewers

Professor Philip A. Gale
School of Chemistry
University of Southampton
Southampton, United Kingdom

Professor Antonella Dalla Cort
Department of Chemistry and IMC-CNR
University La Sapienza
Rome, Italy

Opponent

Professor Anthony P. Davis
School of Chemistry
University of Bristol
Bristol, United Kingdom

ACKNOWLEDGEMENTS

This long journey studying at the university is coming to an end, which started in the first chemistry lectures in the autumn of 2005 and ending with finalizing the PhD studies in June 2016. This has always been the path I wanted to take, to study and learn more about the Nature and the phenomena in it. And the more I have learned, the more amazed I am of all the complexity and beauty in it. But the work has not been the most important part of this journey; it has been the things that I have learned about myself and the people I have met along the way. I want to express my gratitude to the following people for being part of this journey.

First and foremost I want to thank Acad. Prof. Kari Rissanen for giving me the chance to work under his supervision and be a part of his wonderful working group. I am very grateful for the freedom and trust I have received to conduct the work as I have seen fitting. It has been a great chastening experience and I will carry these lessons to wherever I will go. I also want to thank Adj. Prof. Manu Lahtinen for giving me an introduction to the fascinating world of X-ray crystallography, and for the support and patience in this learning experience.

I thank Prof. Phillip A. Gale and Prof. Antonella Dalla Cort for the valuable comments regarding my thesis and I am extremely humbled to have such prestige experts reviewing my work. Matti Nurmi is gratefully acknowledged for the language revision of this thesis.

Prof. Christoph A. Schalley is warmly thanked for the possibility to work in his laboratory, and Dr. Lena Kaufmann, Dr. Karol Nowosinski, Dr. Andreas Springer, Dr. Nora Traulsen, and M. Sc. Hendrik Schröder are thanked for the help in and outside of the lab during my visits in Berlin.

The Department of Chemistry is acknowledged for the financial support for the PhD studies and travel grants.

I want to thank all the people at the chemistry department for creating such a unique and supporting working environment. Adj. Prof. Elina Kalenius is especially acknowledged for her help with the mass spectrometry and for the valuable comments related to my work. Adj. Prof. Juhani Huuskonen is gratefully acknowledged for the help and support during my teaching periods on his courses. Dr. Tanja Lahtinen is warmly thanked for her support while I was working in the teaching laboratory at the organic chemistry department. M. Sc. Esa Haapaniemi is thanked for his help related to the NMR experiments. I want to thank M. Sc. Miia-Elina Minkkinen, M. Sc. Anniina Kiesilä, M. Sc. Ville Holopainen, and M. Sc. Silja Majaharju for their extra pair of hands in the synthesis, crystallizations, and numerous other experiments also presented in this thesis. And laboratory technicians Ms. Johanna Lind and Mrs. Leena Koskela are thanked for their help with the practical things related to the lab work.

These years of doing my PhD studies have been the greatest time of my life because I have met and made friends with so many people from all around the world. I believe I would have never gotten to learn and experience so many

different cultures without these years working in the group of these great people. We have had great times at the department, but especially in the free time hanging out and arranging the most awesome parties. So from the bottom of my heart I express my deepest gratitude to you guys: Filip, Ondrej, Pia, Lotta, Leticia, Lorenzo, Rakesh, Arto, Sahoo, Rosy, Kodi, Nonappa, Chandan, Ralf, Hana, Jens, Biswa, Sandip, and Fangfang. I also want to thank my “non-chemistry” friends Saumyadip, Jussi and Elina, Jaakko, Toni, Petteri, and Johannes for being there and giving a different perspective to life.

This work is dedicated to the memory of my mother Marianne Mäkelä who passed away before this part of my journey was completed. Without her strength and never faltering support even amidst her struggle the ending to this journey would have been much more demanding. I only hope that I possess even a small piece of her strength within me. With that strength there are no obstacles that I cannot overcome. I want to express my deepest gratitude to my family and loved ones for never losing their faith in me: Dad; Sonja, Ismo, Miikka, Tuukka and Miska; Henri, Kati, Peetu, and the newborn. Without you this would not have been possible. I also want to thank my grandmother Airi and all the other relatives and friends for always supporting me. Lastly, I want to thank Marko for all the help and support during the good and tough times.

Tämä työ on omistettu äitini Marianne Mäkelän muistolle, joka poistui keskuudestamme ennen kuin tämä osa matkastani tuli päätökseen. Ilman hänen vahvuuttaan ja loppumatonta tukeaan jopa hänen taistelunsa aikana tämän työn loppuun saattaminen olisi ollut hyvin paljon haastavampaa. Voinkin vain toivoa, että sisältäni löytyy edes pieni osa sitä samaa vahvuutta, sillä sen avulla mikään este ei ole liian suuri ylitettäväksi. Haluan kiittää sydämeni pohjasta perhettäni ja rakkaitani, jotka ovat aina uskoneet minuun: Isä; Sonja, Ismo, Miikka, Tuukka ja Miska; Henri, Kati, Peetu ja uusi tulokas. Ilman teitä tämä ei olisi ollut mahdollista. Haluan myös kiittää isoäitiäni Airia, sekä kaikkia sukulaisia ja ystäviä tuesta. Lopuksi haluan kiittää Markoa kaikesta avusta ja tuesta niin hyvinä kuin vaikeinakin aikoina.

Jyväskylä 11.5.2016

Toni Mäkelä

LIST OF ORIGINAL PUBLICATIONS

This thesis is based on the following original publications which in the text are referred to by their Roman numerals.

- I T. Mäkelä, E. Kalenius and K. Rissanen, Cooperatively Enhanced Ion Pair Binding with a Hybrid Receptor, *Inorg. Chem.* **2015**, *54*, 9154-9165.
- II T. Mäkelä and K. Rissanen, Ion Pair Complexes and Anion Binding in Solution of a Ditopic Receptor, *Dalton Trans.* **2016**, *45*, 6481-6490.
- III T. Mäkelä, A. Kiesilä, E. Kalenius and K. Rissanen, Ion Pair Complexation Studies with Dibenzo-21-Crown-7 and Dibenzo-24-Crown-8 bis-Urea Receptors, *manuscript*.
- IV T. Mäkelä, M.-E. Minkkinen and K. Rissanen, Ion Pair Binding in the Solid-State with Ditopic Crown Ether Uranyl Salophen Receptors, *Inorg. Chem.* **2016**, *55*, 1339-1346.

CONTENTS

ABSTRACT

ACKNOWLEDGEMENTS

LIST OF ORIGINAL PUBLICATIONS

CONTENTS

ABBREVIATIONS

1	INTRODUCTION	11
1.1	Supramolecular Chemistry	11
1.2	Ion Pair Complexation	12
1.3	Crown Ethers and Uranyl Salophens as Ditopic Receptor Scaffolds	15
1.3.1	Ditopic Receptors Based on Crown Ethers	15
1.3.2	Ditopic Receptors Based on Uranyl Salophens	23
1.4	Applications of Ion Pair Receptors.....	27
1.4.1	Solubilization.....	27
1.4.2	Extraction	29
1.4.3	Membrane Transport.....	30
1.4.4	Sensing.....	33
1.5	Multitopic Receptor Systems	34
2	RESULTS AND DISCUSSION	38
2.1	Aim of the Work	38
2.2	Synthesis of Receptors $L^1-L^{6 I-IV}$	39
2.3	Solid-State Studies of $L^1-L^{6 I-IV}$	41
2.3.1	Solid-State Studies of Crown Ether bis-Urea Receptors $L^1-L^4 I-III$.	41
2.3.1.1	Crystal Structures with Alkali and Ammonium Halides $I-III$	43
2.3.1.2	Crystal Structures with Alkali Oxyanions I,III	48
2.3.2	Solid-State Studies of Crown Ether Uranyl Salophen Receptors L^5 and $L^{6 IV}$	51
2.4	Solution Studies with Crown Ether bis-Urea Receptors $I-III$	57
2.4.1	Solution Studies with Receptor $L^2 I$	57
2.4.2	Solution Studies with Receptor $L^1 II$	60
2.4.3	Solution Studies with Receptors L^3 and $L^4 III$	62
2.5	Gas Phase Ion Pair Complexation with Crown Ether bis-Urea Receptors I,III	65
	CONCLUSIONS	68
	REFERENCES.....	71

ABBREVIATIONS

AcO ⁻	acetate
B15C5	benzo-15-crown-5
B18C6	benzo-18-crown-6
BPh ₄	tetraphenylborate
CCI	cation-cation interaction
CDCl ₃	chloroform (deuterated)
CD ₃ CN	acetonitrile (deuterated)
CF ₃ SO ₃ ⁻	triflate
CHCl ₃	chloroform
CH ₂ Cl ₂	dichloromethane
CH ₃ CN	acetonitrile
CID	collision-induced dissociation
CO ₂	carbon dioxide
CO ₃ ²⁻	carbonate
DB21C7	dibenzo-21-crown-7
DB24C8	dibenzo-24-crown-8
DMF	dimethylformamide
DMSO	dimethyl sulfoxide
DNA	deoxyribonucleic acid
ESIMS	electrospray ionization mass spectrometry
HMBC	heteronuclear multiple bond correlation
HMQC	heteronuclear multiple quantum coherence
K	binding constant
MeOH	methanol
MS	mass spectrometry
NH ₄ ⁺	ammonium
NMR	nuclear magnetic resonance
NO ₃ ⁻	nitrate
POPC	1-palmitoyl-2-oleoyl- <i>sn</i> -glycero-3-phosphocholine
ReO ₄ ⁻	perrhenate
SCM	single chain magnet
SMM	single molecule magnet
TBA	tetrabutylammonium
TcO ₄ ⁻	pertechnetate
TMA	tetramethylammonium
tren	tris(2-aminoethyl)amine
UV-Vis	ultraviolet-visible

1 INTRODUCTION

1.1 Supramolecular Chemistry

Jean-Marie Lehn, winner of Nobel-prize in 1987 for his contributions in supramolecular chemistry with Charles Pedersen and Donald Cram, has described supramolecular chemistry as follows: “supramolecular chemistry aims at developing highly complex chemical systems from components interacting by noncovalent intermolecular forces”.¹ In its simple form supramolecular chemistry can be considered as the interaction of “host” and “guest” through interactions beyond covalent bonds, *i.e.* noncovalent or weak interactions, to create complexes. This is simply referred as “host-guest chemistry”. The host can be defined as a “molecular entity possessing convergent binding sites” whereas “the guest possesses divergent binding sites”. The binding site is defined as the area of the host or the guest that is capable of forming weak interactions.^{2,3}

The noncovalent interactions responsible of creating supramolecular systems vary in their strength. Important weak interactions in supramolecular chemistry and natural systems are, for example, ion-ion and ion-dipole interactions, hydrogen bonds, π -interactions (cation- π , anion- π , π - π), and van der Waals forces. Their relative strengths are shown in Table 1. They are weaker than covalent interactions, which can range between 150 - 450 kJ mol⁻¹ for single bonds.⁴ Although the energy of a single interaction is an easily perceived measure of the binding strength, the important factor for the stability of the complex is the sum of all the interactions taking part in the formation of the complex.^{3,4}

Today, host-guest chemistry is only one area of supramolecular chemistry. In recent years, a strong emphasis in supramolecular chemistry has been directed in the development of large molecular systems through self-assembly of smaller chemical entities through various noncovalent interactions.⁵ In this approach, the information within the molecular building blocks is transferred to the resulting supramolecular system. These larger assemblies are again capable of hosting guest molecules via weak interactions, and therefore we can consider

host-guest chemistry to be an integral part of the supramolecular chemistry of self-assembled systems.⁶⁻⁹

The important noncovalent interactions in supramolecular systems play a key role also in many biological processes, and Nature is a huge inspiration for supramolecular chemists developing complex molecular systems with desired functions. Examples of biological systems that depend on noncovalent interactions are, for example, protein folding, enzyme-ligand interactions, formation of the DNA double helix, self-assembly of fibrous proteins in cells from smaller filaments, and ion transport through cell membranes, just to name a few.¹⁰⁻¹² All these systems are finely adjusted for proper function and they are based on noncovalent interactions between the components constituting the system. The essential characteristic in biological systems is the dynamic nature and reversibility of the processes. This is of utmost importance, for example, in the enzyme-mediated reactions, where the product has to be removed from the binding site for the next reaction to take place, i.e. the unfolding of the DNA double helix to reveal the genetic information embedded in the base sequence of the DNA strand.^{3,4,12}

These examples of natural systems exemplify the characteristics that need to be considered when developing supramolecular systems with desired functions. Important factors are the complementarity of the host and guest (size, shape and chemical character), preorganization of the host and cooperativity of the binding.^{3,4,13,14} Examples of ion pair recognition presented in the following chapters elucidate these features in artificial receptor systems.

TABLE 1 Summary of noncovalent interactions and their strength.^{4,15}

Interaction	Strength (kJ mol ⁻¹)
Ion-ion	200-300
Ion-dipole	50-200
Dipole-dipole	5-50
Hydrogen bonding	4-120
Halogen bonding	10-150
Cation- π	5-80
π - π	0-50
van der Waals	< 5

1.2 Ion Pair Complexation

The development of artificial receptors for cations and anions has been an important part of supramolecular chemistry. Cations are present in all living systems and they have critical roles in many biological processes, for example, in nerve signal transduction.¹² Cations are also present in the environment, and increasing amounts of many toxic heavy metals (lead, cadmium, mercury) are

being released into the environment by human actions.³ Because of the inherent nature of cations (size, shape, chemical characteristics), cation receptor chemistry has been a blooming area in supramolecular chemistry for decades, as has been well documented.^{3,12} The more complex nature of anions, varying in their size and shape, having higher solvation energies than cations, and existing usually in narrow pH ranges, has made the development of efficient artificial anion receptors slower compared to cation receptor chemistry.^{3,4,12} Anions also play significant roles in biological systems and in the environment. Chloride is present in the extracellular fluid to balance the ionic strength due to the large sodium and potassium concentration in the body, and it is also present in seawater.³ Hydrogen carbonate and carboxylates are other important biological anions, and nitrates and phosphates have importance as fertilizers but at the same time are major pollutants in water systems.³ Thus a lot of interest has been directed towards developing efficient and selective supramolecular anion receptors utilizing a vast selection of different functionalities in both simple and complex molecular scaffolds.¹⁶⁻²⁰

Ions always exist in the solution with a counter ion to reach charge neutrality. Because of this, ions are rarely completely separated in solution, and especially in weakly polar solvents they can exist as contact ion pairs, whereas in more polar solvents solvent-separated ion pairs can be present.⁴ Thus, the simple cation or anion receptors are actually interacting with ion pairs. The binding of an ion can therefore have a large energetic cost because the ions have to be separated to some extent for the binding to occur. This can have a drastic effect on the binding affinity of the receptor towards the desired ion, and as a consequence affect their use in applications.⁴

Ion pair receptors have garnered growing attention in the last two decades, based on the lessons learned from the development of cation and anion receptors.²¹⁻²⁴ Receptors for ion pair complexation are generally divided into categories according to the structure of the receptor and the nature of the ion pair complex: ditopic receptors with a contact ion pair, a solvent-separated ion pair, or a separated ion pair, cascade receptors, or zwitterionic receptors (Figure 1).^{3,4,22,23} Ditopic receptors have two distinctive binding sites for the cation and anion, while cascade receptors are formed when the first ion binding creates a binding site for the next ion, and receptors for zwitterions (a neutral molecule which bears both positive and negative charge) have binding sites for positively and negatively charged parts of the guest.⁴ Ion pair receptors generally utilize combinations of well-characterized functionalities for cations and anions, for example crown ethers, calixarenes, or Lewis basic groups for cation recognition and hydrogen bonding functionalities (amide and urea groups, imidazolium, pyrrole), Lewis acidic groups or positively charged nitrogen groups for anion recognition. These functionalities can be closely located or reside far away from one another in the receptor scaffold, depending on how the ion pair is to be complexed.^{3,4}

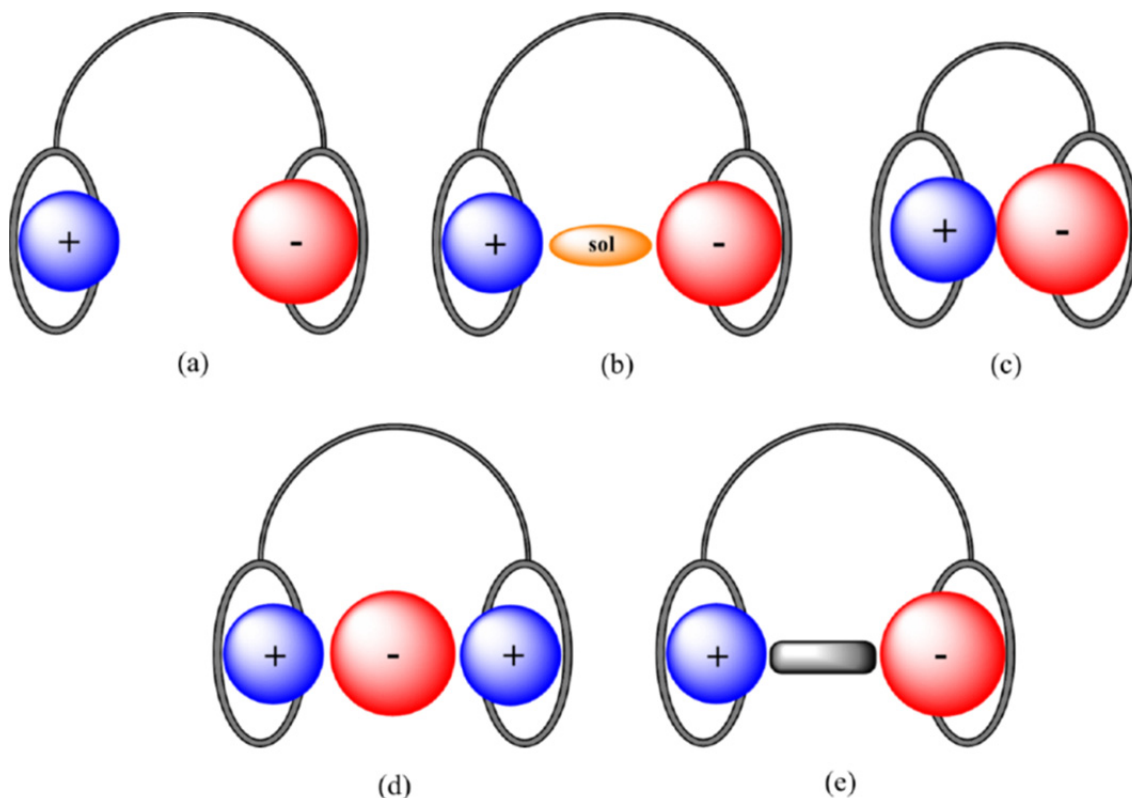


FIGURE 1 Schematic representation of different types of ion pair recognition motifs. Ditung receptors with (a) separated ion pair, (b) solvent-separated ion pair, (c) contact ion pair, (d) cascade receptor, (e) zwitterionic receptor. Figure is modified from reference 23.

One benefit of ion pair receptors over simple cation or anion receptors is that they often show cooperative behaviour. In positive cooperativity, the binding of the first guest induces a change in the host resulting in stronger binding of the second guest. In anti-cooperative binding this phenomenon is reversed, and in non-cooperative binding the binding of the first guest has no effect on the second binding event.^{13,14} The cooperative effects (positive and negative) can be a result of allosteric and electrostatic effects.²²⁻²⁴ Allosteric cooperativity stems from a conformational change in the receptor scaffold upon the binding of the first guest, whereas electrostatic cooperativity results from electrostatic interactions between the bound guests.²²⁻²⁴

Cooperativity is not a simple phenomenon and the factors inducing the process are often not thoroughly understood, even though this effect was observed already with the first ditopic receptor systems. Work by Roelens and coworkers has demonstrated that ion pair binding with even a simple receptor is not necessarily cooperative,²⁵ and that the ion pairing of species not complexed by the receptor should be taken into account to correctly assess the cooperative effects of the guest binding.²⁶ The recent work by Thordarsson and coworkers²⁷ and Flood and coworkers²⁸ have elucidated the matter through extremely detailed studies with their respective molecular systems. The receptor presented by Thordarsson²⁷ is actually a tetratopic receptor, demonstrating the

possibility to develop these receptors for multitopic binding with better selectivity and stronger association with the desired guests. However, the greater complexity of the system also leads to more difficulty in understanding the factors responsible for the selectivity and cooperativity.^{27,28} This system and some other multitopic receptors will be presented in the last part of the introduction.

Although advantageous, a surprisingly limited number of ditopic receptors have been developed.^{22,23} The reason might be the complicated synthesis of the receptors themselves, which are often macrocyclic and can be difficult to obtain. In addition, following the desired binding phenomenon and understanding the role of the multiple ion pair equilibriums present in the system create further challenges. For the sake of simplicity, researchers usually use salts with large non-coordinating counter ions to minimize the effect of the ion pairing with the ions of interest. However, this can be a strong simplification of the system, as shown by Roelens and coworkers.^{25,26}

In the following chapters examples of ditopic receptor systems based on crown ethers (cation recognition motif) and uranyl salophens (anion recognition motif) are presented. Then, examples of applications of different types of ditopic receptors are presented, further underlining the benefits of developing ditopic or multitopic receptor systems.

1.3 Crown Ethers and Uranyl Salophens as Ditopic Receptor Scaffolds

1.3.1 Ditopic Receptors Based on Crown Ethers

Since the ground breaking discovery of crown ethers by Charles Pedersen in 1967, which led to a Nobel prize in chemistry in 1987 with Lehn and Cram,^{29,30} a huge body of work related to the synthesis and use of these macrocyclic molecules has been published.^{3,12,31} Crown ethers can generally be described as macrocyclic structures with heteroatoms (oxygen, nitrogen, sulphur) separated by chains of two or more carbon atoms. The exterior, or the alkyl side, is lipophilic and the interior is hydrophilic, making it possible for crown ethers to exist in different chemical environments. The guest, usually an alkali metal or ammonium cation in the case of oxygen atom donors, can interact with the heteroatoms through ion-dipole interactions or hydrogen bonds to form a complex. The size fit between the guest and the crown ether cavity is a crucial factor for the strength and structure of the complex. For example, 18-crown-6 (crown ether with a total of 18 atoms with 6 oxygen atoms) has a perfect cavity size to accommodate a potassium cation, resulting in high selectivity and strong affinity toward potassium, whereas 15-crown-5 is more suitable for complexing a smaller sodium cation. However, if the guest is too large for the crown ether cavity, it can reside on top of the crown ether plane or be "sandwiched" between two crown ethers.¹² However, the size fit is not the only factor governing

the strength and selectivity of the complexation, and for example solvation, the number of interacting atoms, and electronic factors greatly affect the process.^{3,12} Crown ethers have been utilized in various applications, and probably the best known example is their use in phase-transfer catalysis and anion activation.³ Crown ethers can solubilize inorganic salts in nonpolar media because the formed crown ether - cation complex is lipophilic and thus soluble in apolar solvents. The anion is also transferred to the apolar medium with the cation to maintain the charge balance where it can readily react. Crown ethers have also been functionalized in numerous ways to give, for example, sensors or model systems for ion channels.¹² Selected examples on the use of crown ethers as structural basis for ditopic receptor systems are presented in the following section.

One of the first examples of ditopic receptors was presented by Reetz and coworkers in 1991 (Figure 2).^{32,33} The synthesized receptor (**1**) contained a crown ether attached to an aromatic scaffold for cation complexation and a Lewis acidic boronate group as an anion recognition site. The receptor was shown to dissolve potassium fluoride to dichloromethane (CH_2Cl_2), whereas KCl and KBr were insoluble. The selectivity was further proved by exclusive binding of KF from a mixture containing also KCl, KBr, and KI. The obtained crystal structure with KF proved the formation of an ion pair complex in the suggested binding motif. Although the structure can be considered as having a separated ion pair within the isolated complex, the fluoride anion forms a contact ion pair with the potassium cation complexed in the neighbouring receptor resulting in a polymeric structure.³²

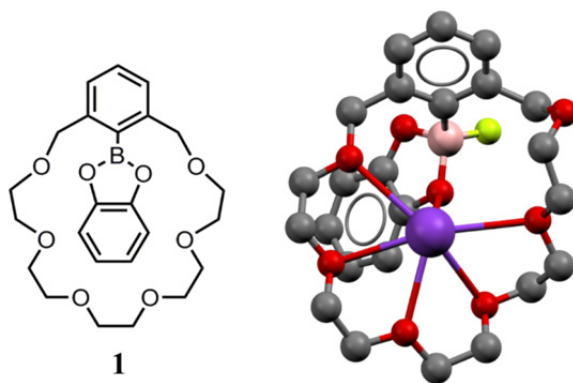


FIGURE 2 Crown ether based Lewis-acidic ditopic receptor **1** prepared by Reetz and coworkers.³² (b) Crystal structure of the receptor with KF (CSD code VOPFEL). Potassium is further coordinated by the fluoride anion and oxygen of the adjacent complex (not shown). Hydrogen atoms have been omitted for clarity.

Smith and coworkers were one of the first groups showing the problems that can arise from ion pairing in solution when using simple anion receptors, and the benefit of utilizing ditopic receptors to overcome this problem.³⁴ They showed that in the presence of small alkali metal cations (Na^+ , K^+) in dimethyl sulfoxide (DMSO), the binding of receptor **2** (Figure 3) with acetate and dihydrogen phosphate is inhibited, whereas the presence of larger Cs^+ does not af-

fect the anion binding. The authors relate this effect to the diminishing anion basicity upon the ion pairing with a cation, or sterical hindrance between the receptor and the anion that result from ion pairing. The inhibition is related to the size and polarizability of the cation. For example, Cs^+ is not ion paired in DMSO and does not affect the anion binding.³⁴ However, when the anion binding affinity of receptor **3** was studied, the binding affinities showed cation and anion dependence. For example, receptor **3** in acetonitrile binds NO_3^- with binding constant (K) 35 M^{-1} . In the presence of Na^+ , the binding constant increases to 130 M^{-1} , whereas in the presence Cs^+ the binding constant is 310 M^{-1} . This effect is both cation and anion dependent, showing reversed behaviour with more basic anions and smaller cations resembling the situation with receptor **2**. This study exemplifies that even with simple systems, the interplay between the anion and cation can strongly affect the desired binding phenomenon.³⁴

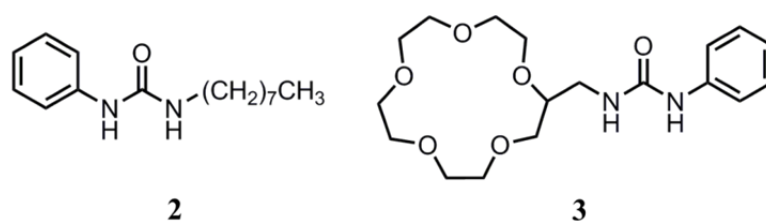


FIGURE 3 Receptors used by Smith and coworkers to show the importance of ditopic nature of the receptor in ion pair binding.³⁴

Smith and coworkers also prepared elegant ditopic receptors for contact and solvent-separated ion pairs.³⁵⁻⁴² Their comprehensive work expands structural studies of these receptors with various ion pair complexes to the utilization of these receptors in ion pair transport through membranes. Receptor **4** (Figure 4) shows positive cooperativity towards anion binding in the presence of small alkali metal cations. For example, the binding constant towards chloride increases from 50 M^{-1} to 410 M^{-1} and 470 M^{-1} in the presence of Na^+ and K^+ , respectively, in DMSO.³⁵ The crystal structure of **4** has revealed a chloroform-separated ion pair with NaCl . Receptor **5** (Figure 4), on the other hand, forms a contact ion pair with KCl in the solid-state due to the smaller cavity compared to **4**.³⁶ However, in solution receptor **5** shows positive cooperativity toward chloride binding only in the presence of K^+ . Receptor **5** has binding constant of 35 M^{-1} towards chloride in DMSO. In the presence of Na^+ the binding constant is 50 M^{-1} , whereas the binding constant with a $[\text{5}\cdot\text{K}]^+$ complex is 460 M^{-1} . This selectivity was explained by the differences in the crystal structures of **5** with NaCl and KCl . In the solid-state complex, the smaller sodium cation resides in the middle of the crown ether ring, bringing the oxygen atoms of the crown ether closer to the complexed anion and creating unfavorable ion-dipole repulsions.³⁶ However, the larger potassium cation is located above the crown ether plane to optimize the ion-dipole interactions, enabling a formation of a contact ion pair with the chloride, which is further hydrogen bonded with the amide groups. Thus, the solid-state complexes could be used to explain the effects ob-

served in the solution.^{35,36} The fairly simple macrobicyclic receptor **5** was also shown to bind neutral guests like urea and primary amides,³⁵ alkylammonium ion pairs with a strong dependence on the counteranions,³⁸ and trigonal oxyanions.⁴² In addition to the extensive structural studies with receptors **4** and **5**, these receptors have also been shown to solubilize inorganic salts into organic media and they have been utilized as NaCl and KCl transporters through lipid membranes.³⁹⁻⁴¹

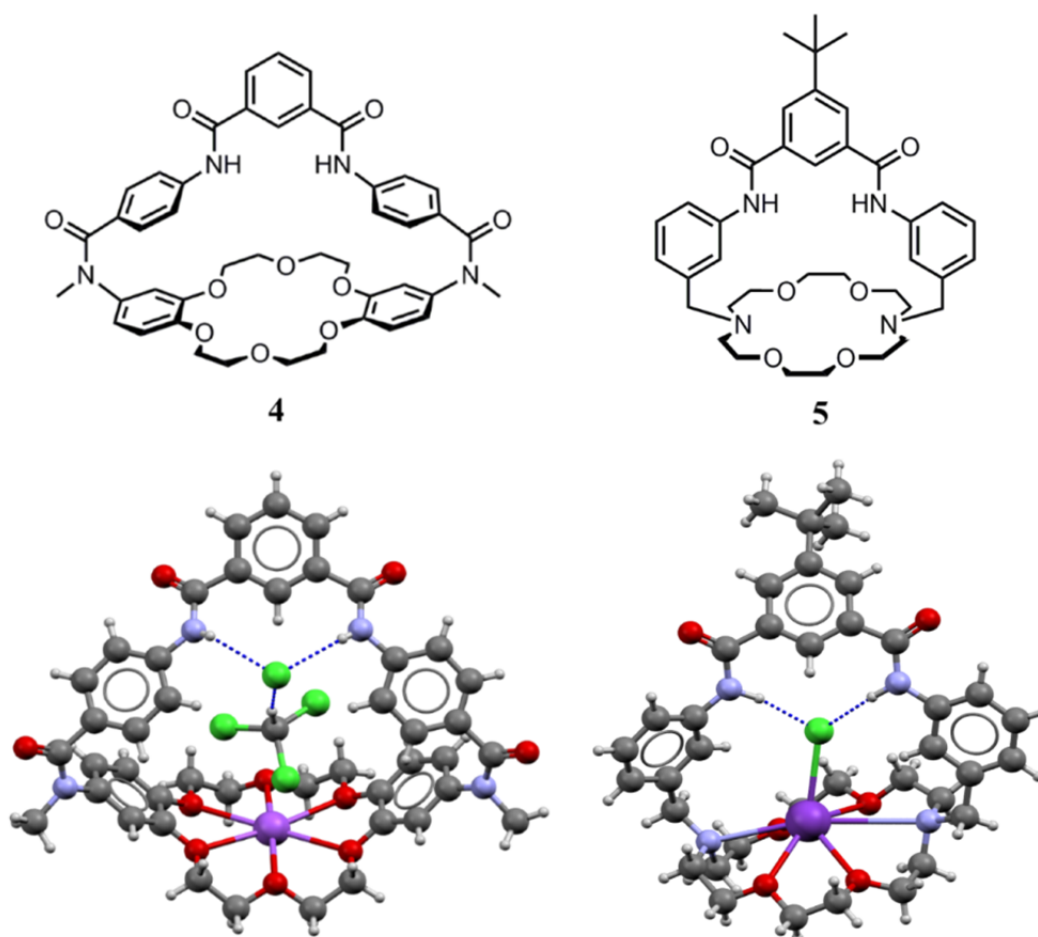


FIGURE 4 Ditopic receptors **4** and **5** designed by Smith and coworkers. Crystal structure of **4**·NaCl·CHCl₃ (CSD code FOQWAJ) has a solvent-separated ion pair complex,³⁵ whereas **5**·KCl (CSD code IBUKEW) has a contact ion pair within the receptor's cavity.³⁶

Barboiu and coworkers have presented extensive studies of utilizing ditopic crown ether ureido molecules in building model systems for cation selective channels.⁴³⁻⁴⁹ Molecules **6** and **7** (Figure 5) present examples of the simple ditopic receptors used in these studies. The receptors were shown to bind alkali metal salts as separate and contact ion pairs in the solid-state depending on the size of the crown ether ring, cation size and the nature of the anion (Figure 5).^{43,45,46} In addition, they were shown to form self-assembled polymeric super

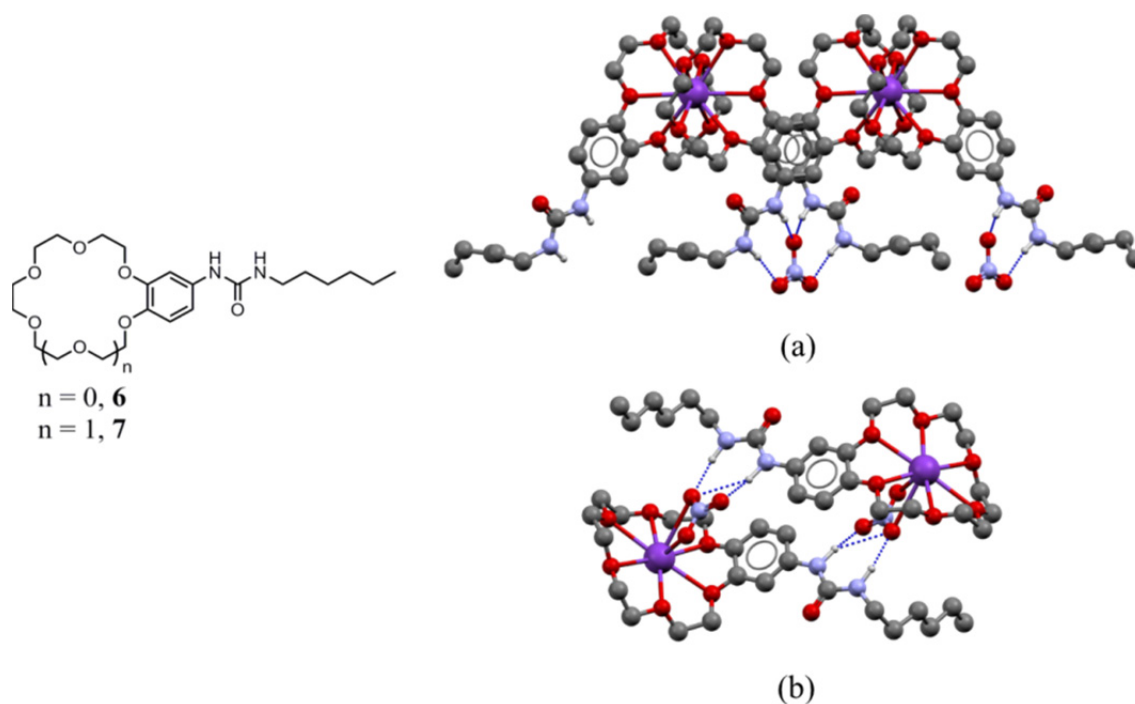


FIGURE 5 Ditopic crown ether ureido molecules prepared by Barboiu and coworkers used as building blocks for artificial K⁺-selective channels.⁴⁹ (a) Crystal structure of **6**·KNO₃ (CSD code XOGBOM), a dimeric assembly formed by K⁺ coordination with two molecules of **6**, where the nitrate is anion hydrogen bonded with the urea groups. (b) Crystal structure **7**·KNO₃ (CSD code XOGBUS). A contact ion pair is formed between crown ether -complexed K⁺ and the NO₃⁻ anion, which is further hydrogen bonded to the urea functionalities.

structures in solution and in lipid bilayers,⁴⁴ and they have been used to create artificial ion channels for selective K⁺ transport.⁴⁹

Similar cholesterol and squaryl crown ether analogues of **6** and **7** have also been used to create artificial model structures of KcsA -channels, naturally occurring potassium-selective ion channels.^{47,48} Because of the importance of ion mobility in many physiological events, ion transport plays a significant role in biological systems. Therefore a lot of attention has been given to develop artificial systems mimicking the behavior of natural ion channels. These structurally simple molecules exemplify beautifully how naturally occurring structures can be mimicked artificially to gain complex functions.⁴⁷⁻⁴⁹

Calixarenes are one of the most utilized molecular scaffolds in creating complex ditopic receptor systems.²¹⁻²³ Beer and coworkers prepared a ditopic receptor based on calix[4]arene scaffold with upper rim functionalization with benzo-15-crown-5 groups (**8**, Figure 6) to study the cooperativity in the complexation of alkali metal salts.⁵⁰ The receptor **8** forms a 1:2 complex with Na⁺ and a 1:1 sandwich complex with K⁺ (monitored by ESI-MS). In the presence of potassium cations (1 equiv as perchlorate, in 1:1 CD₃CN:DMSO), the recognition of chloride, benzoate, and dihydrogen phosphate is enhanced, whereas in the presence of 2 equiv of Na⁺ the anion binding affinity is reduced. The authors correlate the potassium-induced binding enhancement to preorganization

of the receptor scaffold upon K^+ complexation for efficient anion binding and favourable electrostatic interactions between the ionic species. In the presence of sodium cations, however, the electrostatic repulsion between the crown-ether complexed cations pushes the receptor arms further away, thus preventing the anion binding. The cooperativity of K^+ complexation was also supported by using **8** to solubilize $KAcO$ into $CDCl_3$.⁵⁰

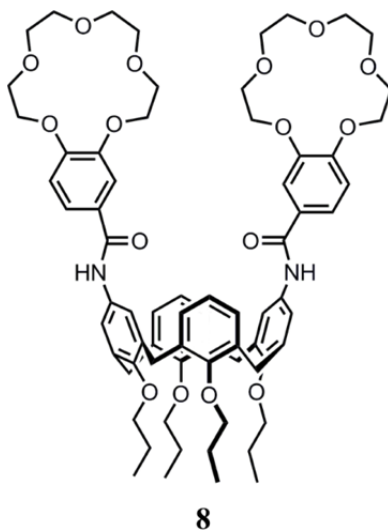


FIGURE 6 Calix[4]arene functionalized ditopic receptor by Beer and coworkers.⁵⁰

Another interesting heteroditopic receptor type utilizing crown ethers by Beer and coworkers is presented in Figure 7.⁵¹⁻⁵³ The heteroditopic Ru^{II} or Re^I bipyridyl bis(benzo-15-crown-5) receptor **9** with amide functionalities for anion recognition has a strong selectivity towards chloride and dihydrogen phosphate depending on the presence of potassium.⁵² When potassium is not present in the system, receptor **9** has stronger affinity towards dihydrogen phosphate compared to chloride in DMSO. However, when 2 equiv of potassium is added (as PF_6^- -salt), a sandwich complex is formed between the potassium and the 15-crown-5 ether rings. According to the authors, this coordination rearranges the amide groups suitably for chloride binding, whereas the receptor conformation is not suitable for binding dihydrogen phosphate. This is another example of allosteric conformational selectivity with ditopic receptors. Similar behaviour was observed also for receptor **10** (Figure 7),^{51,53} which also showed positive cooperativity towards chloride and acetate binding in 1:1 DMSO/ CD_3CN upon potassium complexation, with higher selectivity toward acetate. The crystal structure **10**· KCl consists of a centrosymmetric dimer formed by carbonyl oxygen coordination to the potassium cation in the adjacent complex. The chloride anion is hydrogen bonded with the amide protons and with three aromatic C-H protons. The flexible ethylene linker between the amide groups brings the crown ether closer to the chloride, reinforcing the electrostatic attraction between the cation and the anion.^{51,53}

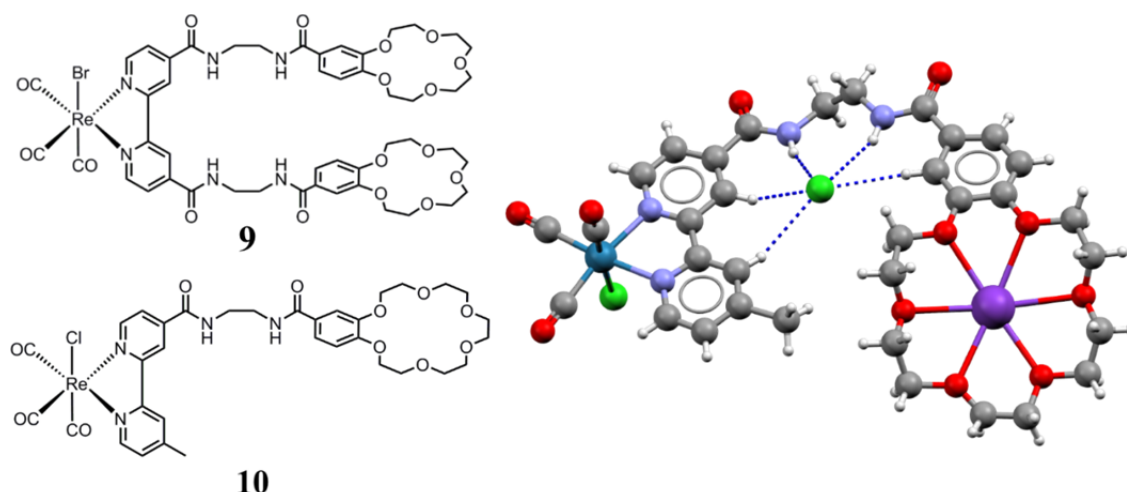


FIGURE 7 Ditopic receptors prepared by Beer and coworkers.⁵¹⁻⁵³ Crystal structure of **10**·KCl (CSD code XIBCOA) consists of a centrosymmetric dimer formed through coordinative bond to the carbonyl oxygen of the adjacent complex (not shown).⁵³

Romanski and coworkers have prepared a large number of ditopic *L*-ornithine based crown ether receptors (see Figure 8 for the general structure), which have shown positive cooperativity towards various anions especially in the presence of sodium. The receptors consist of aza-crown ether connected to *L*-ornithine molecular scaffold having urea and thiourea groups as first anion recognition unit and amide or urea/thiourea functionality as another anion recognition unit (Figure 8).⁵⁴⁻⁵⁷ They also prepared a receptor with a methacrylamide-group to create polymerizable molecules that can be embedded into polymers for extraction of different salts from aqueous media.⁵⁴ The ion pair binding studies have revealed a strong influence of geometric and electrostatic factors in the recognition processes. For example, substituting the thiourea with oxygen-containing urea close to the crown ether leads to higher selectivity of ion pairs due to the stronger coordination of the hard urea-oxygen with the crown ether-complexed sodium cation. This affects the geometry of the receptor and enhances the acidity of the urea-protons, resulting in stronger hydrogen bonds with the anion.⁵⁴⁻⁵⁶ Noteworthy is the selectivity of these receptors towards NaNO_2 , although also other anions (bromide, nitrate) have enhanced affinities towards the receptors in the presence of Na^+ . Further development of their receptor molecules have led to receptors **11** and **12** (Figure 8) with amide functionalities replaced by urea and thiourea groups for even stronger hydrogen bonding interactions with the anions.⁵⁷ Especially receptor **12** has a very high association with NaCl in acetonitrile due to the presence of the thiourea group as a secondary anion recognition unit. These studies nicely demonstrate the effect of different hydrogen bond donor groups on the anion binding efficiency.^{56,57}

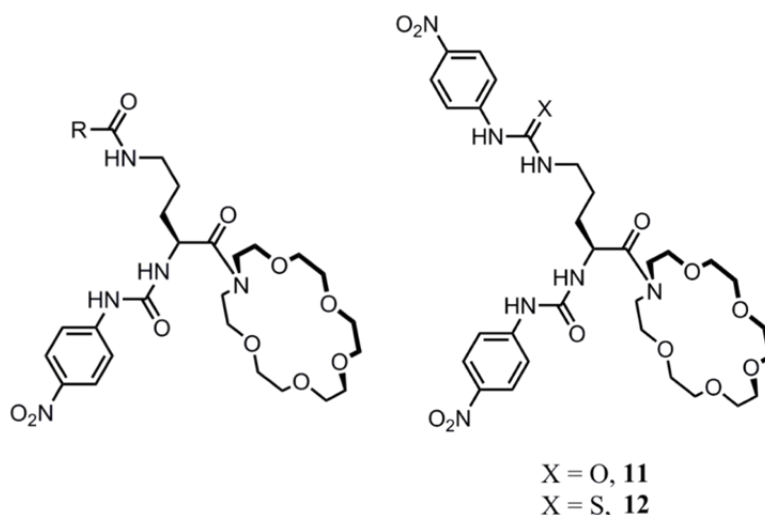


FIGURE 8 Ditopic *L*-ornithine - aza-crown ether receptors prepared by Romanski and coworkers. These receptors have amides (on the left) and urea (**11**) and thiourea (**12**) groups as secondary anion binding groups.^{54,55,57}

A quinolone-substituted crown ether (**13**, Figure 9) was prepared by Albrecht and coworkers to study its ion pair recognition characteristics and to demonstrate its use in solubilizing inorganic salts into CHCl_3 .⁵⁸ The receptor shows positive cooperativity towards halide anions in the presence of potassium cations, and the cooperativity is dependent on the solvent polarity (DMSO vs. 8:1:1 $\text{CD}_3\text{CN}/\text{CDCl}_3/\text{DMSO}$). The ion pair binding motif was suggested to happen via the formation of separated ion pairs supported by the rigidity of the receptor scaffold and the fairly low cooperativity factors obtained with the receptor. However, the receptor was used as a solubilizing agent for inorganic chloride salts, and it was shown that it can be recycled for repetitive use by extracting the solubilized ion pairs into aqueous media.⁵⁸

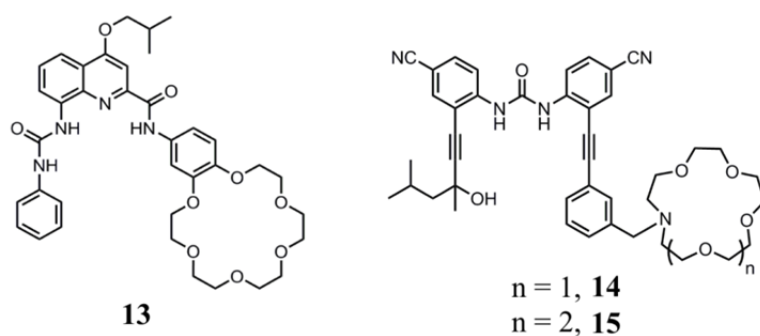


FIGURE 9 Receptors presented by Albrecht and coworkers⁵⁸ (**13**) for salt solubilization, and by Jeong and coworkers⁵⁹ (**14**, **15**) for transmembrane salt transport.

Jeong and coworkers presented the use of receptors **14** and **15** (Figure 9) as M^+/Cl^- symporters through a POPC (1-palmitoyl-2-oleoyl-*sn*-glycero-3-phosphocholine) membrane.⁵⁹ The receptors show cation dependent positive cooperativity towards chloride binding. Receptor **14**, having a 15-aza-crown-5

unit with strong selectivity for Na^+ , has the highest affinity towards chloride in the presence of sodium. Similar behaviour was observed for receptor **15** (with 18-aza-crown-6) in the presence of potassium.⁵⁹ The crystal structure **14**·NaCl shows a contact ion pair formation with the ion pair completely embedded within the organic framework. Selectivity towards the ion pairs was maintained also in the ion pair transport through lipid membranes, in which **14** showed good transport efficiency with NaCl and **15** showed excellent efficiency and selectivity with KCl. Efficient ion pair transport can thus be carefully tuned by selecting the most suitable cation and anion recognition functionalities.⁵⁹

1.3.2 Ditopic Receptors Based on Uranyl Salophens

Since the discovery of uranyl dication ($[\text{UO}_2]^{2+}$) as an efficient functionality towards neutral⁶⁰⁻⁶² and anionic species^{63,64}, it has been utilized in various receptor systems.⁶⁵ In oxidation state +VI the oxygens of the uranyl cation are thermodynamically and kinetically stable, forming complexes with salen and salophen ligands ($\text{N}_2\text{O}_2^{2-}$) in a pentagonal bipyramidal coordination with uranyl oxygens in apical positions.⁶⁵ This leaves the fifth equatorial site of the uranyl group free for further complexation. Due to the hard Lewis acidic nature of the uranyl cation, it can coordinate strongly to anions and solvent molecules.⁶⁵ As an example of its strong anion binding nature, uranyl salophens have been utilized in anion receptors effective also in water by modifying the salophen scaffold with water-soluble sugar groups^{66,67} or embedding the receptors in micellar structures.^{68,69} These examples demonstrate also fluoride recognition in water, a very challenging task due to the small size of the anion and its high solvation energy.^{70,71} Although uranyl salens and salophens have been shown to be efficient anion receptors, their use in ditopic receptor systems is fairly unexplored. Some examples of ditopic uranyl salophens are presented in the following chapter.

The pioneering work of Reinhoudt and his coworkers with uranyl receptors also included some of the first examples of ditopic receptors.⁷²⁻⁷⁴ In Figure 10 are shown examples of ditopic uranyl salen receptors with crown ethers for simultaneous ion pair recognition. Receptor **16** was studied for complexation of KH_2PO_4 . The anion and cation binding studies were performed with ^1H NMR, cyclic voltammetry, and mass spectrometry. Especially the gas-phase studies revealed complexation of the ion pair in addition to the separate complexes of **16** with K^+ and H_2PO_4^- .⁷² Another ditopic receptor was obtained by combining a uranyl salophen unit with a lower rim -functionalized calix[4]arene scaffold, which was shown to bind sodium and dihydrogen phosphate as separate ions (with mass spectrometry).⁷³ Developing their ditopic receptors further, Reinhoudt and coworkers created a calix[4]arene crown-6 based receptor with uranyl salophen as an anion recognition site (**17**, Figure 10).⁷⁴ Receptor **17** was studied as a carrier molecule for CsCl and CsNO_3 through a supported liquid membrane, showing better efficiency in CsCl transport. The authors concluded that for efficient carrier of hydrophilic salts such as CsCl there should be a binding site for both the cation and the anion.⁷⁴

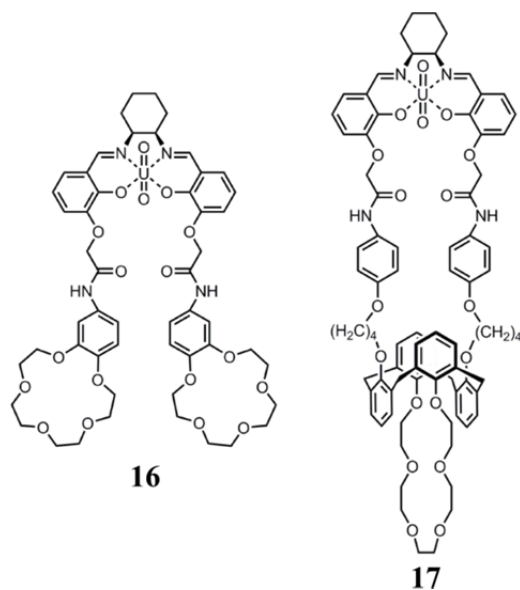


FIGURE 10 Examples of ditopic uranyl salophen receptors prepared by Reinhoudt and coworkers.^{72,74}

Dalla Cort and coworkers presented the use of uranyl salophens with aromatic side arms (Figure 11) as efficient receptors for quaternary ammonium and iminium halides⁷⁵⁻⁷⁷ and alkali halides.^{78, 79} This recognition is based on cation- π and C-H \cdots π interactions between the cation and the aromatic side arms of the receptors.⁷⁵⁻⁷⁹ Solution studies with receptors **19** and **20** towards TMACl and TBACl showed significantly stronger association of both salts with the receptors compared to control receptor **18** without the side arms. Binding affinities determined with ¹H NMR titrations in chloroform showed nearly 14 times stronger association of TMACl with **19** compared to **18**, and with **20** the affinity was 28 times stronger. The affinity of larger TBACl with **19** and **20** was about four times stronger compared to **18**.⁷⁵

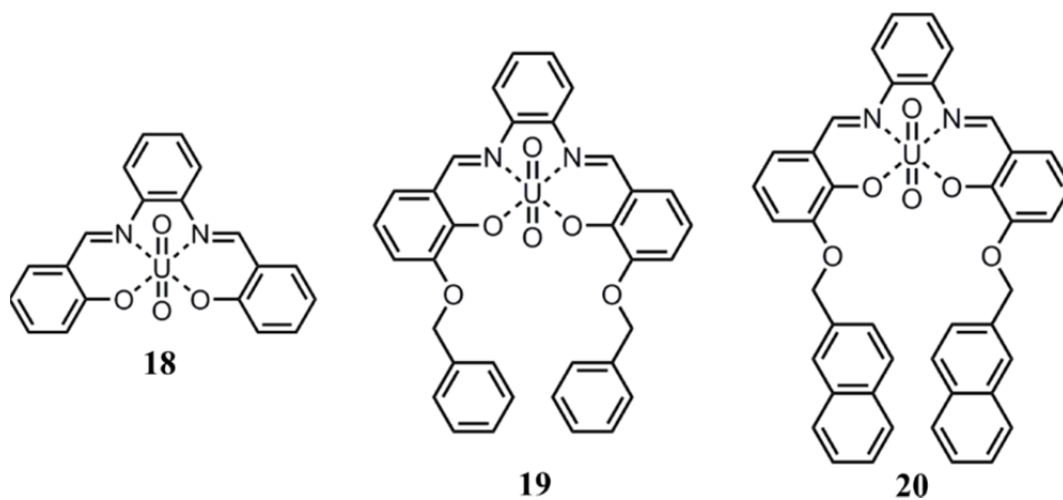


FIGURE 11 Some of the receptors studied by Dalla Cort and coworkers for recognition of alkali and ammonium halides.⁷⁵⁻⁷⁹

Crystal structures **19**·TMACl and **19**·TBACl revealed that the cation forms a contact ion pair with the anion through weak C-H \cdots Cl $^-$ hydrogen bonds (Figure 12).⁷⁵ The high affinity of ammonium salts towards **19** and **20** was explainable by the formation of C-H \cdots O hydrogen bonds to the oxygen in the salophen ligand, and cation- π and C-H \cdots π interactions between the cations and the receptor side arms.⁷⁵

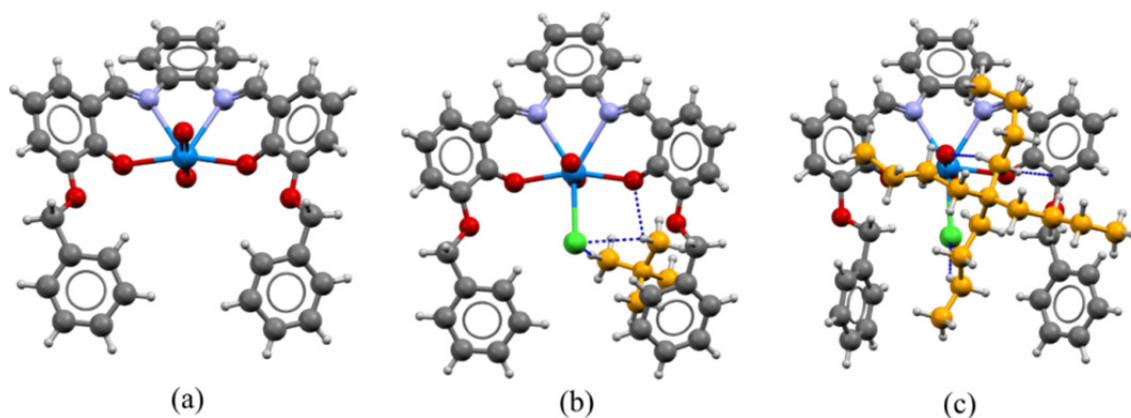


FIGURE 12 Crystal structure of **19** (modified from structure ELUFUM), **19**·TMACl (CSD ELUFUM), **19**·TBACl (ELUGAT).⁷⁵ Weak interactions are presented as dashed lines.

Further studies of **19** and **20** with different ammonium and iminium salts gave evidence that $\pi\cdots\pi$ interactions can also have a role in the ion pair recognition with these receptors.⁷⁶ The solution studies using aromatic guests revealed a stronger affinity towards **20** compared to **19** due to additional $\pi\cdots\pi$ interactions with naphthylene side arms of **20** and the aromatic cations. These interactions were observed also in the solid-state. Another interesting phenomenon with receptors **19** and **20** is the formation of complex supramolecular solid-state aggregates with TMACl.⁷⁵⁻⁷⁷ For example, crystal structure **20**·TMACl (Figure 13a) consists of 4:4 (receptor : ion pair) spherical assemblies in which the receptors enclose four TMACl ion pairs. These aggregates are formed through the various weak interactions described above.⁷⁵⁻⁷⁷

In addition to ammonium and iminium halides, also alkali halide binding was achieved with receptor **19**.⁷⁸ Figure 13b presents the crystal structure of **19**·CsF, which consists of a 2:2 complex of the uranyl salophen receptors with the ion pairs. As expected, the fluoride anion is coordinated to the uranyl center forming a contact ion pair with both cations.⁷⁸ The cation is further coordinated with five receptor oxygens, and additional cation- π interactions are formed with the side arms of the receptors. Similar complexes were obtained also with KCl, RbCl, and CsCl. These aggregates were observed in the gas-phase with mass spectrometry, and the solution studies showed strong binding of Cs $^+$ with the [**19**·Cl] $^-$ complex in acetone, thus supporting the presence of cation $\cdots\pi$ interactions also in solution.⁷⁸

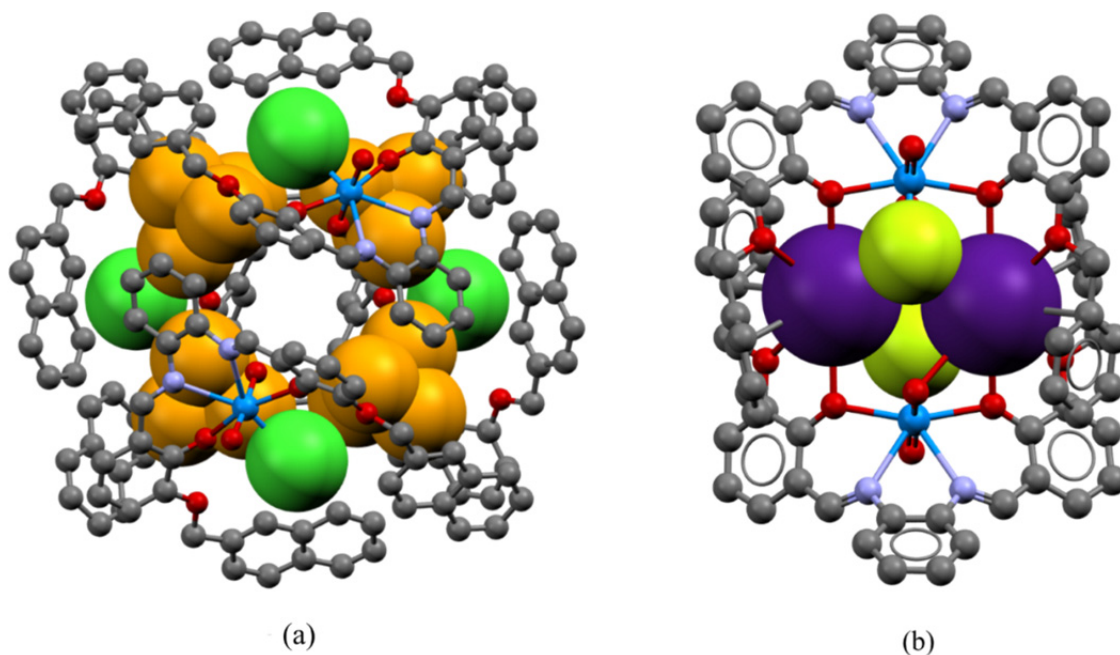


FIGURE 13 (a) Crystal structure of 4:4 supramolecular aggregate of **20** and TMACl (CSD code HEYXOZ).⁷⁶ TMA-cations are shown in orange and chlorides in green. Acetonitrile molecule residing in the middle of the aggregate is omitted. (b) Crystal structure of **19** and CsF (CSD code YALRAF).⁷⁸ Cesium is shown in purple and fluoride in light green.

Chiral ditopic uranyl salen compounds were also developed by Tomaselli and coworkers for enantioselective recognition of chiral ammonium salts of amino acids (Figure 14, receptor **21**)⁸⁰. In addition, receptors **22** and **23** with chiral cavities (Figure 14) were prepared for recognition of achiral and chiral ammonium salts.⁸¹ As in the work presented above, the recognition is based on various cation- π and C-H $\cdots\pi$ interactions between the receptor scaffold and the ammonium cations. These interactions have been proved by NMR methods to be responsible for the solution-state recognition of the ion pairs. The recognition of the amino acids by these receptors has shown that uranyl salens are efficient receptors also for carboxylate anions. The receptor **21** shows a very good enantioselectivity towards the enantiomers of phenylalanine (as TMA salt).⁸⁰ Receptors **22** and **23** have chiral cavities for binding differently sized ammonium guests. In all cases, receptor **23** showed stronger affinity towards the selected ion pairs, resulting from the larger number of weak interactions between the receptor and the cations.⁸¹ For example, binding affinity of **23** with TBACl in chloroform was around 120 times stronger compared to **22**. With smaller TMACl the binding affinity towards **23** was only twice as high as compared to **22**, once again demonstrating the importance of good size fit of the host and the guest for a strong complex to form. **23** was also shown to be able to discriminate some chiral ammonium iodides due to the matching chirality between the host and the guest.⁸¹

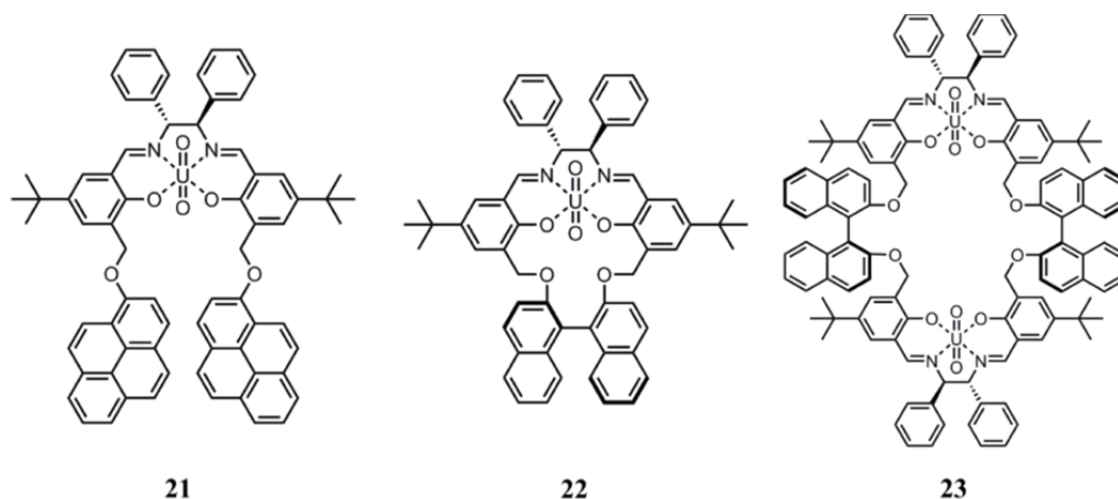


FIGURE 14 Chiral uranyl salen receptors prepared by Tomaselli and coworkers for recognition of chiral salts of amino acids (**21**),⁸⁰ and achiral and chiral ammonium salts (**22, 23**).⁸¹

1.4 Applications of Ion Pair Receptors

Some applications of the ditopic receptors have already been presented in the description of the crown ether and uranyl salophen based receptors. In the following chapter more examples of utilization of ditopic receptors are given, further illustrating the multiple purposes these receptors can have. In addition, different receptor scaffolds are presented to shed light on the multitude of various ditopic receptor systems.

1.4.1 Solubilization

One of the important applications of ditopic receptors is the solubilization of otherwise insoluble salts in organic solvents, which can have importance in synthetic procedures.³ Many of the receptors presented in previous chapters have already been shown to solubilize guests in organic media. For example the crown ether – Lewis base receptor synthesized by Reetz and coworkers (**1**, Figure 2, page 14) dissolved KF in dichloromethane³², and the quinolone-substituted crown ether by Albrecht and coworkers (**13**, Figure 9, page 20) was shown to solubilize salts in chloroform, which then could be extracted into water for repetitive use of the receptor in solubilization.⁵⁸ Reinhoudt and coworkers have shown that a calix[4]arene based receptor (Figure 15, **24**) is able to dissolve sodium halides, and to some extent potassium halides, in chloroform.⁸² The receptor has separate cation and anion binding sites on different sides of the calixarene scaffold. The receptor does not interact with anions without cations due to the internal hydrogen bonding between the urea groups in the upper rim.⁸² However, upon sodium complexation with the ester groups in the lower rim a conformational change takes place in the calixarene framework prevent-

ing the intramolecular hydrogen bonding and enabling the anion to interact with the urea groups. Because of the sodium selectivity of the ethyl ester groups in the lower rim, receptor **24** is capable of dissolving sodium salts selectively in chloroform. Due to the size mismatch of cesium with the cation binding site, no solubilization of cesium salts was observed.⁸²

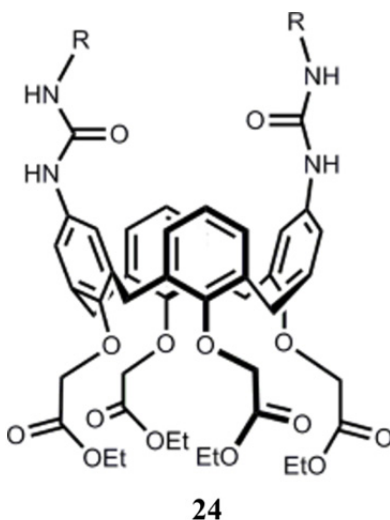


FIGURE 15 Ditopic calix[4]arene based receptor by Reinhoudt and coworkers capable of solubilizing selectively sodium halides in chloroform due to the allosteric effect upon cation complexation.⁸²

Another example of selective guest solubilization was presented by Ghosh and coworkers.⁸³ They prepared a simple dibenzo-18-crown-6 receptor (Figure 16, **25**), which was shown to solubilize solid KCl, KBr, KI, and KNO₃ (but not KF, KAcO, KHSO₄, KH₂PO₄ or any sodium salts) separately into acetonitrile. Interestingly, **25** is able to solubilize KBr selectively from mixtures containing solid KCl, KBr, and KNO₃. Receptor **25** was also shown to interact with bromide most strongly, both without potassium ($K = 851 \text{ M}^{-1}$) and in the presence of potassium ($K = 2455 \text{ M}^{-1}$) in acetonitrile, supporting the selectivity of the solubilization experiments. The bromide selectivity was associated with the suitable size and the charge density of the anion compared to the cavity created by the receptor, and the overall electronic properties of the receptor created by the pentafluorophenyl substituent.⁸³

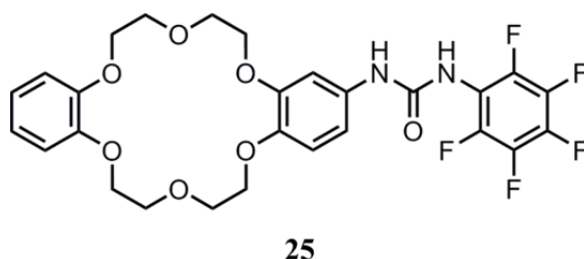


FIGURE 16 Dibenzo-18-crown-6 based urea receptor by Ghosh and coworkers that can selectively solubilize KBr into organic media.⁸³

1.4.2 Extraction

Selective extraction of cations or anions can have important applications, for example, in industrial and environmental processes, where valuable or hazardous ions need to be selectively extracted from waste streams.²³ This has been demonstrated by Beer and coworkers, who developed a tren-based (tris(2-aminoethyl)amine) amide receptor **26** (Figure 17) with benzo-15-crown-5 substituents. The receptor was studied as an extracting agent for the perrhenate anion (ReO_4^-), which is structurally similar to pertechnetate (TcO_4^-), a toxic radioactive anion present in nuclear waste waters.⁸⁴ The affinity of the receptor towards chloride, iodide (same size and charge density as TcO_4^-), and perrhenate was measured to be moderate in chloroform. Not surprisingly, **26** was found to complex sodium cations, and in the presence of 1 equiv of Na^+ the resulting positively charged complex had stronger affinity towards all the studied anions, with the largest increase in binding affinity being with ReO_4^- (20-fold). In addition, receptor **26** was found to effectively extract TcO_4^- from aqueous media resembling nuclear waste water streams, proving the extraction efficiency of ditopic system compared to control receptors with only anion binding sites or simple 15-crown-5 for ion extraction.⁸⁴

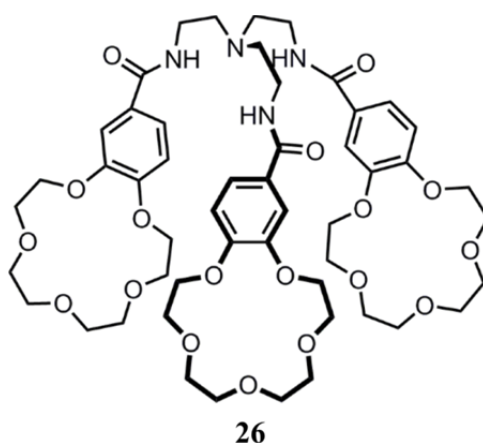


FIGURE 17 Tren-based crown ether receptor for extraction of pertechnetate from aqueous solutions presented by Beer and coworkers.⁸⁴

Extraction can also be achieved by utilizing polymeric structures, as discussed in connection with Romanski's work⁵⁴ (Figure 8, page 19). In addition to having the ditopic receptor in the polymeric matrix, the binding units can be separately attached to the polymer. Sessler and coworkers created poly(methyl methacrylate) polymers decorated with calix[4]pyrroles and benzo-15-crown-5 subunits for anion and cation recognition, respectively, for effective extraction of KF and KCl from aqueous solutions (Figure 18).⁸⁵ Due to high hydration energies of fluoride and chloride, extraction of these anions can be challenging from aqueous media. The cooperative binding of the ion pairs by the matrix is proved by the better extraction efficiency of the ion pairs than expected from the number of calixpyrrole and crown ether subunits within the polymeric ma-

trix alone.⁸⁵ This type of material could be used in medical applications, for example in treating hyperkalemia, exemplifying another important field where selective extraction of ions or ion pairs is desired.^{23,85}

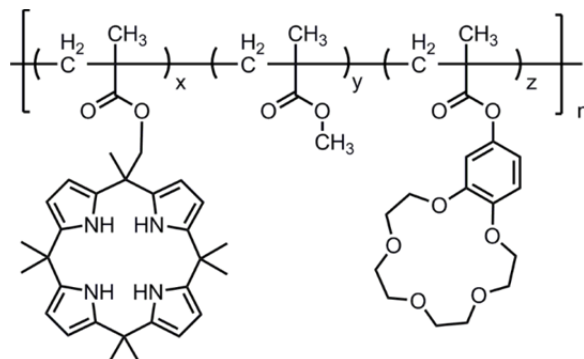


FIGURE 18 Polymer with calix[4]pyrrole and benzo-15-crown-5 subunits capable of extracting KF and KCl from aqueous solution, as shown by Sessler and coworkers.⁸⁵

1.4.3 Membrane Transport

Ion transport through membranes has become an increasingly investigated topic in recent years, and many simple anion receptors have been shown to have promise in membrane transport.^{17,86,87} Channelopathies is a family of diseases in which dysfunction of anion transport across biological membranes causes the symptoms. The best known disease in this family is cystic fibrosis, which results from a disrupted function or lack of CFTR transmembrane ion channel protein, affecting especially chloride transport. It is the most common lethal genetic disease in the white population,⁸⁸ and therefore active synthetic transmembrane ion carriers could have use in clinical applications. In addition, small molecule ion transporters have been shown to induce apoptosis by increasing chloride and sodium concentrations in cells.⁸⁹

Ditopic receptors are interesting for membrane transport applications because they can be utilized as symport carriers for ion pairs. Already the first developed ditopic receptors were studied as transmembrane carriers. For example, the uranyl salophen strapped onto calix[4]arene crown-6 scaffold presented by Reinhoudt and coworkers in 1995 (**17**, Figure 10) was studied as an ion pair transporter,⁷⁴ and the macrobicyclic receptor by Smith and coworkers (**5**, Figure 4) was shown to effectively transport alkali halides through membranes.^{39,40}

Simple calix[4]pyrroles (Figure 19) have been shown to act as efficient anion receptors.^{90,91} In addition, they have been shown to bind ion pairs^{24,92,93} and act as efficient transmembrane carriers.^{94,95} The ion pair recognition of calix[4]pyrroles takes place on the opposite sides of the receptor scaffold. Upon coordination of the anion with the pyrrole hydrogens, the receptor scaffold takes a cone-like conformation. This creates an electron-rich cup that can bind cations through cation- π interactions. Especially a cesium cation has a good

size-fit with the binding site.⁹² Gale and coworkers have presented the use of a simple octamethylcalix[4]pyrrole (**27**, Figure 19) as an efficient transmembrane carrier selective to CsCl over NaCl, KCl, or RbCl.⁹⁴ The ion pair binding motif of the octamethylcalix[4]pyrrole with CsCl had been presented before, supporting the selectivity observed in the membrane transport (Figure 19).⁹²

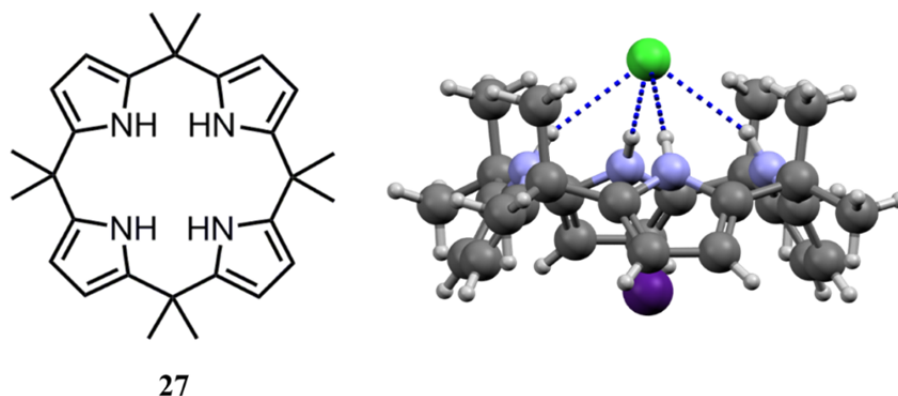


FIGURE 19 Simple octamethylcalix[4]pyrrole **27** has been studied as anion and ditopic receptor, and as a transmembrane carrier.^{90,92,94} Crystal structure **27**·CsCl (CSD code LAMTUP).⁹²

Based upon these preliminary observations, Sessler and coworkers have developed more complex and selective calix[4]pyrrole based receptors.²⁴ A large number of publications present the synthesis of different types of crown-strapped calix[4]pyrroles and their use as ion pair receptors.⁹⁶⁻¹⁰⁴ As an example, oligoether strapped calix[4]pyrrole receptor **28** by Lee, Gale, Sessler and coworkers (Figure 20) has been shown to have an interesting ion-dependent ditopic behavior.¹⁰⁵ The receptor **28** has strong affinity towards fluoride and chloride anions in acetonitrile. The pre-formed [**28**·F]⁻ adduct forms a stable ion pair complex with Cs⁺ within the receptor scaffold. However, addition of Li⁺ and Na⁺ to the receptor-fluoride complex removes the anion from the receptor.¹⁰⁵ The chloride adduct of **28** on the other hand behaves differently as stable ion pair complexes are formed with Li⁺ and Cs⁺ with different binding motifs, and a partial decomplexation of the chloride is observed upon Na⁺ and K⁺ addition. The receptor was also shown to act as a transmembrane ion pair carrier for many alkali metal chlorides working through symport and antiport mechanisms, with highest efficiency being observed with CsCl.¹⁰⁵

Another example of functionalized calix[4]pyrroles is receptor **29** by Sessler and coworkers (Figure 20), which has two binding sites for cations, i.e. crown ether and the ether linkages connecting the calixpyrrole and calixarene units.¹⁰⁶ The receptor shows complicated KF and CsF binding behavior, having different types of cation and anion recognition motifs dependent on the concentration of the guests. In addition, K⁺ can substitute Cs⁺ from the receptor through cation metathesis. Because of the high selectivity toward KF, receptor **29** was also used to extract KF from an aqueous solution into nitrobenzene.¹⁰⁶

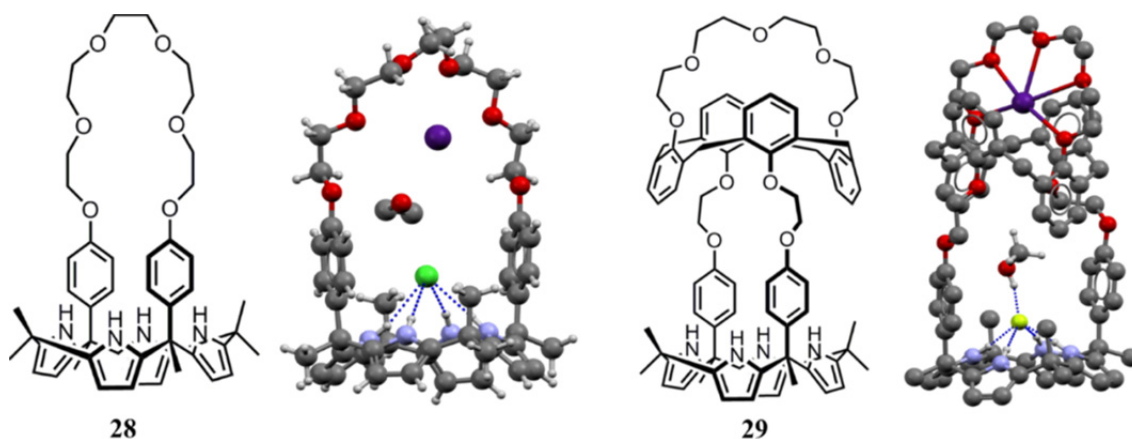


FIGURE 20 Oligoether strapped calix[4]pyrrole by Lee, Gale, Sessler and coworkers (28) and crystal structure 28·CsCl (CSD code DARSEW),¹⁰⁵ a calix[4]pyrrole receptor with calix[4]arene crown-5 by Sessler and coworkers (29) and crystal structure 29·CsF (CSD code GEJCOP).¹⁰⁶

Matile and coworkers have shown a rare example of ditopic transmembrane carriers that utilize anion- π interactions and halogen bonding.¹⁰⁷ For a small molecule to act as an efficient transmembrane carrier it should not bind its guest too strongly. Thus, it was postulated by the authors that receptors working with weak interactions that are difficult to detect otherwise could be utilized to create efficient transmembrane carriers. Receptors 30 and 31 (Figure 21) are based on a calix[4]arene scaffold having a selective binding site for a TMA cation on the upper rim of the molecular scaffold. Receptor 30 constitutes of strongly electron-deficient aromatic rings on the lower rim due to the electron-withdrawing fluorine substituents, and receptor 31 has iodine substituents for halogen bonding interactions.¹⁰⁷

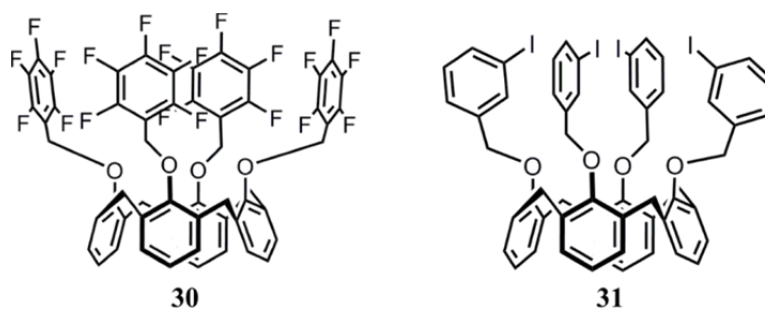


FIGURE 21 Calix[4]arene based ditopic transmembrane carriers that work through anion- π interactions (30) and halogen bonding (31) by Matile and coworkers.¹⁰⁷

Surprisingly, receptor 30 was found to be the most efficient carrier for chloride/TMA and hydroxide/TMA ion pairs from a group of six receptors that are able to form anion $\cdots \pi$ interactions, halogen bonds or hydrogen bonds with the anion. Interestingly, if one of the fluorine substituents in each aromatic ring of receptor 30 was substituted with an iodine atom, the transport activity diminished.¹⁰⁷ This molecule (not shown) forms the strongest complex with the

chloride anion through halogen bonding interactions, which in turn reduces the transport efficiency. The transport activity is regained if the remaining fluorine substituents are changed to hydrogens (receptor **31**), giving a receptor that works through weaker halogen bonding interactions than its perfluorinated analogue. These receptors were selective for the TMA cation, and its presence was necessary for the membrane transport to occur. Although the ion transport activity of these receptors was modest, this study has shown that even very weak interactions that are difficult to detect can be utilized to create transmembrane carriers.¹⁰⁷

1.4.4 Sensing

Sensing of environmentally or biologically relevant ion pairs is an important although still fairly unexplored application of ditopic receptors.²³ For sensing purposes the receptor needs to have a suitable electrochemical or optical sensor within the receptor scaffold. In Figure 22 are presented examples of ditopic receptors with two different sensor units. Receptor **32** by Tucker and coworkers has a ferrocene unit for detecting the ion pair binding.¹⁰⁸ In fact, receptor **32** acts as a simple ON-OFF switch where fluoride binding in acetonitrile through hydrogen bonding turns the receptor solution to yellow. An addition of potassium cations into the $[32 \cdot F]^-$ complex turns the solution clear.¹⁰⁸ This is proposed to result from the weakening of the fluoride interaction with the urea group upon potassium coordination within the crown ether cavity, thus causing the colour change. Ferrocenes have been used in many ditopic receptors as sensor units, and their use in sensing ion pair binding has been recently reviewed by Molina and coworkers.¹⁰⁹

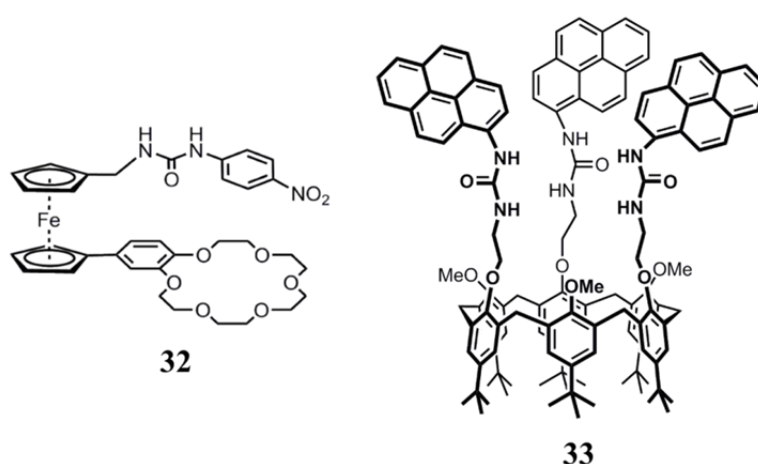


FIGURE 22 Ditopic receptors by Tucker and coworkers (**32**)¹⁰⁸ and Jabin and coworkers (**33**)¹¹⁰ developed for studying ion pair binding through spectroscopic methods.

Pyrenes can be used as photochemical sensing units, as exemplified by calix[6]arene based urea receptor **33** bearing three pyrene units prepared by Jabin and coworkers.¹¹⁰ This receptor has been used to sense anion and ion pair bind-

ing in organic media. The binding could be monitored through UV-Vis and fluorescence spectroscopy because of the photophysical features of the pyrene moiety, and the changes that the guest encapsulation induces in the interactions of the pyrene units. In DMSO, receptor **33** was shown to bind selectively sulfate anions. In CDCl_3 , however, the receptor is capable of forming complexes with ammonium cations only in the presence of sulfate anions.¹¹⁰

1.5 Multitopic Receptor Systems

The receptors presented previously have been ditopic by nature. Even though the field of ion pair binding is fairly new, some reports of more complex multitopic receptors have already been presented that will be discussed in the following chapter. These receptors utilize many structural motifs already discussed, but multitopic receptors are generally structurally larger and their behaviour is more complex.^{27,111-115}

The first supramolecular ion triplet complex of alkaline earth metal halide with a macrocyclic receptor was presented by Luning and coworkers.¹¹¹ The tritopic macrocyclic receptor **34** (Figure 23) consists of two anion binding sites (amides) and a cation binding site (ether oxygens). The receptor was shown to solubilize selectively LiCl in a 95% CDCl_3 /5% DMSO solution but not NaCl or KCl , and similar selectivity was observed with CaCl_2 compared to MgCl_2 and BaCl_2 . The strong complexation of these ion pairs with **34** was observed also in the gas-phase by mass spectrometry, and the solution studies performed by NMR showed considerable conformational changes in the receptor upon guest complexation. It was thus postulated that receptor **34** can bind CaCl_2 as a contact ion triplet in solution and in the gas-phase.¹¹¹

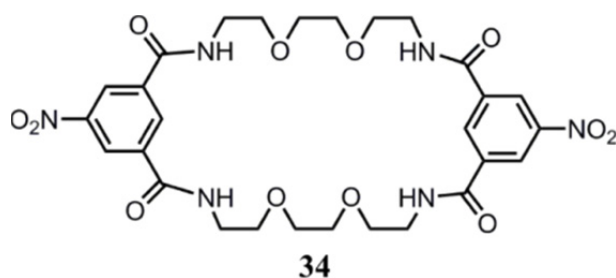


FIGURE 23 Tritopic macrocyclic receptor prepared by Luning and coworkers.¹¹¹

Thordarsson and coworkers developed further the previous receptor scaffold to create a receptor with a larger macrocycle size (Figure 24, **35**).²⁷ Receptor **35** was shown to act as a tetratopic receptor through extremely extensive NMR titration studies, proving the allosteric cooperativity of the receptor in ion pair binding. Without cations present the receptor binds anions (chloride, acetate) very weakly in a polar 9:1 CDCl_3 / CH_3OH solvent mixture. However, in the presence of Ca^{2+} cations the receptor goes through a conformational change,

enabling chloride binding by allosteric positive cooperativity.²⁷ This observation was also supported by the crystal structures of receptor **35** and its $(\text{Ca}(\text{ClO}_4)_2)_2$ complex. In the solid-state the receptor has closed conformation due to intramolecular hydrogen bonding (Figure 24). However, in the presence of Ca^{2+} cations, the macrocycle undergoes a conformational change forming two crown ether-like cavities for Ca^{2+} complexation, “freeing” the amide protons for anion binding.²⁷

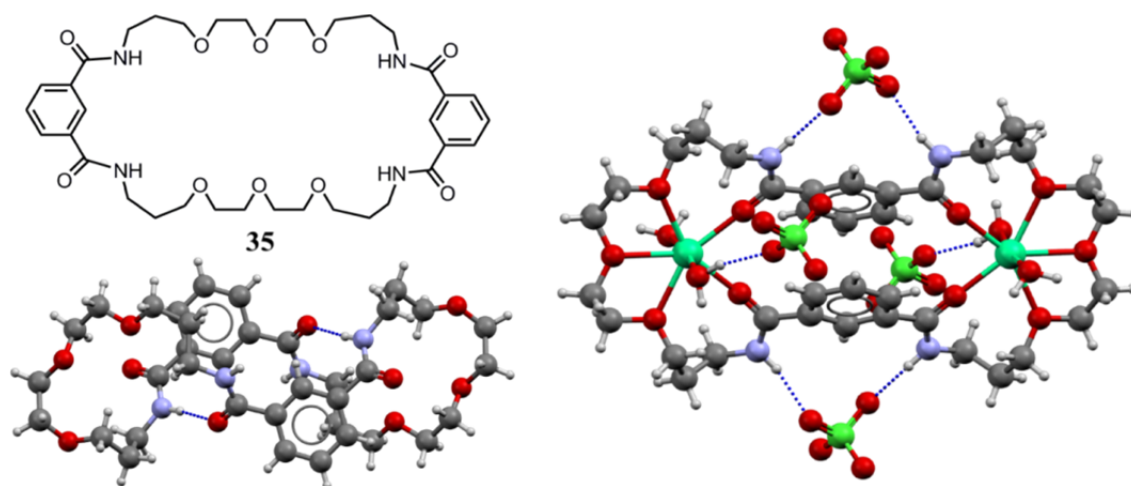


FIGURE 24 Tetratopic receptor presented by Thordarson and coworkers.²⁷ Crystal structures of the receptor (CSD code HOKJUO) and its $\text{Ca}(\text{ClO}_4)_2$ complex (CSD code HOKJOI) is shown. Hydrogen bonds are shown as dashed lines.

Nabeshima and coworkers prepared a calix[4]arene -based multiresponsive host molecule for complexing hard and soft cations and anions (Figure 25, **36**).¹¹² Hard cations are complexed with ester and polyether moieties close to the calix[4]arene framework, soft cations with bipyridine groups on the other end of the receptor and anions with the urea-groups in the middle of the receptor scaffold. NMR and MS studies showed that the receptor **36** is capable of binding Na^+ and Ag^+ both simultaneously and in a stepwise manner, resulting in a very stable $[\mathbf{36} \cdot \text{Ag}^+ \cdot \text{Na}^+]$ complex.¹¹² Receptor **36** alone has a fairly low affinity towards NO_3^- and CF_3SO_3^- anions in 9:1 $\text{CDCl}_3/\text{CD}_3\text{CN}$ ($K = 76 \text{ M}^{-1}$ and $K = 25 \text{ M}^{-1}$, respectively), but both $[\mathbf{36} \cdot \text{Ag}]^+$ and $[\mathbf{36} \cdot \text{Na}]^+$ complexes show strong positive cooperativity towards these anions. For example, towards NO_3^- , $[\mathbf{36} \cdot \text{Ag}]^+$ and $[\mathbf{36} \cdot \text{Na}]^+$ complexes have 30 and 90 times stronger affinity, respectively. However, $[\mathbf{36} \cdot \text{Ag}^+ \cdot \text{Na}^+]$ complex shows remarkable 1500 and 2000 times stronger affinity towards NO_3^- and CF_3SO_3^- , respectively, compared to **36** alone. The enhanced anion binding is thought to result from electrostatic interactions and conformational changes upon cation complexation that can be regulated in a stepwise manner.¹¹²

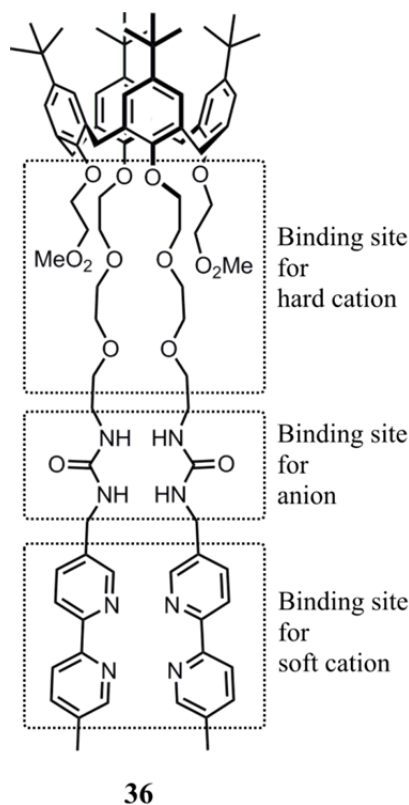


FIGURE 25 Multiresponsive calix[4]arene based receptor by Nabeshima and coworkers.¹¹²

Ballester and coworkers prepared a calix[4]pyrrole based cylindrical homoditopic receptor **37** (Figure 26) for alkylammonium chloride and cyanate ion pair recognition.¹¹³ The ion pair dimers (or ion quartets) interact with the receptor as cascade complexes, thus representing example of cascade receptors (Figure 1, page 12). The structure of the complex $[37 \cdot \text{TBA} \cdot \text{Cl}_2]$ was verified by single crystal X-ray crystallography (Figure 26), and similar solid-state complexes were also obtained with cyanate anions, or as mixed complexes with cyanate and chloride.¹¹³ The structures can be described as having contact and host-separated ion pairs within the same receptor scaffold. The solution studies showed that the complexes are thermodynamically and kinetically highly stable. In addition, the cooperativity of the cascade complex formation is highly dependent on the cation, and thus the cooperativity can be tuned by cation selection.¹¹³

The last example of multitopic receptors is by Jabin and coworkers, also a homoditopic receptor based on calix[6]arene scaffold (**38**, Figure 27).^{114,115} The receptor has been shown to complex linear ammonium cations with doubly charged anions as ion triplets in polar solvents in cooperative manner. In addition, receptor **38** was also shown to solubilize various ammonium sulfate salts in CDCl_3 . The crystal structure of the $[38 \cdot (\text{EtNH}_3^+)_2 \cdot \text{SO}_4^{2-}]$ complex has proven the cascade complex formation also in the solid-state. The complex is stabilized by multiple hydrogen bonds between the sulfate anion and the urea groups. In addition, hydrogen bonds are formed between the ammonium hydrogens and the oxygen atoms of the anion and the ether groups of the receptor.¹¹⁵

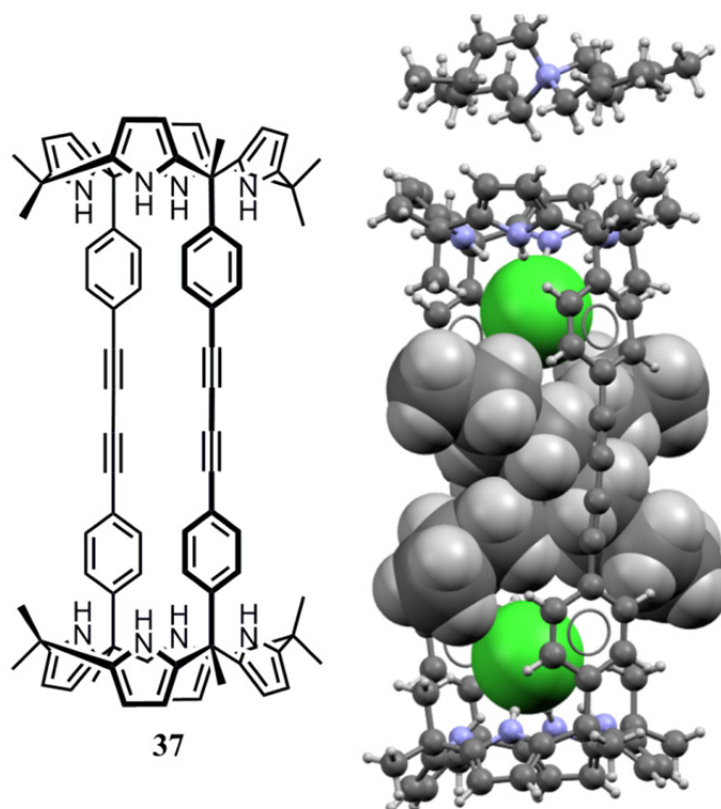


FIGURE 26 Homoditopic calix[4]pyrrole receptor for ion pair dimers prepared by Ballester and coworkers¹¹³ and crystal structure of $[37 \cdot (\text{TBACl})_2]$ (CSD code QEZJEM). One ion pair is complexed as a contact ion pair and the second as receptor-separated ion pair.

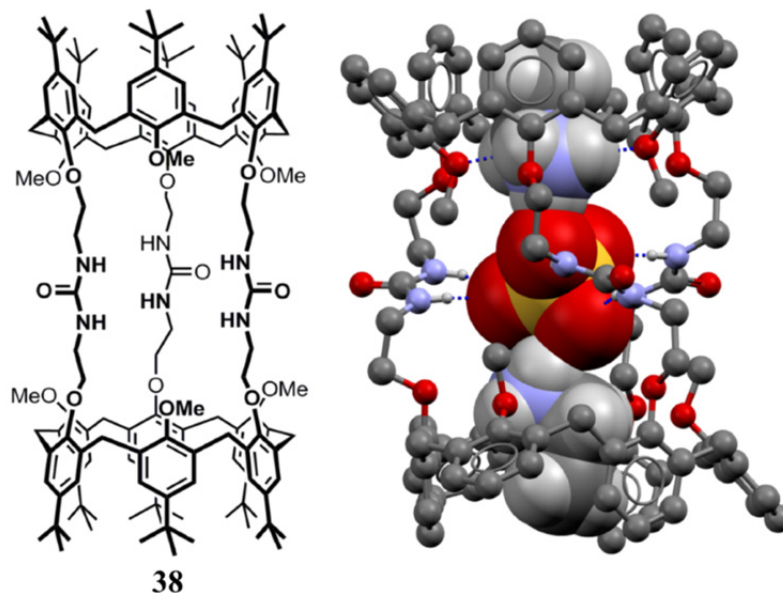


FIGURE 27 Calix[6]arene based cascade receptor by Jabin and coworkers^{114,115} and crystal structure of the complex $[38 \cdot (\text{EtNH}_3^+)_2 \cdot \text{SO}_4^{2-}]$ (CSD code CEYZUD).¹¹⁵ Guests are shown as spacefill models and hydrogen bonding interactions as dashed lines. Tert-butyl groups in the calix[6]arene scaffold are omitted for clarity.

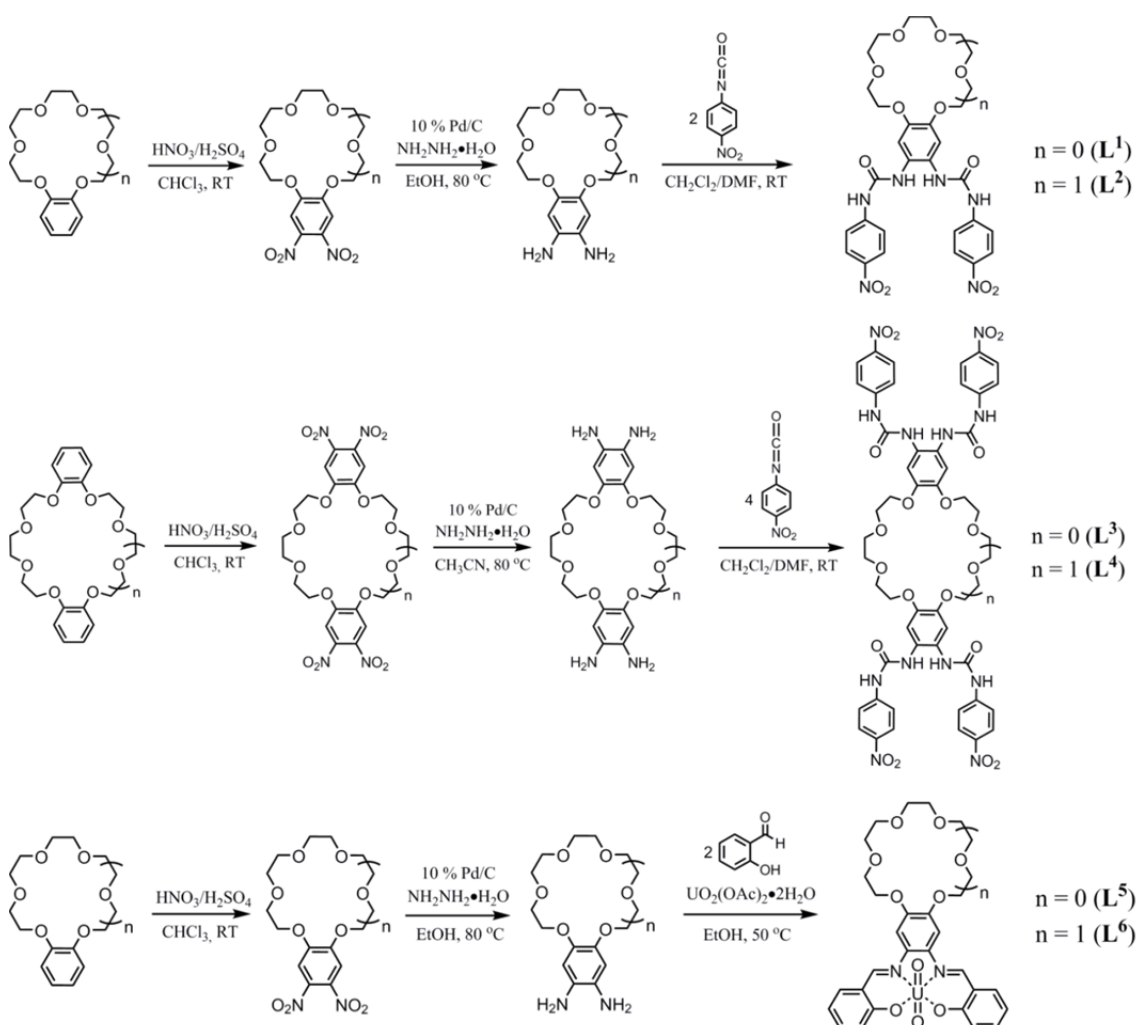
2 RESULTS AND DISCUSSION

2.1 Aim of the Work

The aim of this work was to synthesize a group of ditopic crown ether based bis-urea and salophen receptors and to study their utilization in ion pair recognition in the solid-state with single crystal X-ray crystallography, in solution with nuclear magnetic resonance spectroscopy, and in the gas-phase with mass spectrometry. The primary focuses have been to develop a general methodology for the receptor synthesis, to obtain comprehensive view of the ion pair complexation characteristics of these receptors in different phases, and to relate the functionality of the receptors with the structural information. The results obtained from this work can be used to create stronger and more selective ditopic receptors also effective in more polar media and, as an ultimate goal, to create efficient receptors for ion pair recognition in water.

2.2 Synthesis of Receptors L¹-L⁶I-IV

All the receptors studied were synthesized via three-step reactions modified from literature methods (Scheme 1).¹¹⁶ Starting materials were commercially available benzo-15-crown-5 (B15C5), benzo-18-crown-6 (B18C6), dibenzo-21-crown-7 (DB21C7), and dibenzo-24-crown-8 (DB24C8) compounds. These compounds were nitrated by a two-phase reaction using concentrated nitric acid and concentrated sulfuric acid mixture in chloroform. The nitrated product was obtained by concentrating the organic phase, which resulted in the precipitation of the product, or by direct precipitation of the product by diluting the reaction mixture with water. Generally the purity of the nitrated products was good, although the nitrated products were in some cases recrystallized from suitable solvents. The yields of the nitration reaction were generally good, being between 69 to 77 %. The products were characterized with ¹H, ¹³C, HMBC and HMQC NMR spectroscopy, electrospray ionization mass spectrometry (ESIMS), and single crystal X-ray crystallography.



SCHEME 1 The general synthetic routes and the structures of receptors L¹ - L⁶.

The nitrated products were reduced to di- and tetraamine compounds in anaerobic conditions under inert argon atmosphere and degassed solvents, using hydrazine monohydrate as reducing agent and palladium on activated charcoal (10%) as catalyst. Solvents were degassed prior to the use with simultaneous sonication and argon bubbling through the solvent because of the sensitive nature of the amine compounds towards oxygen. The diamino-15-crown-5 and diamino-18-crown-6 were synthesized in ethanol and the tetraamino-21-crown-7 and tetraamino-24-crown-8 were synthesized in acetonitrile. Generally the yields of reduction step were quantitative or near quantitative with good purity, and the vacuum dried amine compounds were used in the consecutive reactions without further purification because of the instability of the products.

Receptors **L**¹-**L**⁴ with bis-urea functionalities were synthesized by a simple condensation reaction between the di- and tetraamine compounds and 4-nitrophenyl isocyanate in dichloromethane (CH₂Cl₂) using a small amount of dimethylformamide (DMF) to solubilize the starting materials. The reactions were performed under argon atmosphere in degassed solvents. The products precipitated from the reaction mixture with good purity, but in some cases the products were recrystallized. The products were analyzed by ¹H, ¹³C, HMBC, and HMQC NMR spectroscopy, ESIMS, and single-crystal X-ray crystallography. The yields were from moderate to good, varying between 52 and 75%. The 4-nitrophenyl substituent was chosen because of the electron withdrawing nature of the nitro-group and the consequent increased acidity of the urea-protons, resulting in stronger hydrogen bond donation by the urea-group.¹¹⁷ In addition to this, nitrophenyl substituent acts as a chromophore, which can be helpful in studying the ion pair binding in solution by UV-Vis spectroscopy or by naked eye detection.^{118,119}

Crown ether salophen receptors **L**⁵ and **L**⁶ were synthesized by a Schiff-base condensation reaction between the diamine compounds and salicylaldehyde in degassed ethanol under argon atmosphere at 50 °C. In the next step uranyl acetate in ethanol was slowly added to the Schiff-base, resulting in an immediate color change from yellow to red, indicating complexation of the uranyl with the Schiff-base. Products were obtained straight from the reaction mixture as precipitates, or by concentrating the reaction mixture until the product started to precipitate from the solution. The yields of the receptors **L**⁵ and **L**⁶ were moderate (55 and 62 %, respectively). Products were analysed with the methods described before.

2.3 Solid-State Studies of L¹-L^{6 I-IV}

2.3.1 Solid-State Studies of Crown Ether bis-Urea Receptors L¹-L^{4 I-III}

A strong emphasis of this work is in the comprehensive solid-state studies of crown ether bis-urea receptors L¹-L⁴ with different alkali and ammonium halides and oxyanions by single-crystal X-ray crystallography. The obtained crystal structures revealed many general ion pair complexation characteristics of the receptors, and the results have given insight into the way the ion pair affects the solid-state complex formation. The X-ray quality crystals were obtained through numerous crystallization experiments using diffusion and evaporation methods with a large variety of different solvent compositions. The receptors have fairly low solubility in most of the tested organic solvents, possibly due to the strong intra- and intermolecular hydrogen bonding between the receptors themselves (as seen in the crystal structures of L¹ and L², Figure 28), limiting the choice of usable solvents. However, this can also be advantageous in crystallizing the ion pair complexes. In many cases the addition of the guest (dissolved in water or methanol) to the insoluble receptor resulted in enhanced solubility of the complex into the chosen solvent. This has made it possible to utilize also solvents for receptor - ion pair crystallizations that might not seem obvious due to the limited solubility of the receptors themselves. Noteworthy is also the preference of the receptors to crystallize with the ion pairs instead of forming simple solvate structures even in the presence of water or otherwise strongly competing hydrogen bonding solvents (methanol, DMSO, DMF). This further supports the strong affinity of the ion pairs towards the receptors.

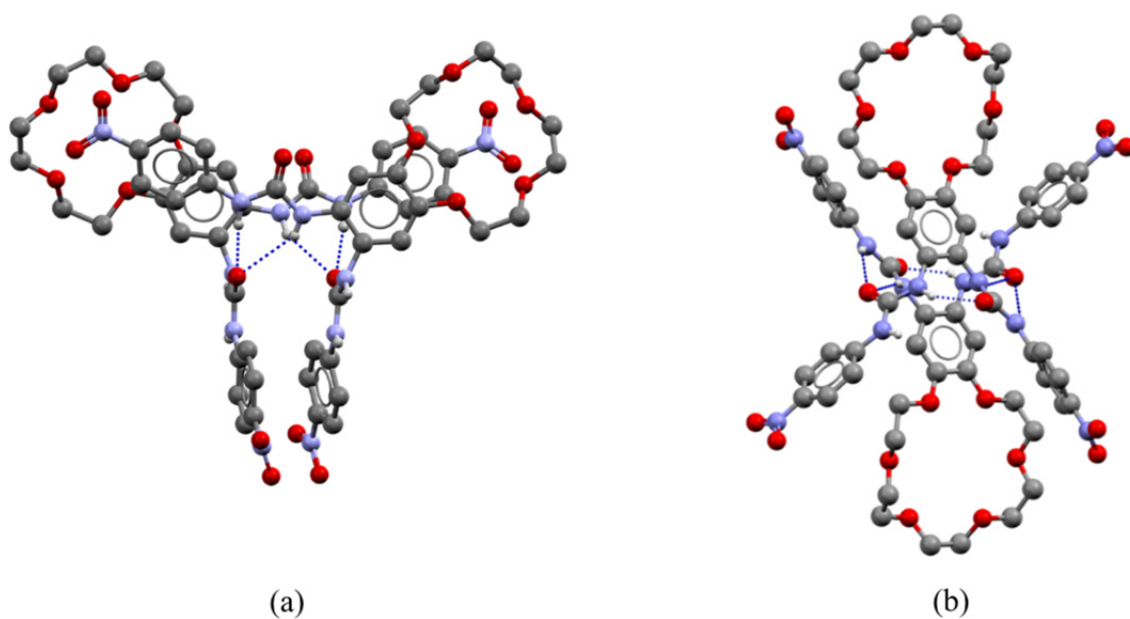


FIGURE 28 Solid-state structures of (a) L^{1 II} and (b) L^{2 I} showing inter- and intramolecular hydrogen bonding interactions (dashed lines) with the receptors. Solvent molecules and non-urea hydrogens have been omitted from the figure for clarity.

Table 2 contains all the crystal structures presented in the publications I-III. The comprehensive solid-state studies with L¹-L⁴ have revealed general features of the ion pair complexation with the crown ether bis-urea receptors in the solid-state, discussed in more detail in the following chapters.

TABLE 2 The crystal structures obtained with receptors L¹-L⁴, their space groups (SG), and the presence of contact (C) or separate (S) ion pair in the structure.^{I-III}

L ¹	SG	C / S ion pair	L ²	SG	C / S ion pair	L ³	SG	C / S ion pair
-	<i>P2₁/n</i>	-	-	<i>P2₁/a</i>	-	Rb₂CO₃	<i>I2/a</i>	S
DMF	<i>P-1</i>	-	KF	<i>P2₁/c</i>	S			
DMSO	<i>P-1</i>	-	KCl	<i>P2₁/n</i>	S	L⁴		
NaCl	<i>P2₁/n</i>	C	KBr_1	<i>P2₁/n</i>	S	RbCl	<i>P2₁/n</i>	S
NaBr	<i>P-1</i>	S	KBr_2	<i>P2₁/c</i>	C	RbI	<i>P2₁/n</i>	S
NaI	<i>I2/a</i>	S	KI	<i>P2₁/c</i>	C	RbOAc	<i>P-1</i>	S
KF	<i>Fdd2</i>	S	KAcO	<i>C2/c</i>	S	CsCl	<i>P2₁/c</i>	S
KCl	<i>P-1</i>	S	K₂CO₃	<i>P2₁/n</i>	S	CsBr	<i>Pca2₁</i>	S
KBr	<i>P2₁/c</i>	S	K₂SO₄	<i>P-1</i>	S/C	CsCO₃CH₃	<i>P2₁/c</i>	S
KI	<i>P2₁/c</i>	S	RbCl	<i>P2₁/c</i>	C	BaCl₂	<i>Pbcn</i>	S
RbF	<i>P-1</i>	S	NH₄Cl	<i>P2₁/c</i>	C			
RbCl	<i>P-1</i>	S	NH₄Br	<i>P2₁/c</i>	C			
RbI	<i>P2₁/c</i>	S						

2.3.1.1 Crystal Structures with Alkali and Ammonium Halides^{I-III}

The first solid-state structure obtained with these receptors was the complex $L^2 \cdot KF$ shown in Figure 29. The structure presents a general interaction motif of L^2 observed in many crystal structures with different ion pairs. The structure consists of a 2:2 assembly of two L^2 molecules, with 2 equiv of KF complexed as separate ion pairs. The dimerization results from coordinative $K^+ \cdots O$ bonds (2.796 Å, 2.970 Å) formed between the crown ether complexed potassium cations and the nitro-group oxygens. The potassium cations are located in the middle of the crown ether rings (2.628 - 3.013 Å), being further coordinated to the carbonyl oxygens in the neighboring molecule (2.644 Å, 2.673 Å, not shown). The dimerization creates a suitable binding site accommodating two fluoride anions hydrogen bonded with the urea-groups ($N \cdots F^-$ distance 2.684 Å - 2.856 Å). The binding site is "capped" by two methanol molecules hydrogen bonded to the fluoride anions ($O \cdots F^-$ distance 2.590 Å and 2.471 Å) showing the importance of the solvent-mediated interactions in the formation of the optimized solid-state complexes with the receptors and ion pairs.

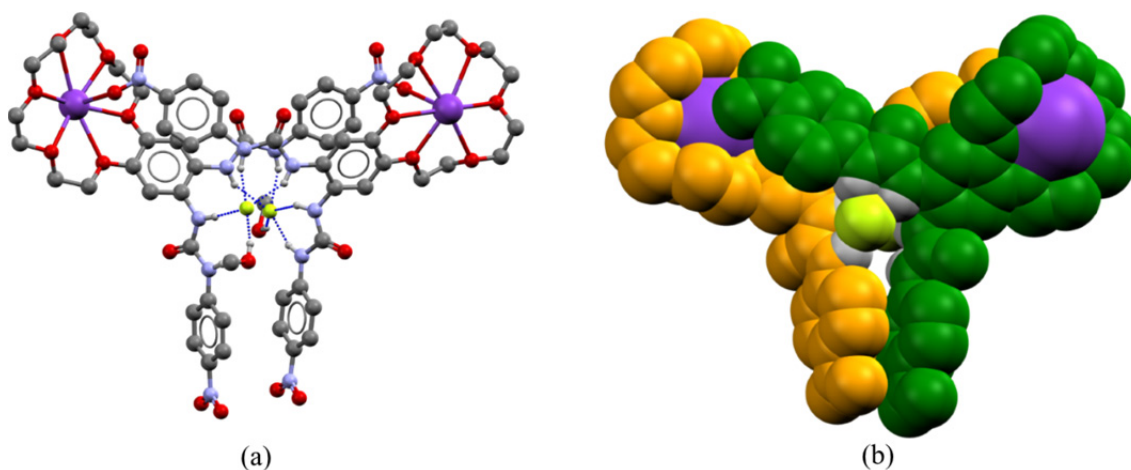


FIGURE 29 Crystal structure $L^2 \cdot KF$ shown as (a) ball-and-stick model and (b) spacefill model.¹ Complex $L^2 \cdot KF$ presents a general ion pair binding motif of L^2 in the solid-state, and similar ion pair complexes were obtained with KCl, KBr, K_2CO_3 , and KAcO.

Isostructural complexes to $L^2 \cdot KF$ were also obtained with KCl and KBr, having strikingly similar solvent mediated interactions. The hydrogen bond distances between the anion and the urea-groups vary between 3.164 Å and 3.311 Å for chloride, and between 3.282 Å and 3.447 Å for bromide. Surprisingly, solid-state structures of L^2 with K_2CO_3 and KAcO have a close resemblance to structure $L^2 \cdot KF$ with similar interaction motif, although the receptor-receptor interactions differ somewhat from $L^2 \cdot KF$ (discussed later). This interaction motif seems to be favoured when the cation size matches the crown ether size of L^2 (potassium), and the counteranion has a strong Lewis basic character and is a strong hydrogen bond acceptor (fluoride, chloride). Bromide is ambiguous in its

behaviour with L^2 ; crystal structures with two different interaction motifs were obtained with KBr.

Figure 30 presents the crystal structure $L^2 \cdot NH_4Cl$, representing another ion pair binding motif of L^2 . The structure consists of a contact ion pair of NH_4Cl with a charge-assisted hydrogen bond ($N \cdots Cl^-$ distance 3.277 Å) between the crown ether -complexed ammonium cation and the chloride anion hydrogen bonded to the urea-group of the adjacent molecule ($N \cdots Cl^-$ distances 3.157 Å and 3.345 Å). Similar structures were also obtained with KBr, KI, RbCl, and NH_4Br . From the obtained complexes it seems obvious that cations too large for the B18C6 ring seems to prefer the formation of a contact ion pair, or if the Lewis basicity and thus the hydrogen bond accepting nature of the anion is weak. The ambiguous nature of the bromide was observed from the crystallization of the $L^2 \cdot KBr$ complex in both binding motifs in a single crystallization experiment.

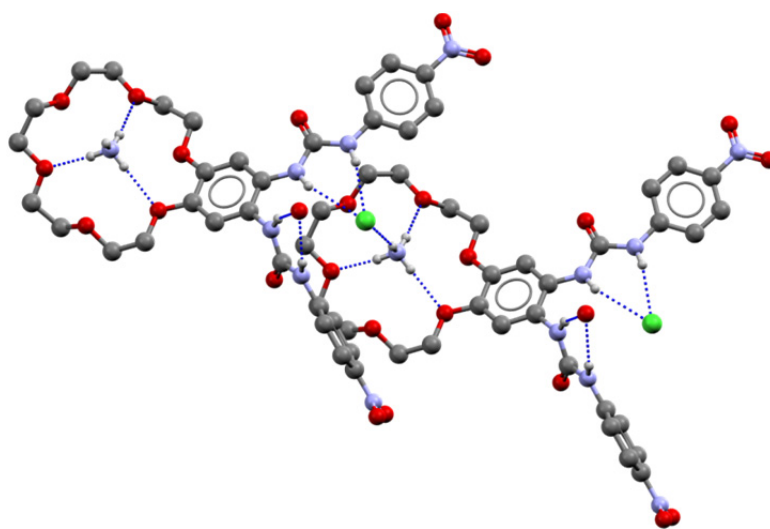


FIGURE 30 Crystal structure $L^2 \cdot NH_4Cl$ representing a second general binding motif of L^2 . The structure consists of a contact ion pair between the crown ether -complexed ammonium cation and the chloride anion. Similar contact ion pair complexes were also obtained with KBr, KI, RbCl, and NH_4Br . Hydrogen bonds are presented as dashed lines and nonbonding hydrogen atoms have been omitted from the figure.

Interestingly, ion pair complexes of L^2 with sodium were not obtained in spite of numerous attempts. This clearly shows that good size-fit between the cation and the crown ether is important for the crystallization process and efficient packing of the ion pair complexes with L^2 . This is supported by the successful crystallization of all the sodium halides except NaF with B15C5-based bis-urea receptor L^1 , where the size fit between the sodium and 15-crown-5 ring is good.

The crystal structure $L^1 \cdot NaCl$ is shown in Figure 31a. It is the only complex of L^1 with a contact ion pair and the crystal structures of L^1 with NaBr and NaI have separate ion pairs in the structure. It is noteworthy that all the sodium

complexes of L^1 are different from one another. In $L^1 \cdot NaCl$ the chloride forms a contact ion pair with the crown ether-complexed sodium cation (2.314 Å, 2.412 Å) and the chloride is further hydrogen bonded with the urea-groups in the adjacent dimers with $N \cdots Cl^-$ distances varying between 3.079 Å and 3.258 Å. Possibly due to the strong point charges of the sodium and chloride and the resulting strong ion pair, weak interactions with the receptor are not sufficient to separate the ions. Although the positions of L^1 molecules in crystal structure $L^1 \cdot NaCl$ resemble those seen in the crystal structures of the 2:2 complexes with L^2 , there are no coordinative bonds between the sodium cations and the nitro-group oxygens in $L^1 \cdot NaCl$. Interestingly, the structure $L^1 \cdot NaCl$ is isostructural with crystal structure L^1 (Figure 28a), where water molecules occupy the same positions as the chloride anions in the complex $L^1 \cdot NaCl$. The hydrogen bonding interactions responsible for the dimerization are identical between the structures. Thus, in crystal structure $L^1 \cdot NaCl$ the packing is solely dependent on the hydrogen bonding interactions, with sodium cations having very little effect on the packing. This is not the case in crystal structures $L^1 \cdot NaBr$ and $L^1 \cdot NaI$, where the sodium cation is always coordinated with a neighbouring receptor molecule and thus participates in the packing of the complexes in the solid-state.

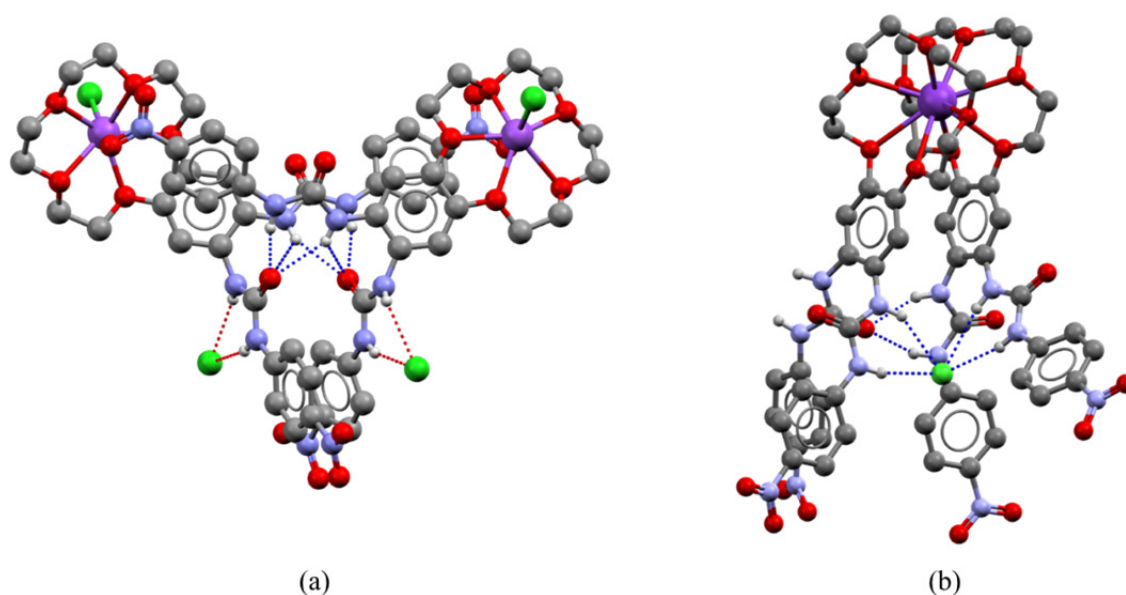


FIGURE 31 (a) Crystal structure $L^1 \cdot NaCl$.¹¹ The structure has a contact ion pair between Na^+ and Cl^- . The structure is very similar to crystal structure L^1 (Figure 28a). (b) Crystal structure $2L^1 \cdot KCl$ presents a general interaction motif of L^1 with potassium and rubidium halides.¹¹

With larger potassium and rubidium cations L^1 forms a dimeric assembly through sandwich complexation of the cation between the B15C5 moieties with a total of ten coordinative bonds formed between the cation and crown ether oxygens (2.778 – 3.109 Å).⁴⁶ In addition, hydrogen bonding between the urea-groups (2.892 and 2.942 Å) further enhances the dimer formation (Figure 31b). The dimerization creates a suitable binding site for the anions, with some of the

urea-groups directed towards the centre of the cavity. The urea groups that are not involved in the anion complexation form hydrogen bonds to the adjacent dimer (2.750 and 2.891 Å). The chloride anion in **2L¹·KCl** is hydrogen bonded with four urea hydrogens with N···Cl⁻ distances between 3.171 Å and 3.389 Å. The complexes with **L¹** and KBr, KI, RbF, RbCl, and RbI are structurally very close to each other having similar hydrogen bonding interactions between the receptor molecules and the anions. In crystal structures **2L¹·RbF** and **2L¹·RbCl** there are also solvent molecules interacting with the anion (MeOH), creating solvent-mediated hydrogen bonding networks. The most complex solid-state structure of **L¹** was obtained with KF, constituting of a tetramer or dimer of dimers. The interactions creating the structure are similar to those observed in the other crystal structures of **L¹**. For example, hydrogen bonding interactions between the dimers in **2L¹·KF** are similar to the structure of **L¹** (Figure 28, page 39), and the dimers are formed by interactions similar to those in **2L¹·KCl** (and other complexes). The fluoride anions are complexed in binding sites similar to those in the crystal structure **2L¹·KCl**, and water molecules create a complex solvent-mediated hydrogen bonding network also participating in the anion complexation. These observations provide information about which interactions are pivotal for the ion pair recognition processes with the crown ether bis-urea receptors, and how the weak interactions are responsible for the solid-state packing of the complexes.

Interestingly, the obtained crystal structures of **L⁴** with rubidium and cesium halides show very similar solid-state structures to potassium and rubidium complexes of **L¹**, as can be seen from the crystal structure **L⁴·CsCl** (Figure 32). The receptor has a doubly folded conformation driven by the optimized Cs⁺···O(crown ether) interactions (3.006 – 3.501 Å) and intramolecular hydrogen bonding between the urea groups (2.849 and 2.925 Å), made possible by the large size and symmetrical structure of the DB24C8 scaffold. The anion resides in a binding pocket similar to that in **2L¹·KCl**, being hydrogen bonded with the urea group in one of the receptor arms (in structure **L⁴·CsCl** the N···Cl⁻ distances are 3.169 Å and 3.411 Å). In other rubidium and cesium halide complexes the anion interacts with two or three receptor arms, and in all the structures solvent molecules (methanol, chloroform, dichloromethane) interact with the anion. Folding of the receptor scaffold leaves the cation open at the topside of the receptor and the cation is further coordinated by solvent molecules (in **L⁴·CsCl** by a methanol molecules) or the nitro group oxygens of the adjacent molecule. Although the general conformation of **L⁴** is very similar in all the obtained crystal structures with rubidium and cesium salts, there are also differences in the receptor arm orientations and weak interactions that follow.

Due to the tritopic nature of the receptors **L³** and **L⁴**, alkaline earth metals were also tested as possible guests for these receptors. The smaller size of the group 2 cations compared to group 1 can result in different receptor conformations because of the differences in optimum crown ether – cation interactions.

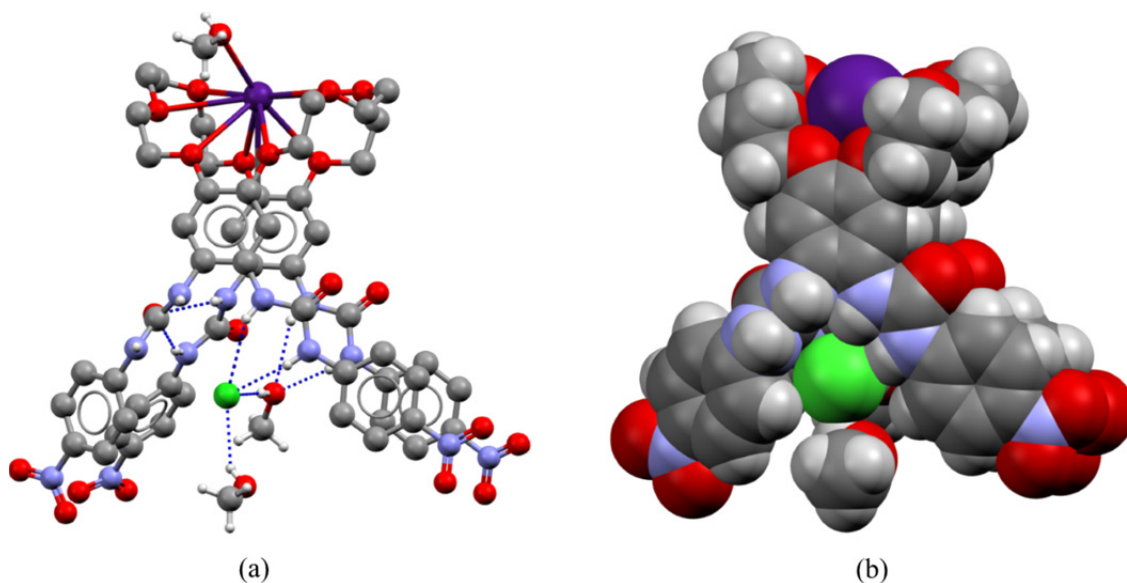


FIGURE 32 Crystal structure $L^4 \cdot CsCl$ as (a) ball-and-stick model and (b) spacefill model.^{III} The methanol molecule coordinated to the cesium cation is hydrogen bonded to the chloride anion in the adjacent complex.

The only obtained solid-state complex of L^3 and L^4 with alkaline earth metals was the crystal structure $L^4 \cdot BaCl_2$ (Figure 33). Truly, the receptor scaffold is in a clearly different conformation compared to $L^4 \cdot CsCl$ with the crown ether ring closed from the topside for optimum coordination between the crown ether oxygens and the barium cation (2.798 – 3.164 Å). This opens the receptor scaffold leaving the cation free for further coordination with solvent molecules (DMF, water) from the underside of the receptor. Each urea group is hydrogen bonded to a chloride anion ($N \cdots Cl^-$ distances being between 3.096 and 3.392 Å), and each anion is hydrogen bonded with two receptor molecules. This structure exemplifies the tritopic nature of the L^4 receptor and the versatile behaviour of these receptors.

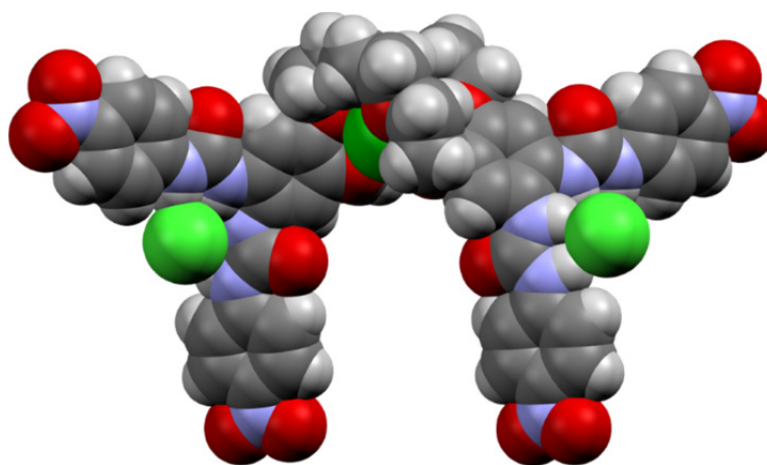


FIGURE 33 Crystal structure $L^4 \cdot BaCl_2$.^{III} Each chloride anion is hydrogen bonded with a neighboring L^4 molecule. The solvent molecules (DMF and water) coordinated to the barium cation and other solvent are omitted from the figure for clarity.

2.3.1.2 Crystal Structures with Alkali Oxyanions^{L,III}

Several solid-state complexes with different alkali oxyanions were obtained in the course of this work, in many cases as a result of serendipity. The first such complex was crystal structure $L^2 \cdot K_2CO_3$ (Figure 34). The complex crystallized from a DMF solution of L^2 with KF as a result of aerial CO_2 fixation into carbonate anion in an organic solution made basic by the presence of the fluoride (and consecutive formation of OH^- from water). There are examples of this phenomenon in the literature.^{92,120} Interestingly, the crystals obtained were red, whereas all the other crystals obtained with the crown ether bis-urea receptors were yellow. This can arise from the charge-transfer complex resulting from cation $\cdots\pi$ interaction between a potassium cation and nitrophenyl substituent (not shown), not observed in any other crystal structure with receptors L^1 - L^4 . The dimeric assembly formed through the anion complexation resembles that seen in the structure $L^2 \cdot KF$ (and other crystal structures with the same binding motif). Because of the larger size of the CO_3^{2-} anion, there are no coordinative bonds between the nitro-group oxygens and potassium cations. Therefore, the dimeric assembly forms solely through the extensive hydrogen bonding between the L^2 molecules and the carbonate anion (11 hydrogen bonds, $N \cdots O$ distances 2.727 – 3.415 Å). The crystal structure $L^2 \cdot KAcO$ (not shown) has a symmetric 2:2 assembly that resembles the structure of $L^2 \cdot KF$, despite the more complex geometry and larger size of the AcO^- anion. The hydrogen bonds between the acetate anions and L^2 molecules and the anion positions in the structure make the coordination between the potassium cations and nitro-group oxygens possible, as in the structure of $L^2 \cdot KF$.

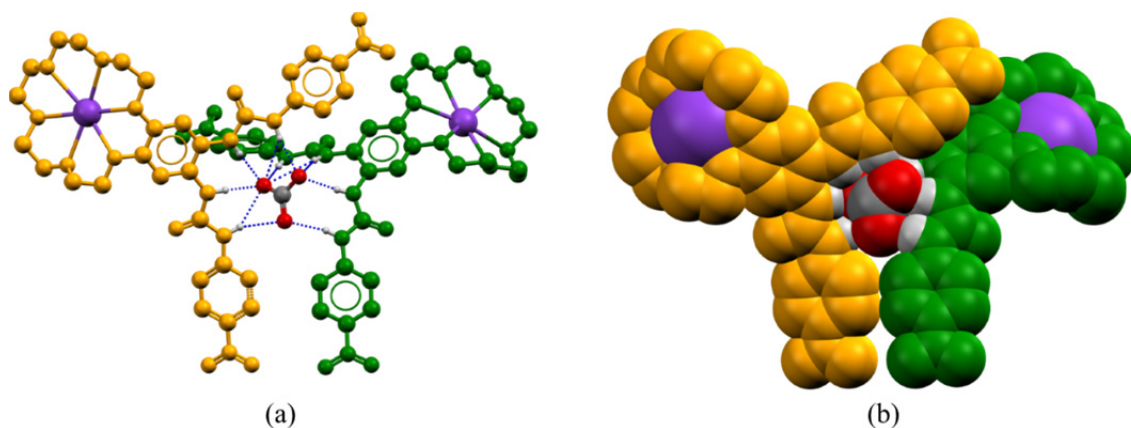


FIGURE 34 Crystal structure $L^2 \cdot K_2CO_3$ presented as (a) ball-and-stick and (b) spacefill models.¹ Carbonate anion is hydrogen bonded with two L^2 molecules with total of 11 hydrogen bonds. In addition, a water molecule is hydrogen bonded to the carbonate anion (not shown).

The crystal structure $L^2 \cdot K_2SO_4$ (Figure 35) differs markedly from all other crystal structures of L^2 , although some characteristics similar to the other structures can be found. $L^2 \cdot K_2SO_4$ consists of a tetrameric assembly formed from two dimers (Figure 35b, blue and green, yellow and red molecules) resulting from a

$K^+ \cdots O(\text{nitro})$ coordination and hydrogen bonds formed by these receptors to the same sulfate anion. Two of the L^2 molecules (yellow and green) are hydrogen bonded to both sulfate anions bringing the two dimers together into a tetrameric assembly. The sulfate anions are hydrogen bonded with the receptors by eight and nine hydrogen bonds ($N \cdots O$ distances 2.768 – 3.311 Å). One sulfate anion is further coordinated to the potassium cation in the next tetrameric assembly (not shown), thus having both a separated and a contact ion pair within one structure. $L^2 \cdot K_2SO_4$ exemplifies the variety of conformations these receptors can have for optimizing the weak interactions for ion pair complexation. It also shows the difficulty of predicting the solid-state structure with a certain ion pair, even though there are general characteristics in all the crystal structures with both spherical halides and geometrically more complex oxyanions.

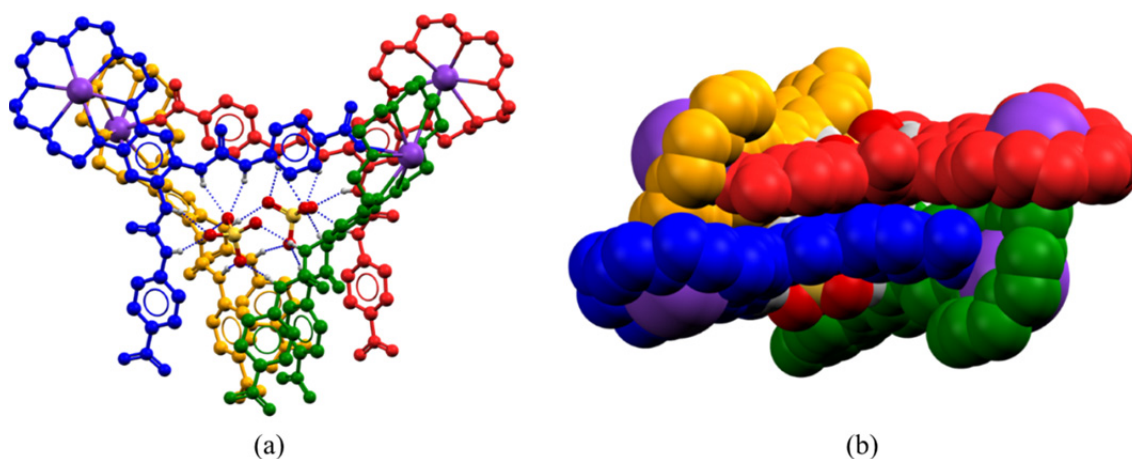


FIGURE 35 Crystal structure $L^2 \cdot K_2SO_4$ presented as (a) ball-and-stick (b) spacefill models.¹ The structure consists of a tetrameric assembly formed through $K^+ \cdots O$ coordination and hydrogen bonding interactions between the sulfate anions and the receptors.

The only crystal structure of L^3 was obtained from fixation of CO_2 into CO_3^{2-} in a DMF solution with an excessive amount of RbF. The crystal structure $L^3 \cdot Rb_2CO_3$ (Figure 36) shows the open conformation of L^3 resulting from the asymmetric structure of the DB21C7 scaffold and the complex coordination behavior between adjacent $[L^3 \cdot Rb]^+$ complexes. Each Rb^+ is located in the middle of the crown ether ring (2.908 – 3.097 Å), coordinated with nitro group oxygen (2.907 Å) of an adjacent receptor (Figure 36). The ninth coordinative bond to Rb^+ is formed with carbonyl oxygen (2.829 Å) in another L^3 molecule (not shown). Part of the structure shown in Figure 36a resembles to the coordination behavior seen in complexes with L^2 , creating a suitable binding site for the anion. In $L^3 \cdot Rb_2CO_3$ the anion interacts with a total of four receptor molecules, forming an extensive hydrogen bonded network (Figure 36c) with hydrogen bond distances between 2.854 Å and 3.413 Å. Despite numerous crystallization experiments, other crystals with suitable quality were not obtained with L^3 , probably due to the conformational freedom of the receptor scaffold and the

difficulty of having optimal weak interactions for the efficient packing of the complexes in the solid-state.

Crystal structures of L^4 with acetate (CH_3COO^-) and carbonate methyl ester ($CH_3CO_3^-$) were also obtained from the basic organic solutions, the acetate being formed from the ethyl acetate solvent, and carbonate methyl ester from CO_2 fixation with CH_3O^- formed from the methanol solvent. In the crystal structure $L^4 \cdot CsCO_3CH_3$ (Figure 37), the L^4 scaffold is also folded double, making further cation coordination possible from the topside (cesium is coordinated by the nitro-group oxygens of the neighboring receptor), in addition to the eight $Cs^+ \cdots O(\text{crown ether})$ coordinative bonds (3.004 – 3.342 Å). Two urea-groups are directed towards the binding site, creating hydrogen bonds with the planar carbonate anion with hydrogen bond distances between 2.763 and 2.924 Å. The other urea groups form hydrogen bonds with solvent molecules and an adjacent receptor molecule (not shown).

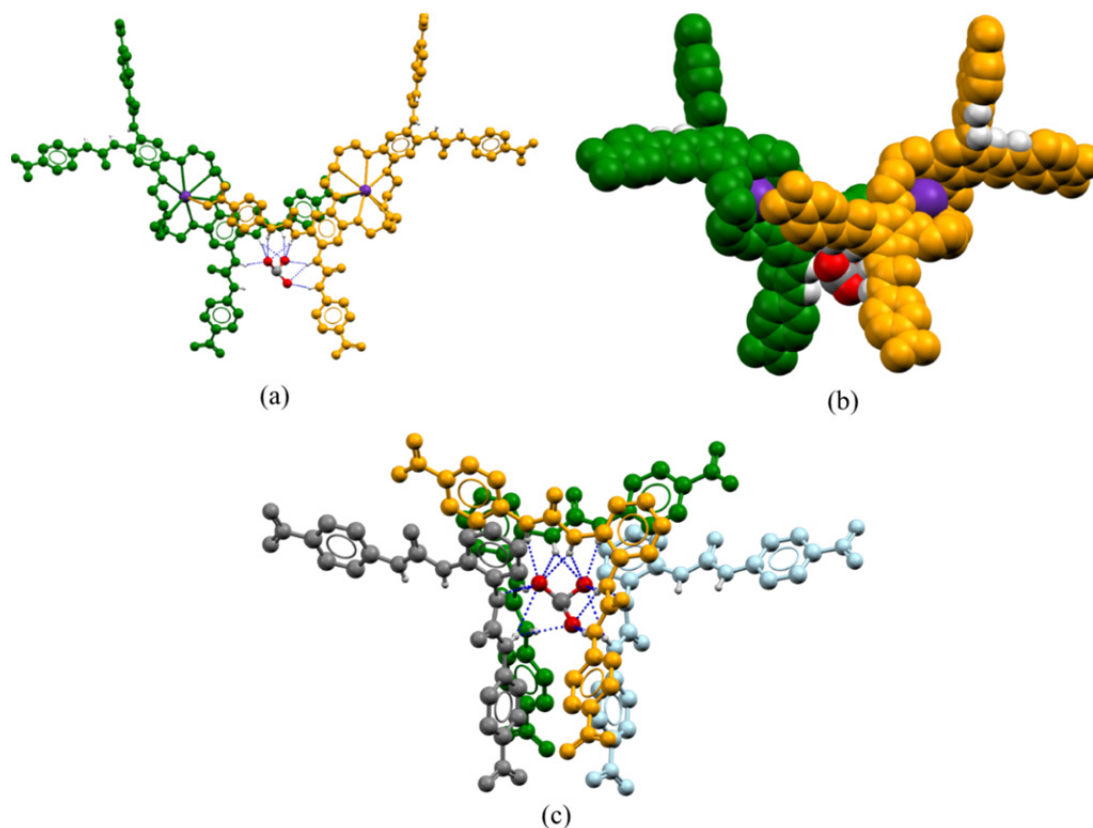


FIGURE 36 Part of the packing in the crystal structure $L^3 \cdot Rb_2CO_3$ shown as (a) ball-and-stick model and (b) spacefill model.^{III} The coordination behavior resembles that seen in crystal structures of L^2 . (c) The carbonate anion is hydrogen bonded with four receptor molecules creating a complex hydrogen bonding network.

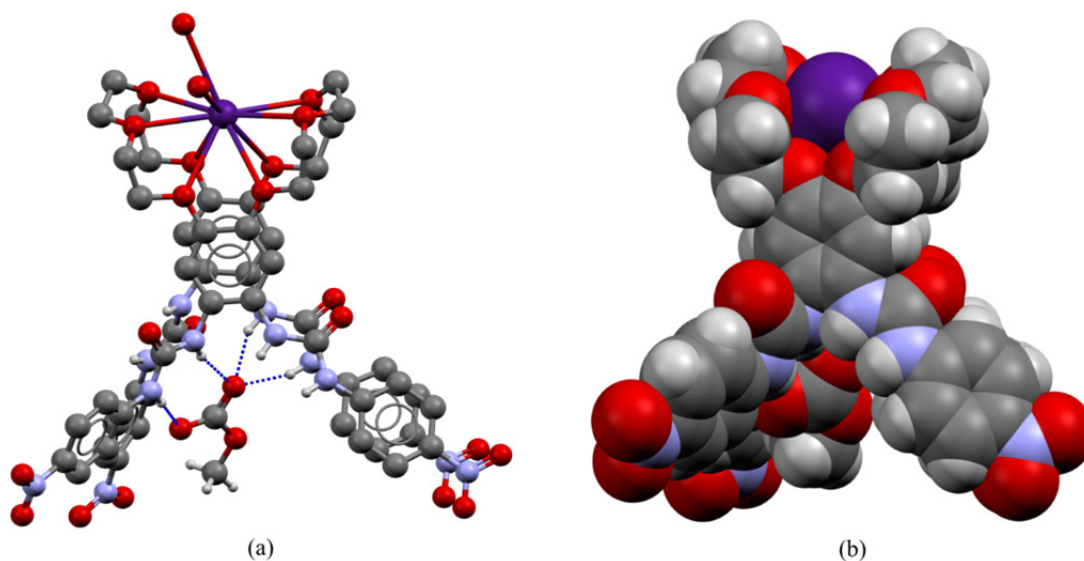


FIGURE 37 Crystal structure $L^4 \cdot CsCO_3CH_3$ presented in (a) ball-and-stick and (b) spacefill models. Solvent molecules interacting with the receptor molecules have been omitted from the figure for clarity.

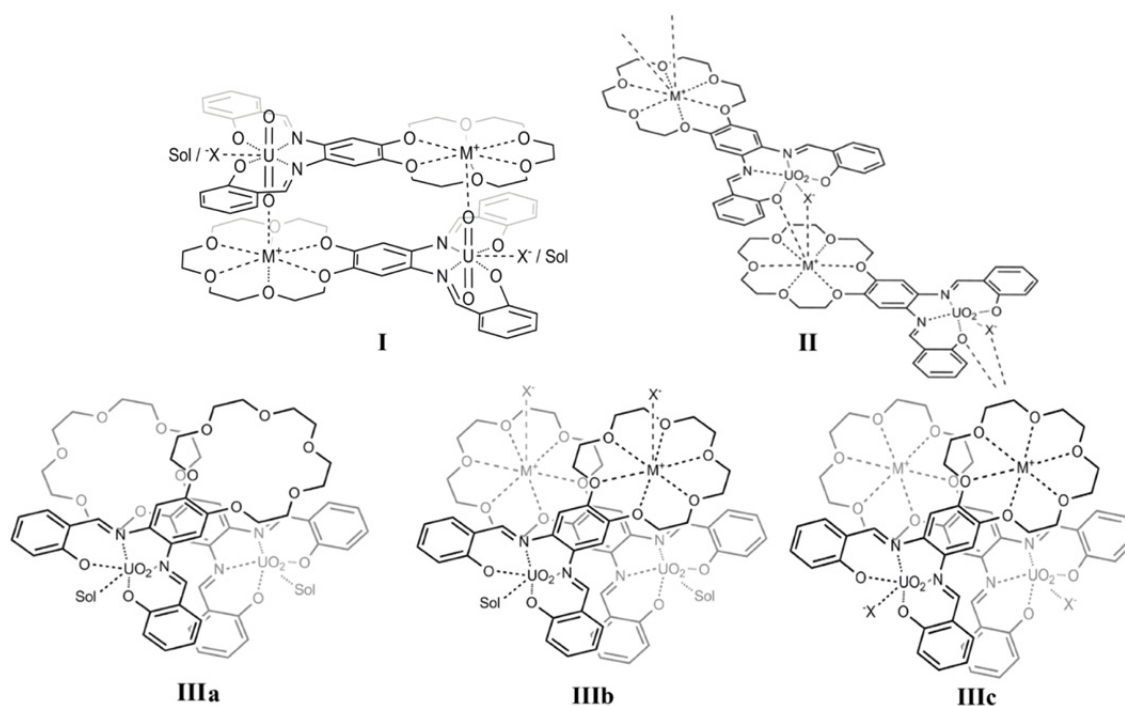
2.3.2 Solid-State Studies of Crown Ether Uranyl Salophen Receptors L^5 and L^6 IV

The behavior of crown ether uranyl salophen receptors L^5 (B15C5) and L^6 (B18C6) as ditopic receptors in the solid-state was studied with comprehensive single-crystal structural analysis with a total of 19 crystal structures (Table 3), out of which 16 were complexes with ion pairs. Interestingly, the obtained solid-state structures revealed three general interaction motifs, defined according to the ion pair binding type or the packing of the receptors. The observed binding motifs are defined as follows: **(I)** separate ion pair; **(II)** contact ion pair; **(III)** stacked packing of receptors, and a schematic presentation of the interaction motifs is shown in Scheme 2. Interaction motifs **(I)** and **(III)** have variety in their constitution as shown in Table 3, whereas interaction motif **(II)** has always the same structure.

TABLE 3 Crystal structures obtained with L^5 and L^6 , their space groups (SG), and the interaction motifs (IM)^a observed in the solid-state complexes.^{IV}

L^5	SG	IM	L^6	SG	IM
H ₂ O	<i>P2₁/c</i>	IIIa	H ₂ O	<i>Cc</i>	IIIa
DMSO	<i>Pbcn</i>	IIIa	NaF	<i>Pbca</i>	IIIc
LiCl	<i>I2/a</i>	Ia	NaBr_1	<i>P-1</i>	Ib
NaBr	<i>P2₁/n</i>	IIIb	NaBr_2	<i>P2₁/m</i>	Ib, II
RbF	<i>P2₁/c</i>	II	NaI	<i>P2₁/c</i>	Ib
CsF	<i>P2₁/c</i>	II	KF	<i>P2₁/n</i>	II
			KCl	<i>P2₁/n</i>	Ia
			KBr	<i>P2₁/n</i>	Ia
			KI	<i>P-1</i>	Ib
			KAcO	<i>P2₁/n</i>	Ia
			RbCl	<i>P2₁/n</i>	II
			CsCl	<i>P2₁/a</i>	II
			NH ₄ Br	<i>P2₁/n</i>	II

^a I: separate ion pair, a: UO₂···X⁻, b: UO₂···Sol; II: contact ion pair; III: stacked packing of receptors, a: UO₂···Sol, b: UO₂···Sol, contact ion pair, c: UO₂···X⁻, separate ion pair. X⁻ = anion, Sol = solvent molecule.



SCHEME 2 General interaction motifs observed with crown ether uranyl salophen receptors L^5 and L^6 .^{IV} (I) structure with separated ion pair; (II) structure with contact ion pair; (IIIa) stacked packing of the receptors with solvent molecules; (IIIb) stacked packing of the receptors with contact ion pair ($L^5 \cdot \text{NaBr}$); (IIIc) stacked packing of the receptors with separated ion pair ($L^6 \cdot \text{NaF}$). The general schemes are presented only for L^6 although similar interaction motifs are observed also with L^5 . M^+ = alkali or ammonium cation, X^- = halide or acetate anion, Sol = solvent molecule.

The crystal structure $L^5 \cdot LiCl$ represents the first example of interaction motif (I) with a separated ion pair in the structure (Figure 38a). This is the only crystal structure obtained with lithium halides and any of the receptors L^1 - L^6 . The lithium cation is coordinated in the middle of the crown ether ring (2.104 – 2.362 Å), and the coordination sphere of the lithium is filled by coordinative bonds with uranyl oxygen in the other molecule of the dimer (2.184 Å) and a water molecule (2.052 Å), which prevents further coordination with the cation. The chloride anion is coordinated to the fifth equatorial site of the uranyl cation with a bond length of 2.806 Å and the anion is further hydrogen bonded with two water molecules.

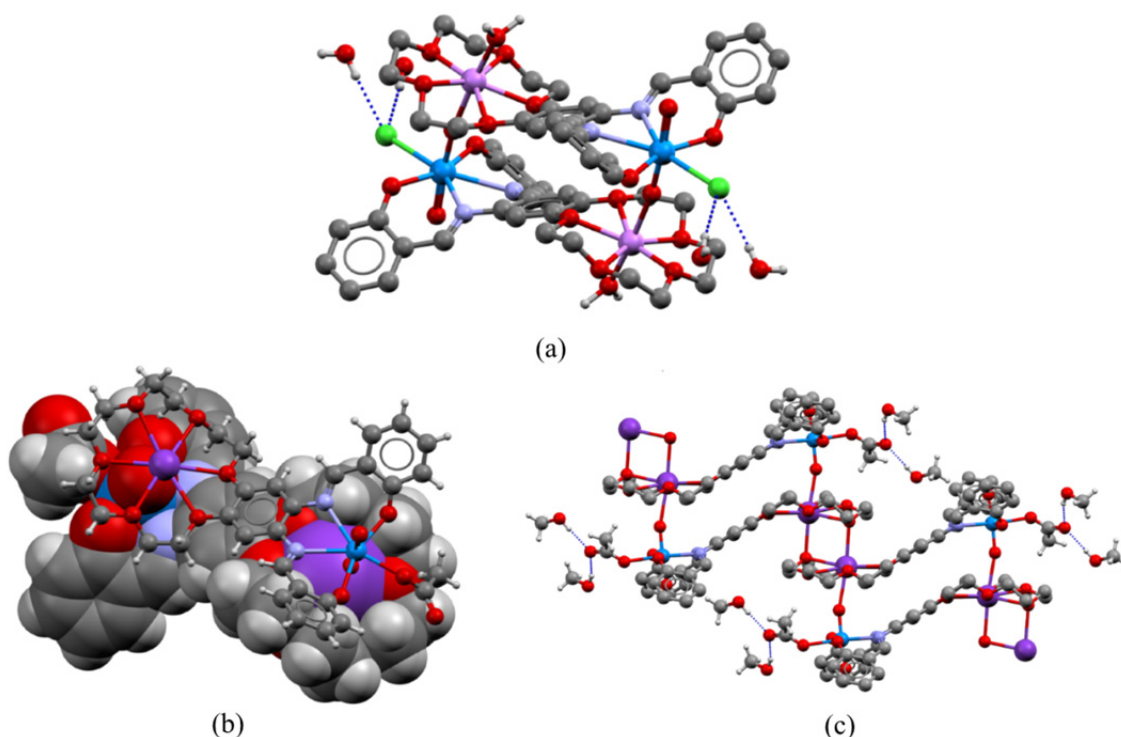


FIGURE 38 Crystal structures of (a) $L^5 \cdot LiCl$ and (b) $L^6 \cdot KAcO$ representing examples of interaction motif (I).^{IV} (c) Part of the packing in crystal structure $L^6 \cdot KAcO$.

Another example of interaction motif (I) is presented in Figure 38b and c. Crystal structure $L^6 \cdot KAcO$ is the only published solid-state complex of uranyl salophens or salens with acetate anions. In the structure, potassium is coordinated in the middle of the 18-crown-6 ring (2.690 – 2.900 Å) with a coordinative bond formed with the uranyl oxygen of the other molecule of the dimer (2.678 Å). The other coordinative bond perpendicular to the plane of the crown ether is formed with crown ether oxygen (2.787 Å) in the adjacent dimeric complex (Figure 38c). This creates a 1-dimensional coordination polymer along the crystallographic a -axis, which is also observed in many other ion pair complexes with L^5 and L^6 . The acetate anion is coordinated to uranyl cation ($U \cdots O^-$ distance 2.356 Å), being further hydrogen bonded with methanol solvate molecules. Hydrogen bonding with the anion and solvate molecules seems to weak-

en the coordinative $U \cdots X^-$ bond, since the observed bond lengths in $L^5 \cdot LiCl$ and $L^6 \cdot KAcO$ complexes are somewhat longer than what is expected from the other uranyl salophen complexes with chloride or oxygen-containing anions.^{IV} Nearly isostructural crystal structures with $L^6 \cdot KAcO$ were obtained with KCl and KBr, but in these complexes there are no solvent molecules interacting with the anion coordinated to uranium ($U \cdots Cl^-$ distance 2.747 Å and $U \cdots Br^-$ distance 2.914 Å).

The last example of interaction motif (I) is presented in Figure 39. The crystal structure $L^6 \cdot NaI$ has similar interactions as observed in crystal structure $L^5 \cdot LiCl$, but in $L^6 \cdot NaI$ the coordination with the cation perpendicular to the crown ether plane is not interrupted by a solvent molecule. Instead, the receptors are stacked with coordinative bonds between the crown ether -complexed sodium cation and the uranyl oxygen of the adjacent receptor (2.306 and 2.361 Å). This creates infinite coordination polymers along the crystallographic a -axis, with 8.203 Å long repeating $\cdots O=U=O \cdots Na^+ \cdots O$ units. Due to the low Lewis basicity of the iodide anion, it is not coordinated to the uranyl center. Instead, a water molecule coordinates with the uranyl (2.476 Å), forming hydrogen bonds with the iodide anion and one of the crown ether oxygens in the adjacent receptor (Figure 39a).

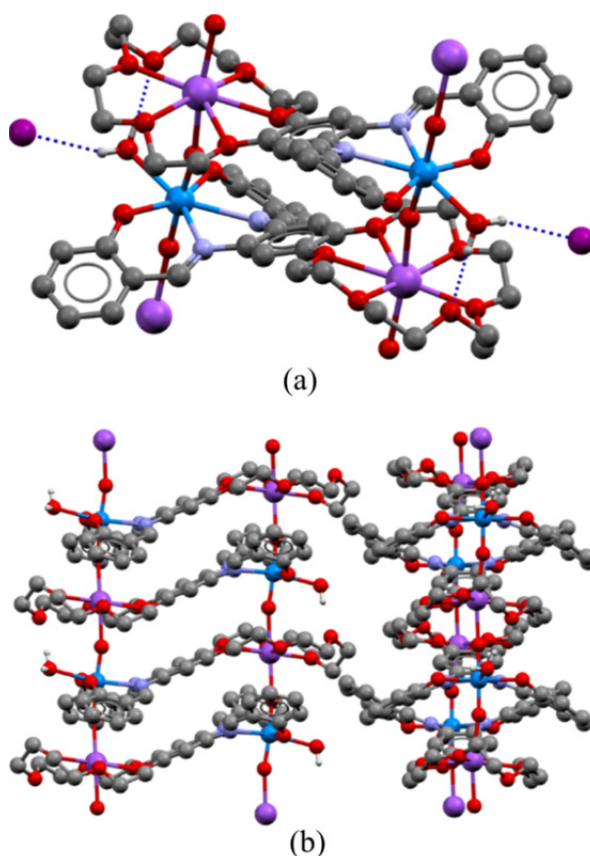


FIGURE 39 (a) Crystal structure $L^6 \cdot NaI$.^{IV} (b) Infinite coordination polymers are formed along the crystallographic a -axis by continuous coordination between repeating $\cdots O=U=O \cdots Na^+ \cdots O$ units (8.203 Å). The iodide anions are omitted from the picture for clarity.

Recently actinides and especially uranium have gained attention in utilizing them in single molecule magnets (SMM) and single chain magnets (SCM). In this type of applications with uranium, a pentavalent uranyl cation (UO_2^+) is coordinated to a transition or alkali metal cation through cation-cation interaction (CCI).¹²¹⁻¹²⁴ A pentavalent UO_2^+ cation is unstable, but salen or salophen scaffolds have been shown to stabilize it.¹²⁵ The polymeric structure obtained with L^6 and NaI gives an intriguing idea for utilizing this type of crown ether salophen scaffold for stabilizing the UO_2^+ cation. In all crystal structures obtained with L^5 and L^6 the uranyl cation is hexavalent UO_2^{2+} , but with a correct reducing agent pentavalent uranyl cation could possibly be obtained, and in the presence of a suitable metal, materials with interesting magnetic characteristics could be created.

In Figure 40 is presented the crystal structure $\text{L}^6\cdot\text{CsCl}$ that represents an example of the interaction motif (II). Other structures with this interaction motif were obtained between L^5 and RbF and CsF, and L^6 with KF, RbCl, and NH_4Br . In the structure $\text{L}^6\cdot\text{CsCl}$ there is a contact ion pair (3.473 Å) between the crown ether-complexed cesium cation (3.052 – 3.504 Å), and the chloride anion coordinated to the uranyl center (2.732 Å). Another coordinative bond to the cation is formed by the oxygen atom in the salophen scaffold (3.025 Å). This type of coordination results in a polymeric structure along the crystallographic *b*-axis.

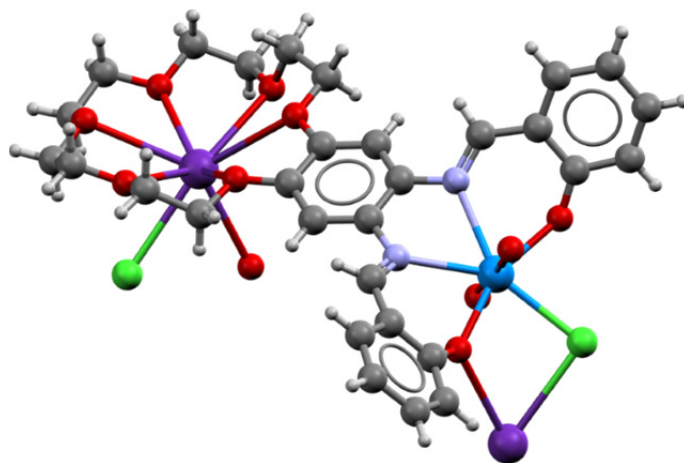


FIGURE 40 Crystal structure $\text{L}^6\cdot\text{CsCl}$ representing the interaction motif (II).^{IV}

The structures with interaction motif (II) have a trend between the size mismatch of the cation and the crown ether ring. If the cation is too large for the crown ether cavity, it resides on top of the crown ether plane. This favors the contact ion pair formation with the anion in the adjacent complex, with the oxygen coordination from the adjacent salophen receptor to the cation further enhancing the contact ion pair formation. Crystal structure $\text{L}^6\cdot\text{KF}$ having interaction motif (II) seems to be contradictory with this, but possibly the ion pairing between potassium and fluoride is too strong to be separated by the receptor to form a complex with interaction motif (I), as happens with other potassium salts. A few attempts at complexation between L^6 and KF resulted repeatedly in

crystal structure $L^6 \cdot KF$ with interaction motif (II). Interestingly, crystal structure $L^6 \cdot NH_4Br$ has also interaction motif (II) with the coordinative bond between the cation and salophen oxygen replaced by a hydrogen bond, and an ion pair contact, although very weak, is formed between the ammonium cation and the bromide anion. The bromide anion is coordinated with the uranyl center at a distance of 2.895 Å.

Interaction motif (III) has the broadest definition and the obtained structures differ from each other. It is defined as a stacking of the receptors at an angle of about 90° to each other through various weak interactions between the receptors and ion pairs (if present). This type of stacking was observed in all solvate structures of L^5 and L^6 , but also in ion pair complexes with $L^5 \cdot NaBr$ and $L^6 \cdot NaF$. There is a lot of structural variety among the obtained structures with solvate structures fairly similar to each other, but the complexes with NaF and NaBr being clearly different from each other. For example, crystal structure $L^5 \cdot NaBr$ (Figure 41) closely resembles the solvate structures of L^5 and L^6 , whereas crystal structure $L^6 \cdot NaF$ has a separated ion pair and a complex solvent-mediated hydrogen bonding network (not shown). Due to the smaller number of solid-state complexes with L^5 , it is difficult to estimate how typical this interaction motif is for L^5 with ion pairs.

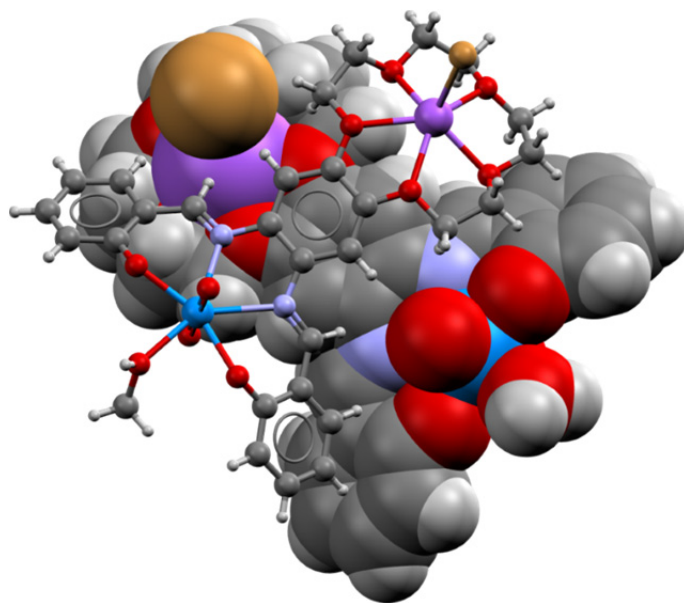


FIGURE 41 Crystal structure $L^5 \cdot NaBr$ representing an example of binding motif III. Water and methanol molecules are coordinated with the uranyl center with a contact ion pair between the sodium and bromide.^{IV}

Although the obtained solid-state complexes of L^5 and L^6 show clear general aspects in their ion pair complexation behavior, some exceptions were also observed. Noteworthy are the two different structures obtained with L^6 and NaBr. Both structures differ from all the other obtained crystal structures with L^5 and L^6 , being also clearly different from each other. These structures can be defined with the interaction motifs described above, but they do not follow

comprehensive description of the structures. It is also interesting that the crystal structure **L⁶·NaBr_2** can be considered as having two different interaction motifs within the same crystal structure. This behaviour might stem from the low Lewis basicity of the bromide anion, the latter not being basic enough to exclusively bind to the uranyl center (as fluoride and chloride), thus competing with the solvent molecules for the uranyl coordination. In addition to this, the size mismatch of sodium cations with the B18C6 scaffold can have a drastic effect on the packing of the receptors in the solid-state, leading to a “confused” behaviour of NaBr with **L⁶**.

2.4 Solution Studies with Crown Ether bis-Urea Receptors^{I-III}

The solution behaviour of ditopic crown ether bis-urea receptors was studied with Job’s plot analysis¹²⁶ and ¹H NMR titrations¹²⁷ to obtain more insight into the effect of the cation complexation towards anion binding. The studies were performed in a fairly nonpolar 4:1 CDCl₃/DMSO-d₆ solution at 303 K. The cations were brought to the solution as their tetraphenylborate (BPh₄) salts and the anions as their tetrabutylammonium (TBA) salts. These ions alone (as TBABPh₄) were tested with **L²** to show the non-interactive behaviour of these ions with the receptor,^I and thus the counter ions were considered as “innocent” to simplify the analysis of the binding behaviour. However, this can be a strong simplification of the system since multiple ion pair equilibria are simultaneously present in it.²⁶ The preliminary studies performed in 9:1 CDCl₃/DMSO-d₆ showed a very strong affinity of chloride with the cationic complexes of **L²**. Because of this, a more polar medium was chosen (4:1 CDCl₃/DMSO) to create more competition between the solvent and the anions towards the receptor. This resulted in a lower affinity of the receptors towards the anions and more reliable results from the binding constant calculations. In addition, DMSO was necessary to solubilize the receptors in otherwise weakly polar chloroform. The cationic complexes were created by measuring equimolar amounts of receptor and MBPh₄ salt in the sample (a 2:1 ratio was used for **L¹** and KBPh₄). The titrations were performed with up to 10 equiv of the studied anion added to the receptor, performed in 17 additions (18 spectra were collected). The chemical shifts obtained from the spectra and the calculated host and guest concentrations were used in a HypNMR2008 program¹²⁸ to calculate the binding constants (*K*) with global fitting^{127,129}.

2.4.1 Solution Studies with Receptor **L²**^I

In Figure 42a and b are shown the spectral changes upon stepwise addition of chloride into the receptor **L²** and the cationic complex [**L²·K**]⁺. In both cases the chloride addition induces seemingly similar downfield shifts in urea-protons H_a and H_b and aromatic proton H_c (Figure 42d)), characteristic of hydrogen bonding interactions between the host and the guest. The behaviour of these shifts is

fairly similar in all the observed signals, but the total chemical shift difference is normally largest for H_a and smallest for H_c . Although the chemical shifts with L^2 and $[L^2 \cdot K]^+$ follow the same trend upon anion additions, plotting the chemical shift differences shows the very different behavior between the two hosts (Figure 42c).

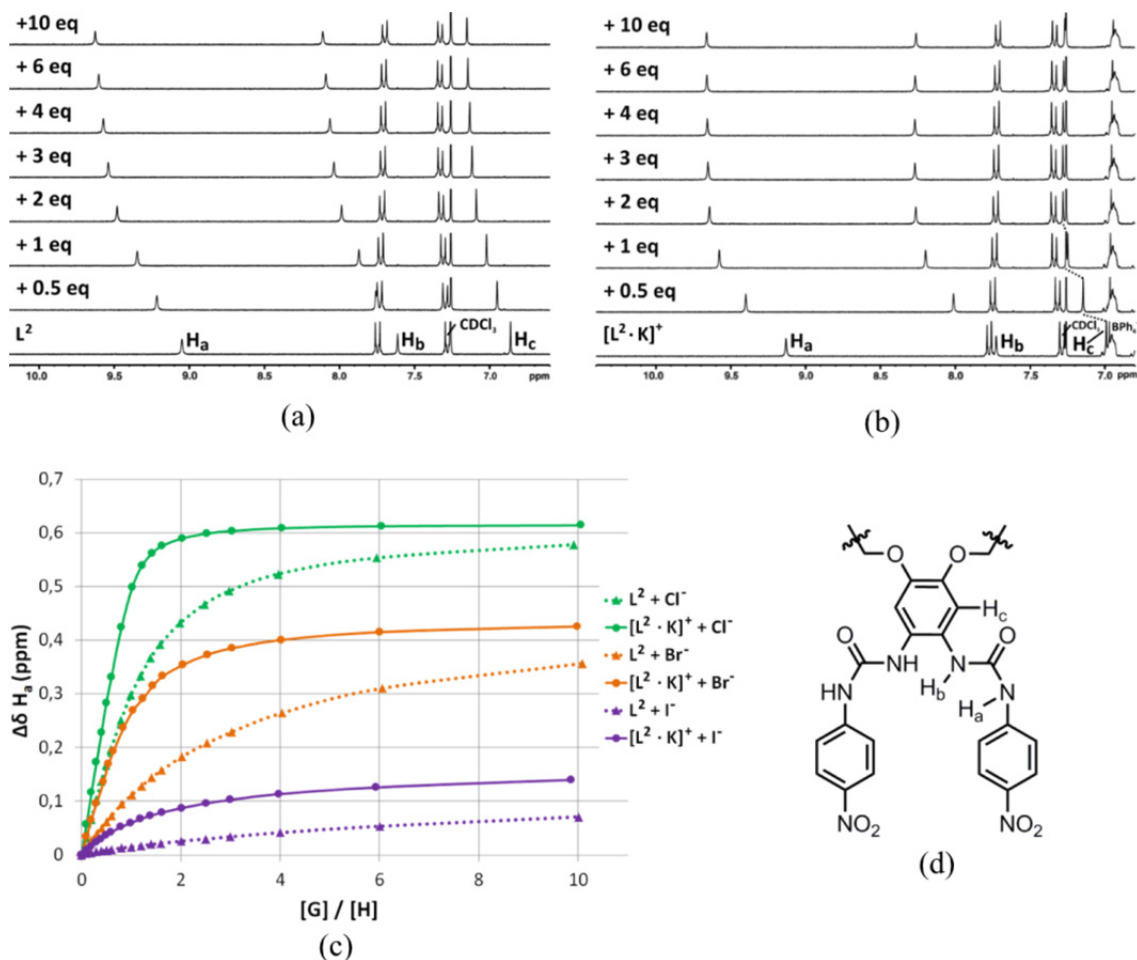


FIGURE 42 Spectral changes of (a) L^2 and (b) $[L^2 \cdot K]^+$ complex upon stepwise chloride addition.¹ (c) Observed chemical shift differences of urea-proton H_a in L^2 (dotted line) and its cationic complex $[L^2 \cdot K]^+$ (solid line) upon addition of chloride (green), bromide (orange), and iodide (purple). (d) Assignment of protons used in the binding studies.

The binding stoichiometry for L^2 and its cationic complexes with the halides was verified to be 1:1 with Job's plot analysis, and this stoichiometry was used to calculate the binding constants for each complexation (Table 4). The obtained 1:1 binding constants for L^2 toward halides (741 M^{-1} for chloride, 163 M^{-1} for bromide, and 34 M^{-1} for iodide) are moderate, and they clearly follow the Lewis basicity and the hydrogen bonding acceptor character of the halides. Similar binding constants for halides were also obtained with a reference receptor without the crown ether (807, 175, and 27 M^{-1} , for Cl^- , Br^- , and I^- , respectively), proving that the crown ether itself has little effect on the anion binding.¹

TABLE 4 Binding constants and fitting errors obtained with HypNMR2008 for L^2 and its cationic complexes $[L^2 \cdot M]^+$ ($M = Na, K, Rb$) with different halides in 4:1 $CDCl_3/DMSO-d_6$ at 303 K using global fitting.

		L^2	$[L^2 \cdot Na]^+$	$[L^2 \cdot K]^+$	$[L^2 \cdot Rb]^+$
Cl ⁻	$K_{11}^{a,b}$	741 ± 10	5381 ± 377	8908 ± 311	6748 ± 382
Br ⁻	K_{11}^b	163 ± 2	1780 ± 55	1549 ± 28	1863 ± 52
	K_{11}^c	-	2118 ± 190	2153 ± 228	- ^d
	K_{21}^c	-	240 ± 178	187 ± 103	- ^d
I ⁻	K_{11}^b	34 ± 2	404 ± 17	374 ± 13	328 ± 13

^a K_{xy} where x = host stoichiometry, y = guest stoichiometry, ^b 1:1 binding model used. ^c 1:1 + 2:1 binding model used. ^d 1:1 + 2:1 binding model was not applicable

Next, the effect of the alkali metal coordination with L^2 in the anion binding affinity was studied. As is seen from the spectra (Figure 42b) and the plotted chemical shift changes (Figure 42c), upon small chloride additions the proton H_a in $[L^2 \cdot K]^+$ complex undergoes a clearly larger chemical shift than in L^2 . This is clear indication of stronger binding of chloride with $[L^2 \cdot K]^+$ compared to L^2 alone. It is also noteworthy that the total chemical shift between the two receptors is fairly similar, although the binding constants are clearly higher for $[L^2 \cdot K]^+$. The halide affinities of the cationic $[L^2 \cdot K]^+$ complex follow the same trend as with L^2 but with remarkably larger binding constants (8908, 1549, and 374 M^{-1} for chloride, bromide and iodide, respectively, Table 4). The cation complexation with L^2 clearly induces a strong turn-on effect towards anion binding. The positive cooperativity can be considered to result from electrostatic interactions between the cation and the anion and the increased acidity of the urea hydrogen induced by the cation complexation in the crown ether ring. The anion-induced chemical shifts for H_b are larger for cationic complexes of L^2 (not shown), whereas the H_a in L^2 undergoes a larger chemical shift upon anion binding when a cation is not present. This can indicate that the crown ether complexed cation can bring the ions closer through electrostatic attraction, thus inducing a larger chemical shift in H_b , which is closer to the crown ether moiety.

Although the Job's plot analysis gave quite explicit results of 1:1 complex formation between L^2 and its cationic complexes with the anions, in the case of bromide also a more complex 1:1 + 2:1 binding model (receptor : anion) could be utilized in binding constant calculations. Job's plot analysis can give unambiguous results if more than a single complex exist in the system,¹²⁷ and thus the results of Job's analysis were considered with caution and more complex binding models were also tested. The 1:1 binding constant for $[L^2 \cdot K]^+$ + Br⁻ complexation from 1:1 + 2:1 binding model was slightly higher (2153 M^{-1}) than binding constant obtained with simple 1:1 binding model (1549 M^{-1}), and the

obtained 2:1 binding constant (187 M^{-1}) is clearly smaller than the 1:1 binding constant. The 1:1 + 2:1 binding model gave a better fit to the observed chemical shifts, and can thus be considered a better model for the observed binding phenomenon. According to the concentration plot obtained from binding constant calculation (not shown), at small bromide concentrations, the guest is complexed as both 1:1 and 2:1 complexes. At higher guest concentrations this dimeric species breaks down to give simple 1:1 complex as the main species. One can speculate that the 2:1 complex could be similar to the 2:2 ion pair complexes observed in the crystal structures of L^2 (Figure 29). It is clear that the data obtained from the titration experiments and the consecutive modelling of the behaviour cannot give an explicit picture of how the host and guest interact in the solution or the exact structures of the complexes. Thus, the results obtained from binding constant calculations have to be considered with caution, and only as a model of the observed phenomenon.

Modelling the iodide binding with the cationic complexes of L^2 using simple 1:1 binding model gave a reasonable fit to the observed chemical shifts. For example the 1:1 binding constant obtained for the $[\text{L}^2\cdot\text{K}]^+$ complex is 374 M^{-1} , being clearly larger than for L^2 alone (34 M^{-1}). As can be seen from the binding constants shown in Table 4, the choice of cation does not seem to have a great effect on the anion binding affinity of L^2 . All the calculated binding constants follow the same trend with the highest affinity of L^2 and its cationic complexes being with chloride and weakest with iodide. There are some differences between the cationic complexes in binding preference for each halide, for example $[\text{L}^2\cdot\text{K}]^+$ has the strongest affinity for chloride, whereas $[\text{L}^2\cdot\text{Rb}]^+$ binds bromide the strongest and $[\text{L}^2\cdot\text{Na}]^+$ has the strongest affinity towards iodide. Thus, from these results it is not reasonable to draw conclusions about the detailed effects of the cation in the anion binding preference.

2.4.2 Solution Studies with Receptor L^1 II

The anion binding behavior of L^1 was studied in a similar manner as with L^2 . The receptor was titrated with chloride, bromide, and iodide, and very similar 1:1 binding constants were obtained (828 , 175 , 32 M^{-1} , respectively, Table 5) compared to L^2 . This is also in accordance with the very similar chemical shift differences with L^1 and L^2 upon stepwise addition of the anions (Figure 43 and Figure 42, respectively). As seen in the crystal structures of L^1 with sodium, potassium and rubidium, the choice of the cation can have a drastic effect on the structure of the cationic complex, and this cation-dependent behaviour might also persist in solution affecting the anion binding behaviour of L^1 . Potassium is known to form 2:1 complexes with B15C5 molecules also in solution.¹³⁰ Indeed, the Job's plot analysis confirmed this also for L^1 , whereas sodium forms 1:1 complexes with L^1 . The anion binding stoichiometry of these complexes was also studied with Job's plot analysis indicating that the same stoichiometries also persist with anion complexation, *i.e.* L^1 binds anions as 1:1 complex in the presence of sodium, and as 2:1 complex in the presence of potassium.

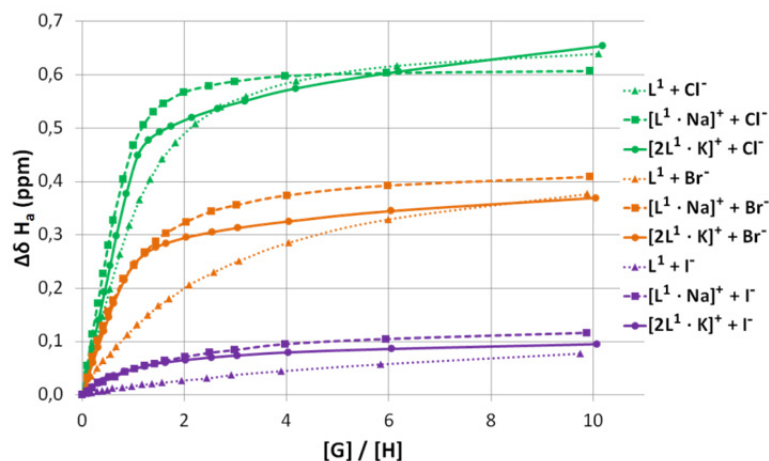


FIGURE 43 Observed chemical shift differences of urea-proton H_a in L^1 (dotted line), its cationic complexes $[L^1 \cdot Na]^+$ (dashed line), and $[2L^1 \cdot K]^+$ (solid line) upon step-wise addition of chloride (green), bromide (orange), and iodide (purple).

When the binding behavior of the sodium and potassium complexes of L^1 was studied in more detail with 1H NMR titrations, clear differences emerged between the complexes (Figure 43). The observed chemical shifts of $[L^1 \cdot Na]^+$ upon chloride complexation resemble those seen with $[L^2 \cdot M]^+$ (Figure 42c), indicating similar behavior towards halide anions between the two receptors. The binding constant calculation using a simple 1:1 binding model for $[L^1 \cdot Na]^+ + Cl^-$ complexation gave a 1:1 binding constant of $7609 M^{-1}$ (Table 5), being in the same range as for $[L^2 \cdot M]^+$ complexes (Table 4). However, the curve obtained in plotting chemical shifts of $[2L^1 \cdot K]^+ + Cl^-$ titration (Figure 43) has a clearly different curve shape than that for $[L^1 \cdot Na]^+ + Cl^-$ titration, suggesting a different type of binding. Utilization of a simple 1:1 binding model for $[2L^1 \cdot K]^+ + Cl^-$ titration data did not give a satisfactory fit between the observed and calculated chemical shifts, and therefore a more complex 1:1 + 1:2 binding model was used. This resulted in a very good fit and a very high 1:1 binding constant ($42247 M^{-1}$), with a remarkably smaller 1:2 binding constant ($96 M^{-1}$). The species distribution obtained from the titration data indicates that with low chloride concentration (< 1 equiv) the concentration of the 1:2 complex is very small, and after 1 equiv the 1:2 complex slowly becomes more abundant. The extremely high 1:1 binding constant of $[2L^1 \cdot K]^+$ with chloride, being clearly higher than that for $[L^2 \cdot K]^+$ ($8908 M^{-1}$), can be explained by having a similar dimeric complex in solution as seen in the crystal structures of L^1 with potassium and rubidium cations. The dimer has a suitable binding site for the anion, bearing more urea-groups capable of forming more hydrogen bonds to the anion compared to $[L^1 \cdot Na]^+$ or $[L^2 \cdot K]^+$ complexes. Interestingly, urea-proton H_b in $[2L^1 \cdot K]^+$ complex undergoes a clearly smaller chemical shift change than H_a (not shown) upon chloride binding, which is reversed from that of $[L^1 \cdot Na]^+$ and $[L^2 \cdot K]^+$ complexes. This can indicate that when the dimeric species $[2L^1 \cdot K]^+$ is formed, the anion cannot have as close an interaction with the cation as in $[L^1 \cdot Na]^+$ and $[L^2 \cdot K]^+$ complexes. This would result in a smaller chemical shift for H_b in the $[2L^1 \cdot K]^+$

complex. The second chloride binding can be hypothesized to result from hydrogen bonding between the anion and the urea group not directed towards the binding site, as seen in the solid-state structures.

TABLE 5 Binding constants and fitting errors obtained with HypNMR2008 for L^1 and its cationic complexes $[L^1 \cdot Na]^+$ and $[2L^1 \cdot K]^+$ with different halides in 4:1 $CDCl_3/DMSO-d_6$ at 303 K using global fitting.^{II}

		L^1	$[L^1 \cdot Na]^+$	$[2L^1 \cdot K]^+$
Cl ⁻	$K_{11}^{a,b}$	828 ± 22	7609 ± 576	-
	K_{11}^c	-	-	42247 ± 20877
	K_{12}^c	-	-	96 ± 29
Br ⁻	K_{11}^b	175 ± 3	1411 ± 69	-
	K_{11}^c	-	-	14713 ± 2657
	K_{12}^c	-	-	51 ± 21
I ⁻	K_{11}^b	32 ± 3	374 ± 16	717 ± 58

^a K_{xy} where x = host stoichiometry, y = guest stoichiometry, ^b 1:1 binding model used, ^c 1:1 + 1:2 binding model used.

The 1:1 binding constants for bromide and iodide are 1411 and 374 M^{-1} , respectively, for the $[L^1 \cdot Na]^+$ complex (Table 5). Again, these are in accordance with the results obtained with the cationic complexes of L^2 . Application of a 1:1 + 2:1 binding model for $[L^1 \cdot Na]^+ + Br^-$ did not give satisfactory results; thus only a simple 1:1 binding model was used. As seen from the chemical shift differences in Figure 43, bromide addition to $[2L^1 \cdot K]^+$ complex induces similar chemical shifts in H_a proton as chloride addition. Indeed, a 1:1 + 1:2 binding model was applicable also for these data, and the obtained 1:1 binding constant was also very high for $[2L^1 \cdot K]^+ + Br^-$ complexation (14713 M^{-1}). For iodide this was not the case, and a simple 1:1 model was used giving a 1:1 binding constant of 717 M^{-1} , which is also clearly higher than that for a $[L^1 \cdot Na]^+$ complex. These results indicate that the structures of the cationic complexes seen in the crystal structures persist also in solution, demonstrating the structure-function correlation between these receptors.

2.4.3 Solution Studies with Receptors L^3 and L^4 ^{III}

The tritopic nature of DB21C7- and DB24C8-based bis-urea receptors L^3 and L^4 can affect their anion binding behaviour compared to the simple ditopic receptors L^1 and L^2 . As before, first the anion binding behaviour of L^3 and L^4 was studied without the alkali metal cations present. Job's plot analysis gave a fairly clear indication of 1:1 complexation between the receptor and the anion, and no

significant differences between L^1 and L^2 were observed. In the ^1H NMR titration experiments, chemical shifts induced by the anions resemble those seen with L^1 and L^2 (Figure 44). Surprisingly, a calculation of the binding constants with a 1:1 binding model resulted in lower binding constants for chloride with both receptors (354 with L^3 and 258 M^{-1} with L^4 , Table 6) compared to L^1 and L^2 , whereas higher binding constants were obtained for iodide (71 with L^3 and 83 M^{-1} with L^4) compared to L^1 and L^2 . Although the obtained binding constants are somewhat different compared to L^1 and L^2 , their anion binding preference is the same, following the basicity of the anions.

In order to study the effect of the cation complexation with L^3 and L^4 towards anion binding, larger rubidium and cesium cations were selected because of their better size-fit with the DB21C7 and DB24C8 cavities. When the chloride binding of the rubidium complexes of L^3 and L^4 was studied with Job's plot analysis, the results indicated the presence of 1:1 and 1:2 complexes. The anion-induced chemical shift changes of $[\text{L}^3\cdot\text{Rb}]^+$ and $[\text{L}^4\cdot\text{Rb}]^+$ both show a different behaviour compared to L^3 and L^4 alone. When compared to previously presented binding curves (Figure 42 and Figure 43), the chemical shift changes observed with $[\text{L}^4\cdot\text{Rb}]^+$ upon chloride addition resemble those seen with $[\text{2L}^1\cdot\text{K}]^+$ upon chloride and bromide additions (Figure 43). The solid-state structures of $[\text{L}^4\cdot\text{Rb}]^+$ and $[\text{2L}^1\cdot\text{K}]^+$ complexes closely resemble each other; thus the similar solution behaviour is logical and supports the use of the same binding model for the observed anion binding behaviour. The binding behaviour of $[\text{L}^3\cdot\text{Rb}]^+$ and $[\text{L}^4\cdot\text{Rb}]^+$ with chloride was modelled with a 1:1 + 1:2 binding model, resulting in 1:1 binding constants of 77965 M^{-1} for $[\text{L}^3\cdot\text{Rb}]^+$ and 95521 M^{-1} for $[\text{L}^4\cdot\text{Rb}]^+$ (Table 6), being larger compared to that of the $[\text{2L}^1\cdot\text{K}]^+$ complex (42247 M^{-1}) but in the same range. Noteworthy is also the higher 1:2 binding constant of $[\text{L}^3\cdot\text{Rb}]^+$ (1318 M^{-1}) compared to that of the $[\text{L}^4\cdot\text{Rb}]^+$ (275 M^{-1}), which is reflected in the binding curve shapes (Figure 44). When the anion binding affinity with the cesium complexes of L^3 and L^4 was calculated using the same binding model, the 1:1 binding constants obtained were lower (22673 M^{-1} for $[\text{L}^3\cdot\text{Cs}]^+$ and 50362 M^{-1} for $[\text{L}^4\cdot\text{Cs}]^+$), possibly due to the larger size and more polarized nature of cesium weakening the electrostatic interactions between the cation and anion.

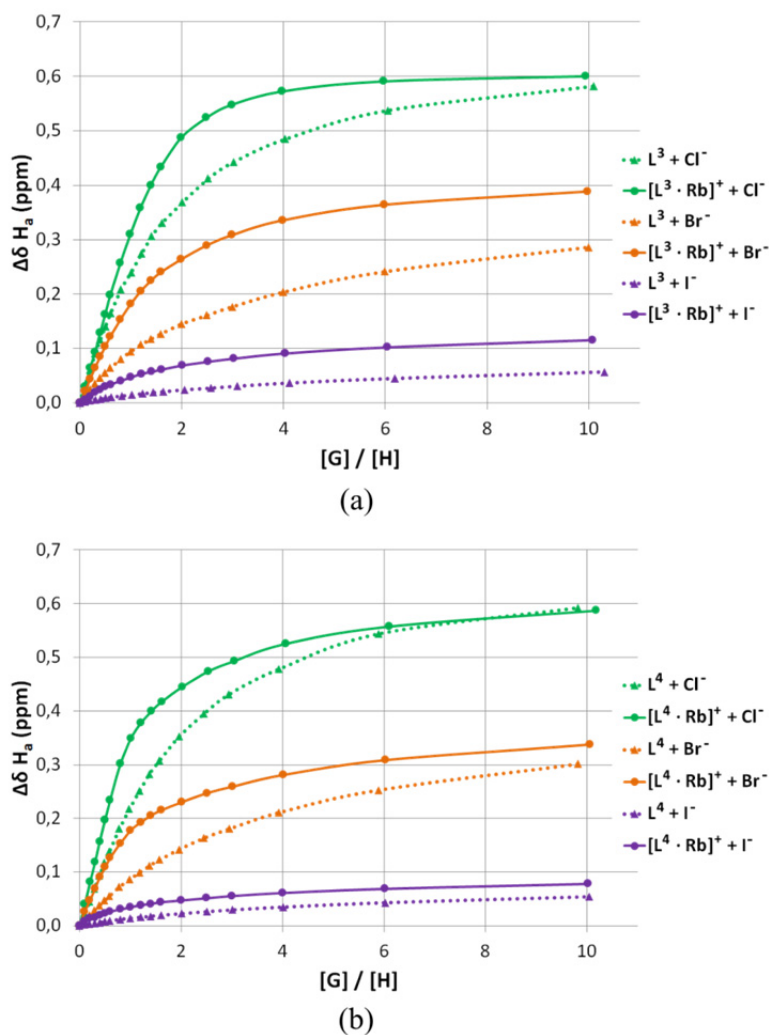


FIGURE 44 Observed chemical shift differences of urea-proton H_a in (a) L^3 and (b) L^4 (dotted lines) and their cationic complexes $[L^3\cdot Rb]^+$ and $[L^4\cdot Rb]^+$ (solid lines) upon addition of chloride (green), bromide (orange), and iodide (purple).

Differences between the cationic complexes of L^3 and L^4 emerge when the bromide binding is studied. The observed chemical shift changes in $[L^3\cdot Rb]^+$ and $[L^3\cdot Cs]^+$ complexes upon bromide addition was best modelled with a 1:1 + 2:1 binding model (indicated also by Job's plot analysis) resulting in 1:1 binding constants of 965 and 688 M^{-1} , respectively (Table 6). These are clearly smaller than any of previously obtained binding constants for bromide. It is possible that the electrostatic interactions are weaker with these cations resulting in only slightly higher 1:1 binding constants than those with L^3 alone (163 M^{-1}). However, the binding behaviour of $[L^4\cdot Rb]^+ + Br^-$ resembles that of chloride (although Job's plot analysis gave uncertain results) as seen in Figure 44b. Indeed, utilizing a 1:1 + 1:2 binding model resulted in very good fit to the obtained data with a 1:1 binding constant of 13020 M^{-1} , once again being close to results obtained with $[2L^1\cdot K]^+$ (14713 M^{-1}). The 1:1 binding constant for $[L^4\cdot Cs]^+ + Br^-$ (5278 M^{-1}) was again lower compared to $[L^4\cdot Rb]^+$ (13020 M^{-1}). As before, a simple 1:1 binding model was utilized for iodide complexation with all the studied

complexes, resulting in slightly higher binding constants than with L^3 and L^4 alone. It is noteworthy that the 1:1 binding constant for $[L^4 \cdot Cs]^+ + I^-$ complexation is higher than that for $[L^4 \cdot Rb]^+$ complex, deviating from the trend in anion binding preference between the rubidium and cesium complexes.

TABLE 6 Binding constants and fitting errors obtained with HypNMR2008 for L^3 , L^4 , and their cationic complexes $[L^3 \cdot M]^+$ and $[L^4 \cdot M]^+$ ($M = Rb, Cs$) with different halides in 4:1 $CDCl_3/DMSO-d_6$ at 303 K using global fitting.

		L^3	L^4	$[L^3 \cdot Rb]^+$	$[L^3 \cdot Cs]^+$	$[L^4 \cdot Rb]^+$	$[L^4 \cdot Cs]^+$
Cl ⁻	$K_{11}^{a,b}$	354 ± 6	258 ± 6	-	-	-	-
	K_{11}^c	-	-	77965 ± 36047	22673 ± 9310	95521 ± 44353	50362 ± 25102
	K_{12}^c	-	-	1318 ± 128	1316 ± 173	275 ± 36	445 ± 61
Br ⁻	K_{11}^b	163 ± 7	124 ± 2	-	-	-	-
	K_{11}^c	-	-	-	-	13020 ± 2510	5278 ± 2100
	K_{12}^c	-	-	-	-	85 ± 12	101 ± 41
	K_{11}^d	-	-	965 ± 89	688 ± 82	-	-
	K_{21}^d	-	-	381 ± 147	183 ± 95	-	-
I ⁻	K_{11}^b	71 ± 4	83 ± 3	337 ± 19	253 ± 12	384 ± 38	440 ± 20

^a K_{xy} where x = host stoichiometry, y = guest stoichiometry, ^b 1:1 binding model used, ^c 1:1 + 1:2 binding model used, ^d 1:1 + 2:1 binding model used.

2.5 Gas Phase Ion Pair Complexation with Crown Ether bis-Urea Receptors^{I,III}

The gas-phase ion pair complexation behavior of L^2 , L^3 , and L^4 was studied by electrospray ionization mass spectrometry. Studies were done by simple complexation experiments, and competition experiments between different ion pairs and receptors towards the same ion pair. Collision-induced dissociation (CID) experiments were performed with L^3 and L^4 to study the structural features of the ion pair complexes.

When the gas-phase ion pair complexation of L^2 with KCl, KBr, KI, and NaI was studied in positive polarization, most abundant ion pair complexes observed were $[L^2+CA+C]^+$ (C = cation, A = anion). In addition, $[L^2+Na]^+$ and $[L^2+K]^+$ ions were always seen in the spectra due to the strong affinity of B18C6 towards these ions. $[L^2-H+2K]^+$ ions were also observed in the complexation experiments following the loss of HCl and supporting the assumption that the anion is hydrogen bonded with the receptor also in the gas-phase. In Figure 45

are shown the results from the bilateral competition experiments of L^2 towards ion pairs KCl/KBr, KBr/KI, and KCl/NaCl. The observed binding preference of the potassium halides follows the basicity of the anions; the strongest affinity of KCl with L^2 is in agreement with the results obtained from the solution studies. Although similar binding constants were obtained for $[L^2+Na]^+$ and $[L^2+K]^+$ towards chloride in solution studies, the clear preference of KCl over NaCl in the gas phase can be attributed to a stronger affinity of K^+ over Na^+ towards B18C6.

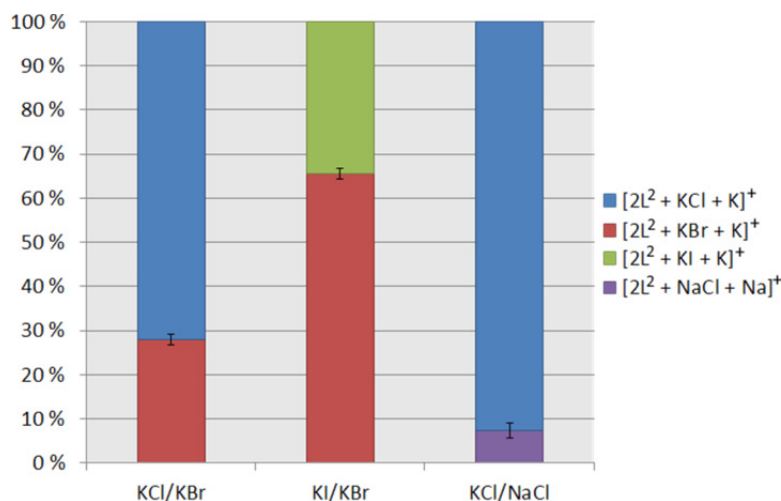


FIGURE 45 Results of competition experiments with L^2 (20 μ M, MeOH) and different ion pairs (1:1:1 ratio).¹

In a similar manner, the gas-phase ion pair complexation of L^3 and L^4 with RbCl, RbBr, RbI, CsCl, CsBr, and CsI was studied with complexation and competition experiments. In negative polarization the ion pair complexes were seen as $[L+CA+A]^-$ ions, and in addition $[L+2A]^{2-}$ (most abundant) and $[L+A]^-$ ions were observed. According to the competition experiments L^3 has a clear preference over RbCl to CsCl (Figure 46a)), being in accordance with the higher affinity of Rb^+ over Cs^+ towards DB21C7 in CH_3CN .¹³¹ Furthermore, the higher relative affinity of L^3 towards RbCl over RbBr is very clear from the competition experiments, and the affinity of L^3 towards RbI is very low. When the relative affinity of L^4 towards RbCl and CsCl was studied, only small preference of CsCl over RbCl was observed. There is a slightly stronger affinity of Cs^+ over Rb^+ towards DB24C8 in highly polar DMF,¹³² which might be reflected in these results. The relative affinities towards CsCl, CsBr, and CsI follow the same trend as the affinities between L^3 and rubidium halides. However, the differences between cesium halides towards L^4 are even more drastic than with L^3 , with $[L^4+CsI+I]^-$ having very low abundance (< 1 %) compared to $[L^4+CsBr+Br]^-$ (Figure 46). The affinity of the receptors L^3 and L^4 toward the same ion pair was also studied with competition experiments. Following the similar trend as in the solution studies, L^4 showed higher affinity towards both RbCl and CsCl, with clearer preference seen for CsCl.

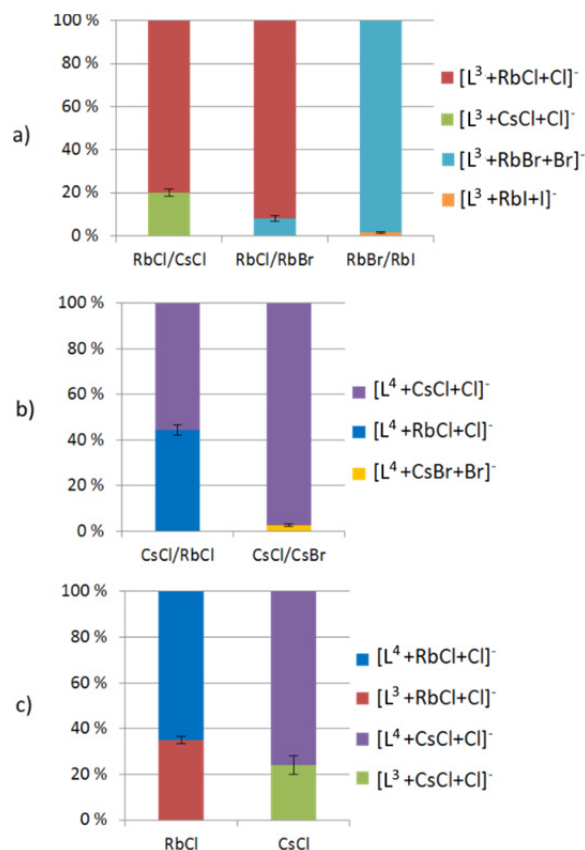


FIGURE 46 Results of competition experiments with (a) L^3 and (b) L^4 (20 μ M, CH_3CN) towards rubidium and cesium halides (with ratio 1:3:3). Graphical view of L^4 and CsBr/CsI is not shown due to the small abundance of $[L^4 + CsI + I]^-$ ions in the experiment (< 1 %). (c) Competition experiment between L^3 and L^4 towards RbCl and CsCl (with ratio 1:1:3).^{III}

CID experiments were performed to gain insight of the structure and the stability of the ion pair complexes in the gas phase. Complexes of receptors L^3 and L^4 showed similar dissociation behavior upon increasing collision energies. The ion $[R+A]^-$ was observed as the first elimination product resulting from the cleavage of an ion pair and a cleavage of HA was seen as the second dissociation event. This suggests that in the gas-phase complex one anion is bound as a contact ion pair with the cation and the second anion is hydrogen bonded with the receptor. Dissociation of the receptor itself was observed with higher collision energies.

CONCLUSIONS

This work describes the synthesis and characterization of six ditopic crown ether-based bis-urea (L^1 - L^4) and uranyl salophen (L^5 , L^6) receptors and studies of their ion pair recognition behaviour.

Single-crystal X-ray crystallography was used to study the ditopic nature of the crown ether bis-urea receptors in the solid-state. With benzo-15-crown-5-based receptor L^1 , two general observations were made in the solid-state: complexes of sodium halides did not show a predictable behaviour, whereas ion pair complexes with larger potassium and rubidium halides always existed as a dimeric assembly through sandwich-complexation of the cation and formation of a separated ion pair complex. Thus it can be concluded that the size fit between the cation and the crown ether cavity plays a key role in the solid-state binding behaviour of L^1 . The receptor L^2 , having a larger benzo-18-crown-6 functionality for cation recognition, has two distinctive solid-state binding motifs with different alkali and ammonium halides and oxyanions. When complexed with a suitably fitted potassium cation, the halide anion basicity seems to have a key role in defining the ion pair binding behaviour. With KF, KCl, and KBr L^2 forms 2:2 (receptor : ion pair) complexes with separated ion pairs in the structure. The complex is formed through various weak interactions between the receptors and the ion pairs, and resembling structures are also formed with potassium oxyanions (CO_3^{2-} , AcO^-). If L^2 is complexed with larger cations (Rb^+ , NH_4^+), or the anion basicity is weak (Br^- , I^-), the solid-state structures are formed through contact ion pair complexation. Potassium bromide was observed in both ion pair binding motifs.

The larger dibenzo-21-crown-7 and dibenzo-24-crown-8 bis-urea receptors L^3 and L^4 , respectively, had distinctive solid-state binding behaviour, but the obtained complexes had structural features strikingly similar to the complexes obtained with L^1 and L^2 . The asymmetric structure of dibenzo-21-crown-7 might explain the difficulty in obtaining solid-state complexes with L^3 , and in the course of this work, in spite of numerous attempts, only one crystal structure with L^3 was obtained ($L^3 \cdot Rb_2CO_3$). Nevertheless, the crystal structure revealed that L^3 has an open conformation forming a very complex network of weak interactions with the neighbouring cation complexes and the carbonate anion. These interactions resemble to those seen in the 2:2 complexes of L^2 , supporting the notion that the observations made with L^2 are more general features in the solid-state ion pair complexation of these types of receptors. Interestingly, the larger and symmetric dibenzo-24-crown-8 scaffold makes it possible for L^4 to have a doubly folded conformation upon ion pair complexation. Its more compact structure compared to L^3 might explain the success in obtaining more crystal structures with rubidium and cesium halides and oxyanions with L^4 . All the obtained alkali metal complexes of L^4 are structurally strikingly similar to the dimeric complexes of L^1 , besides the weak interactions responsible for the complexation. Thus, alkali metal complexes of L^4 can be considered as single-molecule analogues to dimeric assemblies of L^1 . Due to the tritopic nature of L^3

and L^4 , i.e. having one binding site for a cation and two possible binding sites for anions, complexation with earth-alkaline metals was also tested, resulting in crystal structure $L^4 \cdot BaCl_2$. Due to its smaller size compared to rubidium and cesium cations, complexation of Ba^{2+} results in a more open receptor conformation. The two chloride anions are complexed on each side of the receptor, thus proving the tritopic behaviour of these receptors in the solid-state. This structure exemplifies the versatile nature of these receptors, especially in the solid-state ion pair complexation.

The anion binding and ion pair complexation behaviour of L^1 - L^4 in solution was studied with 1H NMR titrations and Job's plot analysis in 4:1 $CDCl_3/DMSO$. Generally, all the receptors had similar moderate binding affinities towards the halides studied (chloride, bromide, and iodide), with the binding preference $I^- < Br^- < Cl^-$ following the basicity of the anions. However, in all the studied cases clear positive cooperativity in anion binding was observed when the receptors were complexed with an alkali metal cation. With receptor L^2 (with a benzo-18-crown-6 functionality), a clear turn-on effect towards anion binding was observed, but this effect was independent of the cation (sodium, potassium, rubidium), as similar anion affinities were observed with all the complexes. A similar turn-on effect in anion binding was seen with L^1 (with benzo-15-crown-5 functionality) and its sodium complexes and the obtained binding affinities were close to the ones obtained with L^2 . However, in the presence of potassium clearly different behaviour emerged. When complexed with larger potassium cations, L^1 forms a dimeric assembly seen in the solid-state complexes also in solution (proved by Job's plot analysis), and this dimeric species has a remarkably stronger affinity towards chloride and bromide compared to an $[L^1 \cdot Na]^+$ complex. Thus the solid-state structures of ion pair complexes can explain the observed behaviour of L^1 . To support this notion, very similar solution behaviour was observed especially with the rubidium complex of L^4 , which also has a similar solid-state structure similar to the $[2L^1 \cdot KCl]$ complex.

In general, both L^3 and L^4 showed similar anion affinity when alkali metals were not present. In addition, the chloride binding with rubidium and cesium complexes of L^3 and L^4 was similar with very high binding affinities. However, the bromide binding between the cationic complexes of L^3 and L^4 differed remarkably, which might result from the different structures of the receptors affecting the selectivity. As a general observation it was seen that the rubidium complexes of L^3 and L^4 had stronger affinities towards the halides, probably resulting from the smaller size of the rubidium ion, and the resulting stronger electrostatic interactions between the cation and anion. Overall, it can be concluded that the positive cooperativity results from attractive electrostatic interactions between the complexed cation and anion, and the possible through-bond electronic effects the cation complexation induces in the receptor. With L^1 and L^4 allosteric cooperativity also exists, as the anion binding behaviour is affected by the structural changes in the receptors upon cation complexation.

The ion pair complexation of L^2 , L^3 , and L^4 was also studied in the gas-phase by mass spectrometry with complexation and competition experiments.

These results mainly support the affinities and selectivities towards the tested ion pairs observed in solution. **L**² showed clear selectivity of KCl over NaCl in the gas phase due to the better size fit of the cation with the crown ether moiety, but this selectivity was not observed in the solution. However, the competition experiments supported the anion selectivity also in the gas phase, as the relative affinity of **L**² towards the tested ion pairs was KI < KBr < KCl. The mass spectrometry studies with **L**³ and **L**⁴ showed similar anion selectivity but with larger differences in selectivity between the tested ion pairs compared to **L**². The competition experiments between the receptors suggested that **L**⁴ has stronger affinity toward both RbCl and CsCl compared to **L**³, possibly due to the more compact structure of the receptor. All in all, the gas-phase studies support the results obtained in solution.

Finally, the crown ether uranyl salophen receptors **L**⁵ (benzo-15-crown-5) and **L**⁶ (benzo-18-crown-6) were studied through comprehensive single-crystal X-ray crystallography analysis with 19 crystal structures. Some general observations on the interactions between the receptors and the ion pairs could be made from the structures. Depending on the nature of the ion pair, and the size fit of the cation with the crown ether, the complexes can be formed as separated ion pairs (interaction motif **I**), or contact ion pairs (interaction motif **II**). Structures with interaction motif **I** had variety in their constitution, as the complexes could exist as isolated dimers (**L**⁵·**LiCl**), dimers forming polymeric structures (i.e. **L**⁶·**KAcO**) or structures consisting of infinite coordination polymers (**L**⁶·**NaI**) through coordination of repeating $\cdots\text{O}=\text{U}=\text{O}\cdots\text{Na}^+\cdots\text{O}$ units. Interaction motif **II** is consistent in its constitution; it is always formed through contact ion pair formation between the anion coordinated to the uranyl centre and the cation complexed in the crown ether of a neighbouring receptor. This interaction motif was observed when the cation resides on top of the crown ether plane due to the poor size fit of the cation and the crown ether (i.e. **L**⁵·**CsF** or **L**⁶·**NH₄Br**). Interaction motif **III** was defined as a more general description of the packing of the receptors in which the receptors stack in about 90° angle to each other through various weak interactions. This interaction motif was observed in crystal structures with receptors alone, and in the presence of ion pairs

REFERENCES

1. Lehn, J. *Proc. Natl. Acad. Sci. U. S. A.* **2002**, *99*, 4763-4768.
2. Kyba, E. P.; Helgeson, R. C.; Madan, K.; Gokel, G. W.; Tarnowski, T. L.; Moore, S. S.; Cram, D. J. *J. Am. Chem. Soc.* **1977**, *99*, 2564-2571.
3. Steed J. W.; Atwood J. L. *Supramolecular Chemistry, 2nd Ed.*, John Wiley and Sons, Ltd., 2009.
4. Steed J. W.; Turner D. R.; Wallace K. J. *Core Concepts in Supramolecular Chemistry and Nanochemistry; 1st ed.*, John Wiley and Sons, Ltd., 2007.
5. Lehn, J. *Science* **2002**, *295*, 2400-2403.
6. Ballester, P. *Chem. Soc. Rev.* **2010**, *39*, 3810-3830.
7. Zarra, S.; Wood, D. M.; Roberts, D. A.; Nitschke, J. R. *Chem. Soc. Rev.* **2015**, *44*, 419-432.
8. Chakrabarty, R.; Mukherjee, P. S.; Stang, P. J. *Chem. Rev.* **2011**, *111*, 6810-6918.
9. Harris, K.; Fujita, D.; Fujita, M. *Chem. Commun.* **2013**, *49*, 6703-6712.
10. Petkau-Milroy, K.; Brunsveld, L. *Org. Biomol. Chem.* **2013**, *11*, 219-232.
11. Uhlenheuer, D. A.; Petkau, K.; Brunsveld, L. *Chem. Soc. Rev.* **2010**, *39*, 2817-2826.
12. Atwood J. L.; Steed J. W. (ed.) *Encyclopedia of Supramolecular Chemistry*. CRC Press, 2004.
13. Hunter, C.; Anderson, H. *Angew. Chem. Int. Ed.* **2009**, *48*, 7488-7499.
14. Mahadevi, A. S.; Sastry, G. N. *Chem. Rev.* **2016**, *116*, 2775-2825.
15. Cavallo, G.; Metrangolo, P.; Milani, R.; Pilati, T.; Priimagi, A.; Resnati, G.; Terraneo, G. *Chem. Rev.* **2016**, *116*, 2478-2601.
16. Evans, N. H.; Beer, P. D. *Angew. Chem. Int. Ed.* **2014**, *53*, 11716-11754.
17. Gale, P. A.; Busschaert, N.; Haynes, C. J. E.; Karagiannidis, L. E.; Kirby, I. L. *Chem. Soc. Rev.* **2014**, *43*, 205-241.
18. Wenzel, M.; Hiscock, J. R.; Gale, P. A. *Chem. Soc. Rev.* **2012**, *41*, 480-520.
19. Gale, P. A. *Chem. Soc. Rev.* **2010**, *39*, 3746-3771.
20. Caltagirone, C.; Gale, P. A. *Chem. Soc. Rev.* **2009**, *38*, 520-563.
21. Kirkovits, G.; Shriver, J.; Gale, P.; Sessler, J. J. *Inclusion Phenom. Macrocyclic Chem.* **2001**, *41*, 69-75.
22. Kim, S. K.; Sessler, J. L. *Chem. Soc. Rev.* **2010**, *39*, 3784-3809.
23. McConnell, A. J.; Beer, P. D. *Angew. Chem. Int. Ed.* **2012**, *51*, 5052-5061.
24. Kim, S. K.; Sessler, J. L. *Acc. Chem. Res.* **2014**, *47*, 2525-2536.
25. Roelens, S.; Vacca, A.; Francesconi, O.; Venturi, C. *Chem. Eur. J.* **2009**, *15*, 8296-8302.
26. Roelens, S.; Vacca, A.; Venturi, C. *Chem. Eur. J.* **2009**, *15*, 2635-2644.
27. Howe, E. N. W.; Bhadbhade, M.; Thordarson, P. *J. Am. Chem. Soc.* **2014**, *136*, 7505-7516.
28. Qiao, B.; Sengupta, A.; Liu, Y.; McDonald, K. P.; Pink, M.; Anderson, J. R.; Raghavachari, K.; Flood, A. H. *J. Am. Chem. Soc.* **2015**, *137*, 9746-9757.
29. Pedersen, C. J. *J. Am. Chem. Soc.* **1967**, *89*, 7017-7036.
30. Pedersen, C. J. *Science* **1988**, *241*, 536-540.
31. Gokel, G. W.; Leevy, W. M.; Weber, M. E. *Chem. Rev.* **2004**, *104*, 2723-2750.

32. Reetz, M. T.; Niemeyer, C. M.; Harms, K. *Angew. Chem. Int. Ed.* **1991**, *30*, 1472-1474.
33. Reetz, M. T.; Niemeyer, C. M.; Harms, K. *Angew. Chem. Int. Ed.* **1991**, *30*, 1474-1476.
34. Shukla, R.; Kida, T.; Smith, B. D. *Org. Lett.* **2000**, *2*, 3099-3102.
35. Deetz, M. J.; Shang, M.; Smith, B. D. *J. Am. Chem. Soc.* **2000**, *122*, 6201-6207.
36. Mahoney, J. M.; Beatty, A. M.; Smith, B. D. *J. Am. Chem. Soc.* **2001**, *123*, 5847-5848.
37. Mahoney, J. M.; Marshall, R. A.; Beatty, A. M.; Smith, B. D.; Camiolo, S.; Gale, P. A. *J. Supramol. Chem.* **2001**, *1*, 289-292.
38. Mahoney, J. M.; Davis, J. P.; Beatty, A. M.; Smith, B. D. *J. Org. Chem.* **2003**, *68*, 9819-9820.
39. Koulov, A. V.; Mahoney, J. M.; Smith, B. D. *Org. Biomol. Chem.* **2003**, *1*, 27-29.
40. Mahoney, J. M.; Nawaratna, G. U.; Beatty, A. M.; Duggan, P. J.; Smith, B. D. *Inorg. Chem.* **2004**, *43*, 5902-5907.
41. Mahoney, J. M.; Beatty, A. M.; Smith, B. D. *Inorg. Chem.* **2004**, *43*, 7617-7621.
42. Mahoney, J. M.; Stucker, K. A.; Jiang, H.; Carmichael, I.; Brinkmann, N. R.; Beatty, A. M.; Noll, B. C.; Smith, B. D. *J. Am. Chem. Soc.* **2005**, *127*, 2922-2928.
43. Barboiu, M.; Vaughan, G.; van, der Lee, A. *Org. Lett.* **2003**, *5*, 3073-3076.
44. Cazacu, A.; Tong, C.; van, d. L.; Fyles, T. M.; Barboiu, M. *J. Am. Chem. Soc.* **2006**, *128*, 9541-9548.
45. Cazacu, A.; Legrand, Y.; Pasc, A.; Nasr, G.; Van der Lee, A.; Mahon, E.; Barboiu, M. *Proc. Natl. Acad. Sci. U. S. A.* **2009**, *106*, 8117-8122.
46. Barboiu, M.; Dumitrescu, D.; van, der Lee, A. *Cryst. Growth Des.* **2014**, *14*, 3062-3068.
47. Sun, Z.; Barboiu, M.; Legrand, Y.; Petit, E.; Rotaru, A. *Angew. Chem. Int. Ed.* **2015**, *54*, 14473-14477.
48. Sun, Z.; Gilles, A.; Kocsis, I.; Legrand, Y.; Petit, E.; Barboiu, M. *Chem. – Eur. J.* **2016**, *22*, 2158-2164.
49. Gilles, A.; Barboiu, M. *J. Am. Chem. Soc.* **2016**, *138*, 426-432.
50. Evans, A. J.; Beer, P. D. *Dalton Trans.* **2003**, 4451-4456.
51. Redman, J. E.; Beer, P. D.; Dent, S. W.; Drew, M. G. B. *Chem. Commun.* **1998**, 231-232.
52. Beer, P. D.; Dent, S. W. *Chem. Commun.* **1998**, 825-826.
53. Uppadine, L. H.; Redman, J. E.; Dent, S. W.; Drew, M. G. B.; Beer, P. D. *Inorg. Chem.* **2001**, *40*, 2860-2869.
54. Romanski, J.; Piatek, P. *Chem. Commun.* **2012**, *48*, 11346-11348.
55. Romanski, J.; Trzaskowski, B.; Piatek, P. *Dalton Trans.* **2013**, *42*, 15271-15274.
56. Piatek, P.; Karbarz, M.; Romanski, J. *Dalton Trans.* **2014**, *43*, 8515-8522.
57. Piatek, P.; Zdanowski, S.; Romanski, J. *New J. Chem.* **2015**, *39*, 2090-2095.
58. Sun, Z.; Pan, F.; Triyanti; Albrecht, M.; Raabe, G. *Eur. J. Org. Chem.* **2013**, *2013*, 7922-7932.
59. Lee, J. H.; Lee, J. H.; Choi, Y. R.; Kang, P.; Choi, M.; Jeong, K. *J. Org. Chem.* **2014**, *79*, 6403-6409.

60. Van Staveren, C. J.; Fenton, D. E.; Reinhoudt, D. N.; Van Eerden, J.; Harkema, S. *J. Am. Chem. Soc.* **1987**, *109*, 3456-3458.
61. Van Doorn, A. R.; Schaafstra, R.; Bos, M.; Harkema, S.; Van Eerden, J.; Verboom, W.; Reinhoudt, D. N. *J. Org. Chem.* **1991**, *56*, 6083-6094.
62. Nijenhuis, W. F.; Van Doorn, A. R.; Reichwein, A. M.; De Jong, F.; Reinhoudt, D. N. *J. Am. Chem. Soc.* **1991**, *113*, 3607-3608.
63. Rudkevich, D. M.; Stauthamer, W. P. R. V.; Verboom, W.; Engbersen, J. F. J.; Harkema, S.; Reinhoudt, D. N. *J. Am. Chem. Soc.* **1992**, *114*, 9671-9673.
64. Rudkevich, D. M.; Verboom, W.; Brzozka, Z.; Palys, M. J.; Stauthamer, W. P. R. V.; van Hummel, G. J.; Franken, S. M.; Harkema, S.; Engbersen, J. F. J.; Reinhoudt, D. N. *J. Am. Chem. Soc.* **1994**, *116*, 4341-4351.
65. Dalla Cort, A.; De Bernardin, P.; Forte, G.; Yafteh Miha, F. *Chem. Soc. Rev.* **2010**, *39*, 3863-3874.
66. Bedini, E.; Forte, G.; De Castro, C.; Parrilli, M.; Dalla Cort, A. *J. Org. Chem.* **2013**, *78*, 7962-7969.
67. Dalla Cort, A.; Forte, G.; Schiaffino, L. *J. Org. Chem.* **2011**, *76*, 7569-7572.
68. Keymeulen, F.; De Bernardin, P.; Giannicchi, I.; Galantini, L.; Bartik, K.; Dalla Cort, A. *Org. Biomol. Chem.* **2015**, *13*, 2437-2443.
69. Cametti, M.; Dalla Cort, A.; Bartik, K. *ChemPhysChem* **2008**, *9*, 2168-2171.
70. Cametti, M.; Rissanen, K. *Chem. Soc. Rev.* **2013**, *42*, 2016-2038.
71. Cametti, M.; Rissanen, K. *Chem. Commun.* **2009**, 2809-2829.
72. Rudkevich, D. M.; Brzozka, Z.; Palys, M.; Visser, H. C.; Verboom, W.; Reinhoudt, D. N. *Angew. Chem. Int. Ed.* **1994**, *33*, 467-468.
73. Rudkevich, D. M.; Verboom, W.; Reinhoudt, D. N. *J. Org. Chem.* **1994**, *59*, 3683-3686.
74. Rudkevich, D. M.; Mercer-Chalmers, J.; Verboom, W.; Ungaro, R.; de Jong, F.; Reinhoudt, D. N. *J. Am. Chem. Soc.* **1995**, *117*, 6124-6125.
75. Cametti, M.; Nissinen, M.; Dalla Cort, A.; Mandolini, L.; Rissanen, K. *Chem. Commun.* **2003**, 2420-2421.
76. Cametti, M.; Nissinen, M.; Dalla Cort, A.; Mandolini, L.; Rissanen, K. *J. Am. Chem. Soc.* **2007**, *129*, 3641-3648.
77. Cametti, M.; Ilander, L.; Valkonen, A.; Nieger, M.; Nissinen, M.; Nauha, E.; Rissanen, K. *Inorg. Chem.* **2010**, *49*, 11473-11484.
78. Cametti, M.; Nissinen, M.; Dalla Cort, A.; Mandolini, L.; Rissanen, K. *J. Am. Chem. Soc.* **2005**, *127*, 3831-3837.
79. Cametti, M.; Nissinen, M.; Dalla Cort, A.; Rissanen, K.; Mandolini, L. *Inorg. Chem.* **2006**, *45*, 6099-6101.
80. Ballistreri, F. P.; Pappalardo, A.; Tomaselli, G. A.; Toscano, R. M.; Sfrassetto, G. T. *Eur. J. Org. Chem.* **2010**, *2010*, 3806-3810.
81. Amato, M. E.; Ballistreri, F. P.; Gentile, S.; Pappalardo, A.; Tomaselli, G. A.; Toscano, R. M. *J. Org. Chem.* **2010**, *75*, 1437-1443.
82. Scheerder, J.; van Duynhoven, J. P. M.; Engbersen, J. F. J.; Reinhoudt, D. N. *Angew. Chem. Int. Ed. Engl.* **1996**, *35*, 1090-1093.
83. Akhuli, B.; Ghosh, P. *Chem. Commun.* **2015**, *51*, 16514-16517.
84. Beer, P. D.; Hopkins, P. K.; McKinney, J. D. *Chem. Commun.* **1999**, 1253-1254.

85. Aydogan, A.; Coady, D.; Kim, S.; Akar, A.; Bielawski, C.; Marquez, M.; Sessler, J. *Angew. Chem. Int. Ed.* **2008**, *47*, 9648-9652.
86. Gale, P. A. *Acc. Chem. Res.* **2011**, *44*, 216-226.
87. Haynes, C. J. E.; Gale, P. A. *Chem. Commun.* **2011**, *47*, 8203-8209.
88. O'Sullivan, B. P.; Freedman, S. D. *The Lancet* **2009**, *373*, 1891-1904.
89. Ko, S.; Kim, S. K.; Share, A.; Lynch, V. M.; Park, J.; Namkung, W.; Van Rossum, W.; Busschaert, N.; Gale, P. A.; Sessler, J. L.; Shin, I. *Nat Chem.* **2014**, *6*, 885-892.
90. Gale, P. A.; Sessler, J. L.; Král, V.; Lynch, V. J. *Am. Chem. Soc.* **1996**, *118*, 5140-5141.
91. Saha, I.; Lee, J. T.; Lee, C. *Eur. J. Org. Chem.* **2015**, *2015*, 3859-3885.
92. Custelcean, R.; Delmau, L. H.; Moyer, B. A.; Sessler, J. L.; Cho, W.; Gross, D.; Bates, G. W.; Brooks, S. J.; Light, M. E.; Gale, P. A. *Angew. Chem. Int. Ed.* **2005**, *44*, 2537-2542.
93. Wintergerst, M. P.; Levitskaia, T. G.; Moyer, B. A.; Sessler, J. L.; Delmau, L. J. *Am. Chem. Soc.* **2008**, *130*, 4129-4139.
94. Tong, C. C.; Quesada, R.; Sessler, J. L.; Gale, P. A. *Chem. Commun.* **2008**, 6321-6323.
95. Kim, D. S.; Sessler, J. L. *Chem. Soc. Rev.* **2015**, *44*, 532-546.
96. Sessler, J. L.; Kim, S. K.; Gross, D. E.; Lee, C.; Kim, J. S.; Lynch, V. M. *J. Am. Chem. Soc.* **2008**, *130*, 13162-13166.
97. Kim, S. K.; Sessler, J. L.; Gross, D. E.; Lee, C.; Kim, J. S.; Lynch, V. M.; Delmau, L.; Hay, B. P. *J. Am. Chem. Soc.* **2010**, *132*, 5827-5836.
98. Kim, S. K.; Gross, D. E.; Cho, D.; Lynch, V. M.; Sessler, J. L. *J. Org. Chem.* **2011**, *76*, 1005-1012.
99. Park, I.; Kim, S.; Lee, M.; Lynch, V. M.; Sessler, J. L.; Lee, C. *Chem. Asian J.* **2011**, *6*, 2911-2915.
100. Kim, S. K.; Vargas-Zúñiga, G. I.; Hay, B. P.; Young, N. J.; Delmau, L.; Mas-selin, C.; Lee, C.; Kim, J. S.; Lynch, V. M.; Moyer, B. A.; Sessler, J. L. *J. Am. Chem. Soc.* **2012**, *134*, 1782-1792.
101. Park, I.; Yoo, J.; Adhikari, S.; Park, J. S.; Sessler, J. L.; Lee, C. *Chem. Eur. J.* **2012**, *18*, 15073-15078.
102. Kim, S. K.; Hay, B. P.; Kim, J. S.; Moyer, B. A.; Sessler, J. L. *Chem. Commun.* **2013**, *49*, 2112-2114.
103. Kim, S. K.; Lee, H. G.; Vargas-Zúñiga, G. I.; Lynch, V. M.; Kim, C.; Sessler, J. L. *Chem. Eur. J.* **2014**, *20*, 11750-11759.
104. Ciardi, M.; Galán, A.; Ballester, P. *J. Am. Chem. Soc.* **2015**, *137*, 2047-2055.
105. Park, I.; Yoo, J.; Kim, B.; Adhikari, S.; Kim, S. K.; Yeon, Y.; Haynes, C. J. E.; Sutton, J. L.; Tong, C. C.; Lynch, V. M.; Sessler, J. L.; Gale, P. A.; Lee, C. *Chem. Eur. J.* **2012**, *18*, 2514-2523.
106. Kim, S. K.; Lynch, V. M.; Young, N. J.; Hay, B. P.; Lee, C.; Kim, J. S.; Moyer, B. A.; Sessler, J. L. *J. Am. Chem. Soc.* **2012**, *134*, 20837-20843.
107. Vargas Jentsch, A.; Emery, D.; Mareda, J.; Metrangolo, P.; Resnati, G.; Matile, S. *Angew. Chem.* **2011**, *123*, 11879-11882.

108. Miyaji, H.; Collinson, S. R.; Prokes, I.; Tucker, J. H. R. *Chem. Commun.* **2003**, 64-65.
109. Molina, P.; Tarraga, A.; Alfonso, M. *Dalton Trans.* **2014**, 43, 18-29.
110. Brunetti, E.; Picron, J.; Flidrova, K.; Bruylants, G.; Bartik, K.; Jabin, I. *J. Org. Chem.* **2014**, 79, 6179-6188.
111. Eckelmann, J.; Saggiomo, V.; Sonnichsen, F. D.; Luning, U. *New J. Chem.* **2010**, 34, 1247-1250.
112. Nabeshima, T.; Saiki, T.; Iwabuchi, J.; Akine, S. *J. Am. Chem. Soc.* **2005**, 127, 5507-5511.
113. Valderrey, V.; Escudero-Adán, E. C.; Ballester, P. *Angew. Chem. Int. Ed.* **2013**, 52, 6898-6902.
114. Moerkerke, S.; Ménand, M.; Jabin, I. *Chem. Eur. J.* **2010**, 16, 11712-11719.
115. Moerkerke, S.; Le Gac, S.; Topić, F.; Rissanen, K.; Jabin, I. *Eur. J. Org. Chem.* **2013**, 2013, 5315-5322.
116. Duggan, S. A.; Fallon, G.; Langford, S. J.; Lau, V.; Satchell, J. F.; Paddon-Row, M. *J. Org. Chem.* **2001**, 66, 4419-4426.
117. Camiolo, S.; Gale, P. A.; Hursthouse, M. B.; Light, M. E. *Org. Biomol. Chem.* **2003**, 1, 741-744.
118. Boiocchi, M.; Del Boca, L.; Gómez, D. E.; Fabbrizzi, L.; Licchelli, M.; Monzani, E. *J. Am. Chem. Soc.* **2004**, 126, 16507-16514.
119. Martínez-Máñez, R.; Sancenón, F. *Chem. Rev.* **2003**, 103, 4419-4476.
120. Ravikumar, I.; Ghosh, P. *Chem. Commun.* **2010**, 46, 1082-1084.
121. Mougel, V.; Chatelain, L.; Pécaut, J.; Caciuffo, R.; Colineau, E.; Griveau, J.; Mazzanti, M. *Nat. Chem.* **2012**, 4, 1011-1017.
122. Chatelain, L.; Walsh, J. P. S.; Pécaut, J.; Tuna, F.; Mazzanti, M. *Angew. Chem. Int. Ed.* **2014**, 53, 13434-13438.
123. Mougel, V.; Chatelain, L.; Hermle, J.; Caciuffo, R.; Colineau, E.; Tuna, F.; Magnani, N.; de Geyer, A.; Pécaut, J.; Mazzanti, M. *Angew. Chem. Int. Ed.* **2014**, 53, 819-823.
124. Mougel, V.; Horeglad, P.; Nocton, G.; Pécaut, J.; Mazzanti, M. *Angew. Chem. Int. Ed.* **2009**, 48, 8477-8480.
125. Horeglad, P.; Nocton, G.; Filinchuk, Y.; Pecaute, J.; Mazzanti, M. *Chem. Commun.* **2009**, 1843-1845.
126. Renny, J. S.; Tomasevich, L. L.; Tallmadge, E. H.; Collum, D. B. *Angew. Chem. Int. Ed.* **2013**, 52, 11998-12013.
127. Thordarson, P. *Chem. Soc. Rev.* **2011**, 40, 1305-1323.
128. Frassinetti, C.; Ghelli, S.; Gans, P.; Sabatini, A.; Moruzzi, M. S.; Vacca, A. *Anal. Biochem.* **1995**, 231, 374-382.
129. Lowe, A. J.; Pfeffer, F. M.; Thordarson, P. *Supramol. Chem.* **2012**, 24, 585-594.
130. Kirkovits, G. J.; Zimmerman, R. S.; Huggins, M. T.; Lynch, V. M.; Sessler, J. L. *Eur. J. Org. Chem.* **2002**, 2002, 3768-3778.
131. Katsuta, S.; Kuwano, T.; Ito, Y.; Takeda, Y. *J. Chem. Eng. Data* **2005**, 50, 1313-1318.
132. Goff, C. M.; Matchette, M. A.; Shabestary, N.; Khazaeli, S. *Polyhedron* **1996**, 15, 3897-3903.